Vietnam National University Ho Chi Minh City
University of Science
Faculty of Physics
Department of Theoretical Physics

ICISE, Quy Nhon, VietNam
Institute For Interdisciplinary Research in Science and Education
Theoretical Physics Group

———————— * ————————

BACHELOR THESIS

AXION AND ITS DIRECT DETECTION PROCESSES

Nguyen Huy Hien

Supervisor: Dr. Dao Thi Nhung

HO CHI MINH CITY - 2021

Contents

List of Figures

List of Tables

Abstract

In 2020 XENON1T experiment,has observed an excess the known background for the electron recoil energy in the range [3,5] KeV. A promissing explanation for this excess by is given by a hypotheretical particle, axion.The particle is a pseudo-Goldstone boson resulted from the spontaneous symmetry breaking of the $U(1)_{PQ}$. That was proposed by Peccei-Quinn the 1977 to solve the long standing problem of the Standard Model, the strong CP problem. The aim of this thesis two folds. We first try to understand the strong CP problem and its connection with the chiral anomaly. We then review the axion solution and the generation of axion mass and its effective couplings with photons, fermions and nucleons at the Λ_{QCD} scale. Then, we discuss a particular axion model, SMASH, and apply the coupling formulas that have been built into this model. The second aim of this thesis is to study three direct detection axion processes: inverse Primakoff scattering, Compton-like scattering and axioelectric effect. We have performed the canculation of the cross sections in detail and compared with the results quoted shortly in literature. There are difficulties arising in these calculation due to the involvement of the compound electrons in atom. We have to apply the QFT and the quantum mechanics and make use of the experimental data from measurements of the photon scattering in material. We then investigated the dependence of the cross sections on axion couplings and its mass. We observed that the cross section of these three processes depend strongly on the value of the interaction coupling and the axioelectric effect has the largest contribution for the axion energy in the region $10^{-}1$ to 10 KeV..

Acknowledgements

I would like to express my most sincere and honest gratitude to my supervisor, Dr. Dao Thi Nhung, for offering me an interesting topic in this thesis. She gave me very valuable advice and detailed feedback during my work and it is my honor and fortunate to work with her.

I am grateful to Prof. Tran Thanh Van, the Theoretical Physics group of the Institute For Interdisciplinary Research in Science and Education (IFIRSE) as well as the Interdisciplinary Science and Education (ICISE) for giving me the opportunity to work and support me during my four - month internship.

I also acknowledge Associate Prof. Nguyen Quoc Khanh, Dr. Vu Quang Tuyen, Dr. Vo Quoc Phong, Dr Nguyen Huu Nha, Dr. Phan Hong Khiem, Mr. Dang Ngoc Chau for their enthusiastic lectures at the department of Theoretical Physics, Vietnam National University Ho Chi Minh City - University of Science

I would like to wholeheartedly thank my seniors Phan Anh Vu and Ho Quoc Trung for helping me during my study at the university.

Finally, I want to give my special thank to my parents for their unconditional sacrifice and great love, without them I would never become the person I am today.

Introduction

Particle physics is known as the study of the nature of matter. Several experiments provide some scientific evidences for the existence of some particles which are not in the Standard Model. At the Laboratori Nazionali del Gran Sasso (LNGS), Italy, the XENON1T experiment, utilizing a two-phase liquid xenon time projection chamber, was primarily designed to search for Weakly Interacting Massive Particles (WIMPs). From low-energy electronic recoil data recorded with the XENON1T detector, one observed an excess over known backgrounds at low energies in 2020. The excess can be explained by a hypothetical particle arising from the Peccei-Quinn theory to solve the strong CP problem, axion.

The work of this thesis focuses on understanding the nature of the axion and how it interact with particles in the Standard Model (SM). We aim further to understand how the axion can be detected in experiments like XENON by studying the three main detection processes. We organize the thesis as follows.

In the first chapter, We start with the introduction of the $U(1)_A$ problem and then review the strong CP problem and the axion solution. We then compute the axion mass arising from the light quark masses and its mixing with pion mesons.

In the second chapter, we will answer the questions: *"Does axion interact with elementary particles like photons, quarks, leptons in the standard model?"*, *At what energy levels will the interaction take place?*. I first review the chiral anomaly which is used to compute the axion couplings with gluons and photon. We then discuss the disappearance of the axion-gluon couplings at Λ_{QCD}. The model dependent and independent part of the axion to photon, fermions, nucleons will be discussed in detail. I will briefly introduce the coupling constraint which is derived from astrophysics.

In the final chapter, we will explore axion detection processes and calculate the scattering amplitudes and cross sections of those processes using quantum field theory and quantum mechanics. We numerically evaluate the cross sections and its dependence on axion couplings and mass. We review the usage of these cross sections in explaining the access in the XENON1T at the end of this chapter. We summarize our results in the summary part. In the two appendices we present details of the computation of the amplitude and differential cross section for the Compton-like scattering.

Chapter 1

Axions

Our universe was born 13.7 billions years ago by a huge explosion from which everything was created. From the tiniest particles such as electrons, quark and neutrino...to atoms, molecules to the largest galaxies. However, most of the matter that we can see and measured is only a small fraction of the whole universe. In fact, the larger amount of matter is invisible and undetectable by our instruments.

Elementary particle physics is described by the gauge theory of the standard model including the electromagnetic , weak and strong interactions . But there is still an unresolved problem in the theory that cannot explain why the predicted violation in weak interactions, that is the charge conjugation times parity (CP) symmetry, is not observed in strong interactions. In 1977, Roberto Peccei and Helen Quinn postulated a solution to the strong CP problem. This results in a new particle,Wilczek named this new hypothesized particle the "axion". It is a particle beyond the Standard model. Because of appearance in the theory makes one try to find evidence of its existence.

In chapter 1 of this thesis we will present a general theory of the axion. We will learn about what is the $U(1)_A$ problem (in section. (1.1)) . We then move on to the Strong CP problem and its solution in section. (1.2). Finally we will come to an important result which is the expression for the mass of axion in section. (1.3)

1.1 The $U(1)_A$ Problem

$U(1)_A$ problem arises from giving the mass of pion which is related to the mass of up quark and down quark (u, d). The reason for us to consider only u and d flavors is that their masses are of the same order and much smaller than the Λ_{QCD} scale. It is also possible to consider three light quarks (u,d,s), that would lead to the same conclusion. Now, we consider QCD Lagrangian that describe the interactions between quarks and gluons with two flavors

$$\mathcal{L}_{QCD} = \bar{u}(i\gamma^\mu \mathcal{D}_\mu - m_u)u + \bar{d}(i\gamma^\mu \mathcal{D}_\mu - m_d)d - \frac{1}{4}G^a_{\mu\nu}G_{a,\mu\nu}, \tag{1.1}$$

where, γ^μ are Dirac matrices connecting the spinor representation to the vector representation of the Lorentz group. $G^{\mu\nu}_a$ are the gluon field strength tensors with $a = 1, 2, ..., 8$. $\mathcal{D}_\mu$ represents the covariant derivative and is defined as

$$\mathcal{D}_\mu = \partial_\mu + igT_\alpha G^\alpha_\mu, \tag{1.2}$$

where T^α is generator in the fundamental representation of $SU(3)$ group ($\alpha = 1, 2, ..., 8$). and g is the strong coupling and G^α_μ is the gluon files. The masses of u and d are quarks denoted by m_u and m_d

In Driac representation

$$\psi = \psi_L + \psi_R, \tag{1.3}$$

where

$$\psi_L = \frac{1}{2}(1 - \gamma^5)\psi = P_L\psi \tag{1.4}$$

$$\psi_R = \frac{1}{2}(1 + \gamma^5)\psi = P_R\psi. \tag{1.5}$$

The P_L, P_R operators satisfy the following conditions

$$P_L^2 = P_L, \qquad P_R^2 = P_R, \qquad P_L^2 + P_R^2 = 1, \qquad P_R P_L = P_L P_R = 0. \tag{1.6}$$

We can rewrite the Lagrangian (1.1) as

$$\begin{aligned}\mathcal{L}_{QCD} = -\frac{1}{4}G^a_{\mu\nu}G_{a,\mu\nu} + i\bar{u}_L\not{D}u_L + i\bar{d}_L\not{D}d_L + i\bar{u}_R\not{D}u_R + i\bar{d}_R\not{D}d_R \\ +\bar{u}_L m_u u_R + \bar{d}_L m_d d_R + \bar{u}_R m_u u_L + \bar{d}_r m_d d_L.\end{aligned} \tag{1.7}$$

by defining left-handed quarks q_L and right-handed quarks q_R doublet as

$$q_L = \begin{pmatrix} u_L \\ d_L \end{pmatrix}, \qquad q_R = \begin{pmatrix} u_R \\ d_R \end{pmatrix}, \qquad \bar{q}_L = \begin{pmatrix} \bar{u}_L & \bar{d}_L \end{pmatrix}, \qquad \bar{q}_R = \begin{pmatrix} \bar{u}_R & \bar{d}_R \end{pmatrix}, \tag{1.8}$$

QCD Lagrangian becomes

$$\mathcal{L}_{QCD} = -\frac{1}{4}G^a_{\mu\nu}G_{a,\mu\nu} + i\bar{q}_L\not{D}q_L + i\bar{q}_R\not{D}q_R + \bar{q}_L M q_R + \bar{q}_R M^\dagger q_L, \tag{1.9}$$

where M is mass matrix of quarks

$$M = \begin{pmatrix} m_u & 0 \\ 0 & m_d \end{pmatrix}. \tag{1.10}$$

If the masses of up quark and down quark are zero, QCD Lagrangian will be invariant under four 4 global symmetries $S = SU(2)_L \times SU(2)_R \times U(1)_V \times U(1)_A$ with $U(1)_V, U(1)_A$ symmetries called vector and axial. We can write the transformations of left and right - handed quarks doublet corresponding to $SU(2)_L, SU(2)_R, U(1)_V$ symmetries

$$q_L \longrightarrow q'_L = g_L \begin{pmatrix} u_L \\ d_L \end{pmatrix}, \qquad q_R \longrightarrow q'_R = g_R \begin{pmatrix} u_R \\ d_R \end{pmatrix} \tag{1.11}$$

$$q_L \longrightarrow q'_L = e^{i\theta_V} \begin{pmatrix} u_L \\ d_L \end{pmatrix}, \qquad q_R \longrightarrow q'_R = e^{i\theta_V} \begin{pmatrix} u_R \\ d_R \end{pmatrix}, \tag{1.12}$$

with $g_L \in SU(2)_L$, $g_R \in SU(2)_R$ and $e^{i\theta_V} \in U(1)_V$. Under $U(1)_A$ symmetry the transformation looks pretty interesting

$$q_L \longrightarrow q'_L = e^{i\theta\gamma^5}\begin{pmatrix} u_L \\ d_L \end{pmatrix} = \begin{pmatrix} (1+i\theta\gamma^5)P_L u \\ (1+i\theta\gamma^5)P_L d \end{pmatrix} = e^{-i\theta}\begin{pmatrix} u_L \\ d_L \end{pmatrix}$$
$$q_R \longrightarrow q'_R = e^{i\theta\gamma^5}\begin{pmatrix} u_R \\ d_R \end{pmatrix} = \begin{pmatrix} (1+i\theta\gamma^5)P_R u \\ (1+i\theta\gamma^5)P_R d \end{pmatrix} = e^{i\theta}\begin{pmatrix} u_R \\ d_R \end{pmatrix}. \tag{1.13}$$

From Eqs. (1.11) and (1.13) the mass term of Lagrangian explicitly breaking $SU(2)_L \times SU(2)_R \times U(1)_A$ symmetries while $U(1)_V$ is still perfect symmetry in the presence of quark masses. This $U(1)_V$ symmetry corresponds to the baryon number conservation in the QCD Lagrangian, we however donot concern about that in this sector. In order to have Lagrangian to be invariant under the S symmetry, we pretend for a moment that the masses are not constants but fields. Then we can assign transformation properties to M. Under $SU(2)_L \times SU(2)_R$ and $U(1)_A$, we define the mass matrix transform as

$$M \longrightarrow M' = g_L M g_R^\dagger \tag{1.14}$$
$$M \longrightarrow M' = e^{-i\theta} M e^{-i\theta}. \tag{1.15}$$

Our QCD lagrangian was written in theory electroweak scale. However, at Λ_{QCD} and below this scale experiments show us that the vacuum state of QCD has a non-zero expectation value for the quark billinears (see Ref. [21])

$$\langle 0|\bar{u_L} u_R|0\rangle = \langle 0|\bar{d_L} d_R|0\rangle \neq 0, \tag{1.16}$$

which implies that these condensates spontaneously breaks symmetry. Specifically, $SU(2)_L \times SU(2)_R$ break down to its diagonal $SU(2)_D$ that is the symmetry where the left and the right quark doublets transform in the same matrix as $q_L \to g_D q_L, q_R \to g_D q_R$ with g_D in $SU(2)_D$. This $SU(2)_D$ symmetry associated to the isospin symmetry in nuclear physics. The $U(1)_A$ is also spontaneously broken by these condensates. As with any spontaneous symmetry breaking, there will exist Goldstone bosons: These are called the pions and are expressed in terms of the matrix

$$U = exp\Big(\frac{i}{f_\pi} F^a(x)\sigma_a\Big), \tag{1.17}$$

where $\sigma_{1,2,3}$ are Pauli matrix and σ_0 is identity matrix. The pions are typical referred to $F^3 = \pi^0$ and $F^{1,2} = \pi^{1,2}$ corresponding to breaking of $SU(2)_L \otimes SU(2)_R$. $F^0 = \eta$ is associated with the breaking of $U(1)_A$ and is called η the boson associate with the breaking group. In our cases there are four Goldstone bosons. If quarks are massless these Goldstone bosons would be massless. The spontaneous braking of $SU(2)_L \times SU(2)_R$ to $SU(2)_D$ can be described well by introducing a set of scalar files as in the nonlinear sigma model or the Gell-mann Levy model. We will not go into the detail of these scalar fields. What we focus here are the Goldstone boson and assume that other scalar states having non-zero expectation value with heavy masses are already integrate out. We can write Eqs. (1.17) in matrix form

$$U = \exp\Big(\frac{i}{f_\pi} A\Big), \qquad A = \begin{bmatrix} \eta + \pi^0 & \sqrt{2}\pi^- \\ \sqrt{2}\pi^+ & \eta - \pi^0 \end{bmatrix}, \qquad \pi^\pm = \frac{\pi^1 \pm i\pi^2}{\sqrt{2}}, \tag{1.18}$$

with π^0, π^+, π^- are the physical pion fields. We require that the U matrix transform under $SU(2)_L \times SU(2)_R$ as $e^{i\theta} g_L U g_R^\dagger e^{-i\theta}$. It is easy to see that the term such as $\mathrm{tr}\big(UU^\dagger\big)$ is equal to 1 therefore these pions donot have masses. Because of quark masses explicitly break $SU(2)_L \times SU(2)_R \times U(1)_A$ symmetry, which in turn implies that pions and boson η are not massless Goldstone bosons, but massive pseudo-Goldstone bosons. To derive the mass of the bosons, we will can use Chiral Lagrangian. Note that, this lagrangian is used at energies below Λ_{QCD}

$$\mathcal{L}_{mass} = v_\pi^3 \,\mathrm{tr}\Big(M^\dagger U + M U^\dagger\Big), \tag{1.19}$$

with our requirement for the transformation of U and M matrices we can easily see that the Lagrangian in (1.19) is invariant under $SU(2)_L \times SU(2)_R \times U(1)_A$.

According to Eqs. (1.10), (1.18) and expanding the expression U to the second order, we obtained the mass matrix

$$\mathcal{V} = 2\frac{v_\pi^3}{f_\pi^2}(m_u + m_d)\pi^+\pi^- - \frac{v_\pi^3}{f_\pi^2}\begin{pmatrix}\pi^0 & \eta\end{pmatrix}\begin{pmatrix} m_u + m_d & m_u - m_d \\ m_u - m_d & m_u + m_d\end{pmatrix}\begin{pmatrix}\pi^0 \\ \eta\end{pmatrix}, \tag{1.20}$$

we can choose the matrix $P = \begin{pmatrix} 1 & 1 \\ -1 & 1\end{pmatrix}$ to diagonalize mass matrix in Eqs. (1.20)

$$\begin{pmatrix} m_u + m_d & m_u - m_d \\ m_u - m_d & m_u + m_d\end{pmatrix} \longrightarrow \begin{pmatrix} 2m_d & 0 \\ 0 & 2m_u\end{pmatrix}. \tag{1.21}$$

We see that the mass squared of $\pi^+ = 2\frac{v_\pi^2}{f_\pi^2}(m_u + m_d) = \frac{1}{2}(m_{\pi^0}^2 + m_\eta^2)$. However, in experiment we find that $m_{\pi^0} \approx m_{\pi^+} \approx 140 MeV$ while $m_\eta \approx 960 MeV$. The mass of boson η is far too high compared to that of pions. The absence of a satisfactory candidate for the fourth Goldstone boson is known as the $U(1)_A$ problem Ref.[37].

1.2 Strong CP Problem And Axion

The resolution of the U(1) A problem came through the realization by 't Hooft (Ref.[34]) that the QCD vacuum has a more complicated structure. The complicated QCD vacuum makes the $U(1)_A$ is not a good symmetry of QCD Lagrangian even in the limit of vanishing quark masses. 't Hooft noticed that that if under $U(1)_A$ like transform

$$q_f \longrightarrow e^{i\gamma_5 \alpha/2} q_f, \qquad q_f : \text{are quark fields} \tag{1.22}$$

an anomalous extra term $\mathcal{L}_\theta$ is added to the QCD Lagrangian (Eqs. (1.9)).

$$\mathcal{L}_\theta = \theta_{QCD} \frac{g^2}{32\pi^2} G^{\alpha,\mu\nu} \tilde{G}_\alpha^{\mu\nu}, \tag{1.23}$$

where, g is the strong coupling constant, $G^{\alpha,\mu\nu}$ is the gluons field strength tensor and. Its dual $\tilde{G}_\alpha^{\mu\nu}$ is given by $\frac{1}{2}\epsilon_{\mu\nu\sigma\rho} G_\alpha^{\sigma\rho}$ The term $\mathcal{L}_\theta$ is Lorentz and gauge invariant. So this term should be included in the SM Lagrangian. This term conserves C but violates P and T, and thus it also violates CP. This mean that even at classical

level, the QCD Lagrangian contains $U(1)_A$ symmetry but this symmetry is broken at quantum level. So $U(1)_A$ is also called the anomalous symmetry. The resolution of the $U(1)_A$ problem, however, gives rise to a new problem that the appearance of CP violation in strong interactions. We have no experimental evidences for this.

Now, at electroweak scale, QCD Lagrangian is

$$\mathcal{L}_{QCD} = -\frac{1}{4}G^a_{\mu\nu}G_{a,\mu\nu} + i\bar{q}_L\not{D}q_L + i\bar{q}_R\not{D}q_R + \bar{q}_L M q_R + \bar{q}_R M^\dagger q_L + \mathcal{L}_\theta, \tag{1.24}$$

in general quark mass matrix can be complex. In simple case, we redefined Eqs. (1.10) as

$$M_2 = \begin{pmatrix} m_u e^{i\beta_u} & 0 \\ 0 & m_d e^{i\beta_d} \end{pmatrix}, \tag{1.25}$$

with β is a phase constant. Under $U(1)_A$ transformation for quarks in lagrangian (1.24),

$$u_L = e^{-i\frac{1}{2}\beta_u}u_L, \qquad u_R = e^{i\frac{1}{2}\beta_u}u_R. \tag{1.26}$$

Similarly for d quark. These rotation belong to $U(1)_A$ transformation and it produces the anomalous term

$$\mathcal{L}_{\text{anomolous}} = (\beta_u + \beta_d)\frac{1}{32\pi^2}G^{\alpha,\mu\nu}\tilde{G}^{\sigma\rho}_\alpha = \frac{1}{32\pi^2}arg(Det(M_2))G^{\alpha,\mu\nu}\tilde{G}^{\sigma\rho}_\alpha \tag{1.27}$$

Under $U(1)_A$ transformation, QCD lagrangian become

$$\mathcal{L}'_{QCD} \supset \bar{q}_L M'_2 q_R + \bar{q}_R M_2'^\dagger q_L + \frac{\theta_{QCD} + arg(Det(M_2)}{32\pi^2}G^{\alpha,\mu\nu}\tilde{G}^{\sigma\rho}_\alpha, \tag{1.28}$$

where

$$M_2 = \begin{pmatrix} m_u e^{i2\beta_u} & 0 \\ 0 & m_d e^{i2\beta_d} \end{pmatrix}. \tag{1.29}$$

In general, M_2 is a complex mass matrix of N generations. To go to a physical basis, one must diagonalize this mass matrix and when one does so, in general, one performs $U(1)_A$ transformation that changes θ_{QCD} by $arg(Det(M_2))$. In the SM this mass matrix M is generated from the Yukawa coupling of up-type quarks and down-type quarks. The angle of the determinant of the mass matrix can be written as $arg(Det[Y_u Y_d])$. We however keep it as $arg(Det(M_2))$ to be independent of models . In the full theory, the coefficient of the $\epsilon_{\mu\nu\sigma\rho}G^{\alpha,\mu\nu}G^{\sigma\rho}_\alpha$ term is

$$\bar{\theta} = \theta_{QCD} + arg(Det(M_2)). \tag{1.30}$$

The effective CP-violating parameter (Eq. (1.30)) is a sum of a QCD contribution θ_{QCD} and the electroweak piece $arg(Det(M_2)$ which related to the phase structure of quark matrix. The CP-violating term is not invariant under CP transformations, so it could could give a large effect to the CP-violating observables . We consider an example of such observables, the neutron electric dipole moment. This term also contributes to the neutron electric dipole moment (nEDM) of order Ref. [25]

$$d_n \cong \frac{\bar{\theta}m_q e}{m_N^2}, \qquad m_q = \frac{m_u m_d}{m_u + m_d}, \tag{1.31}$$

where m_N is the neutron mass. Recent experimental bound on the neutron electric dipole moment $|d_n| < 3 \times 10^{-26} e$ cm (Ref. [25]) implied $\bar{\theta} < 1.3 \times 10^{-10}$. This low $\bar{\theta}$ value is unnatural because there seems to be no reason in the SM why $\bar{\theta}$ must be so small. Eqs. (1.30) tell us that either both contributions are really small, or that they cancel each other out themselves, leading to a fine tuning of both parameters. The question of why $\bar{\theta}$ the parameter that emerges from two independent contributions is so small, is known as "**the Strong-CP problem**".

There are three possible "solutions" to the strong CP problem

- An additional chiral symmetry
- Unconventional dynamics
- Spontaneously broken CP

In fact, another possible solution is that one of quark has zero mass then one can rotate it with an arbitrary angle, therefore one can make $\bar{\theta}$ to be zero exactly. However experiments have shown that quarks are massive particles, so this simple solution has been ruled out.

In this thesis, I going to follow the first solution.

Peccei and Quinn (1977) suggested a possible dynamical solution to the strong CP problem. If the mechanism holds in nature then $\bar{\theta}$ actually vanishes, and there is no need to explain a small number like 10^{-10} cropping up in the theory. They postulated that the Lagrangian of the Standard Model was invariant under an additional global $U(1)$ chiral symmetry - $U(1)_{PQ}$ which is spontaneously broken at the energy scale, f_a , resulting in the appearance of a new bosonic field, the $a(x)$ field and its coupling to gluons.

$$\mathcal{L}_a = \chi \frac{a(x)}{f_a} \frac{g^2}{32\pi^2} G^{\alpha,\mu\nu} \tilde{G}_{\alpha,\mu\nu}, \tag{1.32}$$

where χ is a model dependent parameter, and f_a a free parameter that is well known as the Peccei-Quinn scale. The $a(x)$ field is called an axion field which is the massless Nambu-Goldstone boson of the broken $U(1)_{PQ}$ symmetry (Ref.[38]). However, this latter will become a pseudo-goldstone boson at low energy.

After the spontaneous breaking of $U(1)_{PQ}$, this Lagrangian must be augmented by axion interactions:

$$\mathcal{L} = \mathcal{L}_{SM} + \Big(\bar{\theta} + \chi \frac{a(x)}{f_a}\Big) \frac{g^2}{32\pi^2} G^{\alpha,\mu\nu} \tilde{G}_{\alpha,\mu\nu} + \mathcal{L}_{int}[\frac{\partial_\mu a(x)}{f_a}, J^\mu] - \frac{1}{2} \partial_\mu a \partial^\mu a, \tag{1.33}$$

where the third term in Eq. (1.33) indicates the kind of interactions the axion field can participate in with the other fields in the theory and the third term is the kinetic energy term for the axion field. Peccei-Quinn treated $\bar{\theta}$ not as a parameter, but as a dynamical variable and set

$$\bar{\theta}_{eff}(x) = \bar{\theta} + \chi \frac{a(x)}{f_a}, \tag{1.34}$$

which allows different states with a vacuum state at $\bar{\theta}_{eff}(x) = 0$ leaving no strong-CP violation.

$$\langle a \rangle = -\frac{f_a}{\chi} \bar{\theta}. \tag{1.35}$$

We see that axion field can be seem as fluctuation field. We can rewrite Eq. (1.34) as

$$\bar{\theta}_{eff}(x) = \chi \frac{a(x)_{phy}}{f_a}, \qquad a(x)_{phy} = a(x) - \langle a \rangle \,, \tag{1.36}$$

when we redefine Lagrangian in Eq. (1.33)

$$\mathcal{L} = \mathcal{L}_{SM} + \chi \frac{a(x)_{phy}}{f_a} \frac{g^2}{32\pi^2} G^{\alpha,\mu\nu} \tilde{G}_{\alpha,\mu\nu} + \mathcal{L}_{int}[\frac{\partial_\mu a(x)_{phy}}{f_a}, J^\mu] - \frac{1}{2} \partial_\mu a_{phy} \partial^\mu a_{phy} \tag{1.37}$$

It turns out that imposing a $U(1)_{PQ}$ symmetry is equivalent to imposing CP conservation on the QCD Lagrangian. Note that, axion is a pseudo- scalar field so CP-odd. It is lead to the second term in Eq. (1.37) being CP-even. Under $U(1)_{PQ}$ transformation the CP-violating lagrangian $\mathcal{L}_\theta$ become CP conserving. For strong interactions, CP conservation is desirable.

1.3 The Axion mass

In the classical approach developed up to now, the axion emerges as a goldstone boson with zero mass. However, at low energy (Λ_{QCD}), axion will have mass which is model independent. We apply the same method that is used to generate mass for mesons as done in the section (1.1). Now we consider Lagrangian

$$\mathcal{L}_a = \frac{a(x)_{phy}}{f'_a} \frac{g^2}{32\pi^2} G^{\alpha,\mu\nu} \tilde{G}^{\sigma\rho}_{\alpha} + \bar{q}_L M q_R + \bar{q}_R M^\dagger q_L, \qquad f'_a = \frac{f_a}{\chi} \tag{1.38}$$

We can make the first term in Eq (1.38) vanish by an chiral trasformation

$$q \longrightarrow e^{-i\gamma^5 \frac{a}{4f_a} I_{2\times 2}} \begin{pmatrix} u \\ d \end{pmatrix}. \tag{1.39}$$

In order to the mass term in Eqs. (1.38) conserve under transformation above, we can define a chiral transformation for the two-by-two quark matrix

$$M \longrightarrow M' = e^{i\frac{a}{4f_a}} M e^{i\frac{a}{4f_a}}. \tag{1.40}$$

At QCD energy, we have the low energy Lagrangian that we presented in section. (1.1) simply as

$$\mathcal{L}_{mass} = v_\pi^3 \, \mathrm{tr}\Big(M' \Sigma^\dagger + \Sigma M'^\dagger\Big) \tag{1.41}$$

We remind that

$$\Sigma = exp\Big(\frac{i}{f_\pi} B\Big), \qquad B = \sum_{a=1}^{3} F^a(x)\sigma_a = \begin{bmatrix} \pi^0 & \sqrt{2}\pi^- \\ \sqrt{2}\pi^+ & -\pi^0 \end{bmatrix} \tag{1.42}$$

and that v_π in Eq. (2.40) is an energy scale related to chiral condensates. Note that we have considered here only the pi mesons that responsible for the breaking

of $SU(2)_A$ not as in (1.18) where the meson η was included to break $U(1)_A$. The axion here can be made to be like η meson but it is the remnant part of the beaking of the $U(1)_{PQ}$, and it is associated with a PQ scale which is much larger than the pi meson scale. Consequently, we cam expand Eq. (1.41)

$$\begin{aligned}
\mathcal{L}_{mass} &= v_\pi^3 \,\mathrm{tr}\Big(Me^{i\frac{a}{2f_a}I_{2\times2}}e^{-i\frac{B}{f_\pi}} + Me^{-i\frac{a}{2f_a}I_{2\times2}}e^{i\frac{B}{f_\pi}}\Big) \\
&\approx v_\pi^3 \,\mathrm{tr}\bigg(M(2I_{2\times2}) - M(B - \frac{a}{2f_a}I_{2\times2})^2\bigg) \\
&\approx v_\pi^3 2(m_u+m_d) - v_\pi^3 \,\mathrm{tr}\left\{M\begin{bmatrix}\frac{\pi^0}{f_\pi} - \frac{a}{2f_a} & \sqrt{2}\pi^- \\ \sqrt{2}\pi^+ & -\frac{\pi^0}{f_\pi} - \frac{a}{2f_a}\end{bmatrix}^2\right\} \\
&\approx v_\pi^3 2(m_u+m_d) - v_\pi^3 m_u\Big[\Big(\frac{\pi^0}{f_\pi} - \frac{a}{2f_a}\Big)^2 + \frac{2\pi^-\pi^+}{f_\pi^2}\Big] \\
&\qquad\qquad - v_\pi^3 m_d\Big[\Big(\frac{\pi^0}{f_\pi} + \frac{a}{2f_a}\Big)^2 + \frac{2\pi^-\pi^+}{f_\pi^2}\Big] \\
&\supset 2m_u v_\pi^3\Big[1 - \frac{1}{2}\Big(\frac{\pi^0}{f_\pi} - \frac{a}{2f_a}\Big)^2\Big] + 2m_d v_\pi^3\Big[1 - \frac{1}{2}\Big(\frac{\pi^0}{f_\pi} + \frac{a}{2f_a}\Big)^2\Big] \\
&\supset 2m_u v_\pi^3 \cos\left(\frac{\pi^0}{f_\pi} - \frac{a}{2f_a}\right) + 2m_d v_\pi^3 \cos\left(\frac{\pi^0}{f_\pi} + \frac{a}{2f_a}\right),
\end{aligned} \tag{1.43}$$

and making use of some standard trigonometric formulae, we eventually obtain potential formulae

$$\begin{aligned}
\mathcal{V}(a,\pi^0) &= -2v_\pi^3(m_u+m_d)\cos\left(\frac{\pi^0}{f_\pi}\right)\cos\left(\frac{a}{2f_a}\right) + 2v_\pi^3(m_u-m_d)\sin\left(\frac{\pi^0}{f_\pi}\right)\sin\left(\frac{a}{2f_a}\right) \\
&= -2v_\pi^3(m_u+m_d)\cos\left(\frac{a}{2f_a}\right)\Big[\cos\left(\frac{\pi^0}{f_\pi}\right) + \tan(\phi_a)\sin\left(\frac{\pi^0}{f_\pi}\right)\Big] \\
&= -2v_\pi^3(m_u+m_d)\frac{\cos\left(\frac{a}{2f_a}\right)}{\cos(\phi_a)}\cos\left(\frac{\pi^0}{f_\pi} - \phi_a\right),
\end{aligned} \tag{1.44}$$

where the minus sign obviously comes out from the fact that the potential enters the Lagrangian with a change of sign ($\mathcal{L} = \mathcal{T}_{kenic} - \mathcal{V}$) and we defined

$$\tan(\phi_a) = \frac{m_u - m_d}{m_u + m_d}\tan\left(\frac{a}{2f_a}\right) \tag{1.45}$$

From Eq (1.45), we can see that

$$\begin{aligned}
\frac{1}{\cos(\phi_a)} &= \sqrt{1+\tan^2(\phi_a)} \\
&= \frac{1}{\cos\left(\frac{a}{2f_a}\right)}\sqrt{\cos^2(\frac{a}{2f_a}) + \Big(\frac{m_u-m_d}{m_u+m_d}\Big)^2\sin^2(\frac{a}{2f_a})} \\
\Rightarrow \frac{\cos\left(\frac{a}{2f_a}\right)}{\cos(\phi_a)} &= \sqrt{1 - \frac{4m_u m_d}{(m_u+m_d)^2}\sin^2(\frac{a}{2f_a})},
\end{aligned} \tag{1.46}$$

Using the Gell-Mann-Oakes-Renner relation

$$m_\pi^2 = 2\frac{v_\pi^3}{f_\pi^2}(m_u + m_d), \tag{1.47}$$

The potential is

$$\mathcal{V}(a,\pi^0) = -m_\pi^2 f_\pi^2 \sqrt{1 - \frac{4m_u m_d}{(m_u+m_d)^2}\sin^2(\frac{a}{2f_a})}\cos\left(\frac{\pi^0}{f_\pi} - \phi_a\right) \tag{1.48}$$

We can integrate out the pion field by simply noticing that the previous expression can be minimized with respect to pions by choosing $\langle\phi_a\rangle = \frac{\langle\pi_0\rangle}{f_\pi}$. We get the effective potential acting on the axion, derived in Ref. [13],

$$\mathcal{V}(a) = -m_\pi^2 f_\pi^2 \sqrt{1 - \frac{4m_u m_d}{(m_u+m_d)^2}\sin^2(\frac{a}{2f_a})}. \tag{1.49}$$

The effective potential is minimized by $\langle a\rangle = 0$. This is satisfying Eq. (1.36) $\langle a_{phy}\rangle = 0$ when axion is physic state in this case. We can extract the axion mass from the previous formula very easily, by simply expanding the potetial $\mathcal{V}(a)$ up to the quadratic order in a

$$\begin{aligned}
\mathcal{V}(a) &\approx -f_\pi^2 m_\pi^2\Big[1 - \frac{1}{2}\frac{4m_u m_d}{(m_u+m_d)^2}\sin^2(\frac{a}{2f_a})\Big] \\
&\approx -f_\pi^2 m_\pi^2\Big[1 - \frac{1}{2}\frac{4m_u m_d}{(m_u+m_d)^2}\Big(\frac{a}{2f_a} - \frac{1}{6}\frac{a^3}{8f_a} + ...\Big)^2\Big] \\
&\approx f_\pi^2 m_\pi^2 \frac{1}{2}\frac{m_u m_d}{(m_u+m_d)^2}\frac{a^2}{f_a^2} + ...
\end{aligned} \tag{1.50}$$

Eq. (1.50) tell us that the axion mass is only related to that of the neutral pion by means of some QCD parameters

$$m_a^2 = f_\pi^2 m_\pi^2 \frac{m_u m_d}{(m_u+m_d)^2} = \frac{z}{(1+z)^2}\frac{m_\pi^2 f_\pi^2}{f_a^2}, \qquad z = \frac{m_u}{m_d}. \tag{1.51}$$

choosing $z = 0.48$, pion mass $m_\pi = 135$ MeV and pion decay is $f_\pi = 92$ MeV we get

$$m_a = 5.70\mu\text{eV}\frac{10^{12}\text{GeV}}{f_a}, \tag{1.52}$$

where, of course, the dependence on f_a still remains. Based on Eq. (1.52) we have two main axion model branches are

- f_a small $\longrightarrow$ m_a large: Visible axion
- f_a large $\longrightarrow$ m_a small: Invisible axion.

Due to the lack of experimental evidence for the axion with large m_a and large couplings with SM particles, the visible axion model is completely rule out. At the moment only the invisible axion model can survive the experimental data. We concentrate on the invisible axion model in this thesis.

Chapter 2

Interactions of Axions

A variety of experiments to search for evidence of an axion with a large decay constant have been proposed. In order to interpret the results of any of experiments, it is necessary to have a firm theoretical prediction of how the axion couples to particles in the SM. As we have seen in the chapter 1, the Lagrangian of the SM and an axion is an effective theory which results from a high energy theory that respects the global $U(1)_{PQ}$ symmetry. The interactions of axion with other particles in the SM arise from dimension 5 operators and they are suppressed by the large scale f_a at which $U(1)_{PQ}$ symmetry is broken. The second breaking of the SM model local gauge group $SU(2)_L \times U(1)_Y$ at the EW scale gives masses for SM model particles and shapes the strength of EW weak interaction. At this EW scale the axion is still a massless particle. The third stage happens at the Λ_{QCD} scale, where the QCD condensate states form and break the chiral symmetry, $SU(2)_L \times SU(2)_R$, of the QCD Lagrangian with only two lightest quarks. The masses of Goldstone bosons such as axion, pi mesons and their interactions are generated from mass terms of the two light quarks and the QCD decay constants of hardronic states at the QCD scale. There are many possible high energy theories that results different couplings strengths of the axion to SM particles at the first stage. However the second and the third stages are the same for every models. Therefore many of axion couplings contains model independent and model dependent parts. We will understand how the two contributions to the axion couplings arise in this chapter.

This chapter contains three sections. We discuss the generic couplings of axion to the SM particles in section (2.1) with an emphasize on the anomaly in subsection (2.1.1). We then introduce an particular example of a high energy theory, called SMASH, in section (2). Finally we present some experimental bounds on the axion couplings from astrophysics in section (2.3).

2.1 Axion Couplings

2.1.1 The Chiral Anomaly

In the section, we will briefly discuss the fermionic axial current. We assume that there exist fermionic field multiplet ψ, and it has strong and electromagnetic interactions. The fields in this multiplet are massless. The Lagrangian of the multiplet has a chiral symmetry of $SU(n)_A$ where $\psi \to e^{i\gamma_5 \alpha_a \tau^a}\psi$. This symmetry is associated with a general symmetry or τ^a is proportional to identity matrix in the

case of abelian symmetry axial current $J^{5a}_{\mu} = \psi\gamma_{\mu}\gamma_5\tau^a\psi$ where τ^a is generators of an non-abelian global or abelian symmetry. This current is not conserve so it has an anomaly which can be calculate by

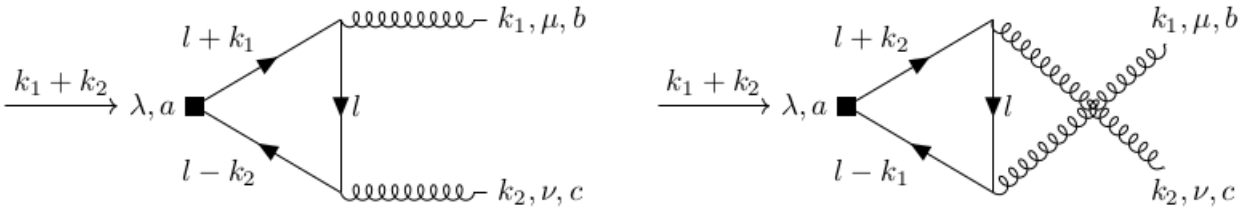

Figure 2.1: Two triangle diagrams contribute to the anomaly of current axial. The two external spring-shaped lines denote the gluon fields.

We consider the evaluation of a peculiar matrix element :

$$\langle k_1 k_2|\partial_\mu J^{5,\lambda}_a|0\rangle \sim \mathcal{M}^{T,\lambda,\mu\nu}_{a,b,c}(k_1+k_2)_\lambda, \tag{2.1}$$

where $\mathcal{M}^{T,\lambda,\mu\nu}_{a,b,c}$ is Fourier transformation of matrix element $\mathcal{M}^{\lambda,\mu\nu}_{a,b,c}$ and can be calculated by

$$\mathcal{M}^{T,\lambda,\mu,\nu}_{a,b,c} = -\int \frac{d^4l}{(2\pi)^4}\mathrm{tr}\Big(\tau^a\gamma^\lambda\gamma^5\frac{i}{\not{l}+\not{k}_1}T^b\gamma^\mu\frac{i}{\not{l}}T^c\gamma^\nu\frac{i}{\not{l}-\not{k}_2} + \tau^a\gamma^\lambda\gamma^5\frac{i}{\not{l}+\not{k}_2}T^c\gamma^\mu\frac{i}{\not{l}}T^b\gamma^\nu\frac{i}{\not{l}-\not{k}_1}\Big), \tag{2.2}$$

where we have assumed fermionic fields in ψ being massless. After several complicated mathematical transformations, , see for example the appendix of [Daniele Lombardi' Thesis]

$$\langle k_1 k_2|\partial_\lambda J^{5,\lambda}|0\rangle = -\frac{g^2}{32\pi^2}d^{abc}\epsilon_{\mu\nu\sigma\rho}\langle k_1 k_2|G^{\mu\nu}_b G^{\sigma\rho}_c|0\rangle\,, \tag{2.3}$$

where $d^{abc} = \mathrm{tr}\Big(\tau^a\big\{T^b, T^c\big\}\Big) = 2\,\mathrm{tr}\big(\tau^a T^b T^c\big)$. T^b is the operator of the respentation of the $SU(3)_C$ to which ψ belongs and $G^{\mu\nu}$ is the gluon field strength tensor. From eq. 2.3 we see that if the chiral symmetry group is SU(N) where $tr[t^a] = 0$ the axial vector current is conserved. However if the chiral symmetry is $U(1)$ then $tr[t^a] \neq 0$ then the axial vector current is not conserved, although the Lagrangian is symmetric under the chiral symmetry. The Eq. (2.3) is known as the Adler-Bell-Jackiv anomaly which was first noticed in Ref. [2]. If we replace gluon external lines by photons then one obtains the same expressions as Eq. (2.3) but the T^b is replaced by the electric charged matrix, and the gluon field strength tensor is replaced by the photon field strength tensor.

We now consider only the U(1) chiral symmetry, in particular the $U(1)_{PQ}$ symmetry and derive the anomaly for the PQ current which will be used in the next section. From now on we will work using the language of Weyl spinor for convenience. The Dirac spinor is just a combination of two Weyl spinors: one left-handed and one-right handed. The right handed can be written in terms of the left-handed spinor by taking the charge conjugation. So it is in principle can work in the theory with

only left-handed Weyl spinor as we will proceed in the rest of this chapter. Because $U(1)_{PQ}$ symmetry is exactly anomalous, divergence of PQ current corresponding to an extra term. We consider Lagangian with two the left-handed component Weys spinor

$$\mathcal{L} = \psi_i i\bar{\sigma}_\mu \partial \psi_i. \tag{2.4}$$

Under $U(1)_{PQ}$ transformation $\psi_i \longrightarrow \exp(i\alpha X_i)\psi_i$ where X_i is PQ charge we get

$$J^\mu_{PQ} = -X_i \psi_i \bar{\sigma}^\mu \psi_i, \tag{2.5}$$

where we can understand that X_i has the same role as τ^a in (2.2). Since in the Eq. (2.3) the axial current got contributions from the left and the right-handed Weyl spinor, we now take only the left-handed one then

$$\begin{aligned}
\partial_\mu J^\mu_{PQ} &= \frac{1}{2}\frac{g^2}{32\pi^2} d^{abc} \epsilon_{\mu\nu\sigma\rho} F^{\mu\nu}_b F^{\sigma\rho}_c \\
&= \frac{g^2}{32\pi^2} d^{abc} F^{b,\mu\nu} \tilde{F}_{c,\mu\nu} \\
&= \mathrm{tr}\Big(X_i T^b T^c\Big) \frac{g^2}{16\pi^2} F^{b,\mu\nu} \tilde{F}_{b,\mu\nu} \\
&= X_i \,\mathrm{tr}\Big(T^b T^c\Big) \frac{g^2}{16\pi^2} F^{b,\mu\nu} \tilde{F}_{c,\mu\nu},
\end{aligned} \tag{2.6}$$

For the case of strong interaction, $F^{\mu\nu}_b$ is gluon field strength tensor and we have n quarks

$$\partial_\mu J^\mu_{PQ} = \sum_{i=1}^{n} X_i T(R) \frac{g^2}{16\pi^2} G^{b,\mu\nu} \tilde{G}_{b,\mu\nu} = N \frac{g^2}{16\pi^2} G^{b,\mu\nu} \tilde{G}_{b,\mu\nu}, \tag{2.7}$$

where $N = \sum_{i=1}^{n} X_i T(R)$ and $T(R)$ is index of $SU(3)_c$ representation.

For the case of electromagnetic interaction, $F^{\mu\nu}_b$ is electromagnetic field strength tensor and we have m charged fermions,

$$\partial_\mu J^\mu_{PQ} = \sum_{i=1}^{n} X_i Q^2 D_f \frac{g^2}{16\pi^2} F^{b,\mu\nu} \tilde{F}_{b,\mu\nu} = E \frac{g^2}{16\pi^2} F^{b,\mu\nu} \tilde{F}_{b,\mu\nu}, \tag{2.8}$$

where $E = \sum_{i=1}^{n} X_i Q^2 D_f$, Q is electric charge and D_f the dimension of the representation, $D_f = 3$ for one quark and $D_f = 1$ for one charged lepton.

As final remark this PQ current anomaly give rise to the effective couplings of the axion to gluons and photons. It will from the model dependent part of these couplings. In the following section we will consider how the further stages of symmetry breaking contribute to the model-independent part of the axion couplings.

2.1.2 Axion- Photon Coupling

We now work in a generic model which have K scalar fields (K is larger than one) which also carry PQ charges. After PQ symmetry breaking there will be only one that becomes axion. The remaining particles are not Goldstone bosons. If

electroweak symmetry is also broken. Some of them can be for example Goldstone bosons eateen by the W and Z bosons. We first write all fermionic fields as left-handed, two-component Weyl spinors ψ_i. Now, the Lagrangian will contain Yukawa couplings

$$\mathcal{L} = \partial_\mu \varphi_n \partial^\mu \varphi^n + \sum_{i=1}^{K} \psi_i i\bar{\sigma}^\mu \partial \psi_j + \lambda_{n,i,j} \psi_i \varphi_n \psi_i + \kappa_{n,i,j} \psi_i \varphi_n^\dagger \psi_j + h.c, \tag{2.9}$$

where φ^n denotes complex scalar field. We can assume that each ψ_i, φ_n have PQ charge X_i, Z_n. The Lagrangian must must be invariant under the $U(1)_{PQ}$ transformation

$$\begin{aligned} \psi_i &\longrightarrow \exp(i\alpha X_i)\psi_i \\ \varphi_n &\longrightarrow \exp(i\alpha Z_n)\varphi_n, \end{aligned} \tag{2.10}$$

requiring $Z_n + X_j + X_i = 0$ for term $\lambda_{n,i,j}$ and $-Z_n + X_j + X_i = 0$ for $\kappa_{n,i,j}$ term. Note that the two terms can not exists simultaneously if we require non vanishing Z_n. The PQ current corresponding to this symmetry is

$$J^{PQ} = \sum_n (iZ_n \varphi_n \partial_\mu \varphi_n^* - iZ_n \varphi_n^* \partial_\mu \varphi_n) - \sum_{i=1}^{n} X_i \psi_i \bar{\sigma}^\mu \psi_i. \tag{2.11}$$

Using linear sigma model for φ_n, after the spontaneous breaking of PQ symmetry we give

$$\varphi_n = \frac{1}{\sqrt{2}}(V_n + \rho(x)_n) \exp\left(i\frac{\epsilon(x)_n}{V_n}\right) \tag{2.12}$$

where V_n, is the vacuum expectation value of φ_n, and $\rho(x)$ and $\epsilon(x)$ are fields. The mass of ρ is of order $\sqrt{\lambda}V_n$, where λ is some coupling in the Higgs potential; Its mass will be large. The $\rho(x)$ fields will be ignored (We will see this more clearly in the next section, when we consider a particular model). We obtain

$$\varphi \approx \frac{1}{\sqrt{2}}(V_n + i\frac{\epsilon(x)_n}{V_n}) \tag{2.13}$$

The PQ current becomes

$$J^{PQ} = \sum_n Z_n V_n \partial_\mu \epsilon(x)_n + \sum_i (X_i)\bar{\psi}_i \bar{\sigma}^\mu \psi_i \tag{2.14}$$

Here we give an important definition of the axion: the axion field is the sum of the goldstone boson fields $\epsilon(x)$

$$a = \sum_n f_a^{-1} Z_n V_n \epsilon_n(x), \qquad f_a = \sqrt{\sum_n V_n^2 Z_n^2}. \tag{2.15}$$

Note that this choice is unique. We can see that, under PQ transformation (2.10)

$$\varphi_n' = \frac{1}{\sqrt{2}}(V_n + \rho(x)_n) \exp\left(i\frac{\epsilon(x)_n + \alpha V_n Z_n}{V_n}\right). \tag{2.16}$$

Goldstone boson transform as

$$\epsilon(x) \longrightarrow \epsilon(x)_n + \alpha V_n Z_n. \tag{2.17}$$

Substituting Eq.(2.17) into Eq. (2.15), one gets

$$a \longrightarrow a + f_a \alpha. \tag{2.18}$$

This is the transformation of axion under $U(1)_{PQ}$. The Eq. (2.18) means that axion is a field but it shifts a contant under the $U(1)_{PQ}$, one then can treated it as a phase of the U(1) transformation. Thanks to this shift symmetry, the θ_{QCD} parameter in the QCD Lagrangian can be rotated away by a proper shift of the axion. Combining Eqs. (2.13), (2.14) and (2.11) we get

$$J_\mu^{PQ} = f_a \partial_\mu a + \sum_i (X_i) \bar{\psi}_i \bar{\sigma}_\mu \psi_i \tag{2.19}$$

Now, we consider the 4-divergence of PQ the current. Because the first term of (2.19) is the current of complex field. It is a conserved current. Thus, divergence of this current is zero. The second term is the fermionic current under PQ transformation (a kind of chiral transformation) and this is not conserved current. We have a anomaly that appears due to the triangle-loop contribution

$$\partial_\mu J_{PQ}^\mu = N \frac{e^2}{16\pi^2} G^{b,\mu\nu} \tilde{G}_{b,\mu\nu} + E \frac{e^2}{16\pi^2} F^{b,\mu\nu} \tilde{F}_{b,\mu\nu}. \tag{2.20}$$

A interesting idea comes from Noether's theorem: the Goldstone boson can be is coupled to its symmetry current and the current is anomalous (see Ref. [27]). We can get lagrangian for interaction of axion - gluon and axion - photon

$$\mathcal{L} = \frac{a}{f_a} \partial_\mu J_{PQ}^\mu = N \frac{a}{f_a} \frac{e^2}{16\pi^2} G^{b,\mu\nu} \tilde{G}_{b,\mu\nu} + E \frac{a}{f_a} \frac{e^2}{16\pi^2} F^{b,\mu\nu} \tilde{F}_{b,\mu\nu} \tag{2.21}$$

Usually one will normalize $f_a \longrightarrow f_a' = \frac{f_a}{N}$ when the term axion-photon

$$\mathcal{L} = \frac{E}{N} \frac{a}{f_a'} \frac{e^2}{16\pi^2} F^{b,\mu\nu} \tilde{F}_{b,\mu\nu} = \frac{1}{2} g_{a\gamma\gamma}^0 a F^{b,\mu\nu} \tilde{F}_{b,\mu\nu} \tag{2.22}$$

with axion-photon coupling

$$g_{a\gamma\gamma}^0 = \frac{\alpha}{2\pi f_a'} \frac{E}{N}. \tag{2.23}$$

Here I would like to note that, for some papers Ref. [27], [33] interaction lagrangian of axion and photon is written as (2.22) some others [8], [20] is

$$\mathcal{L} = \frac{E}{N} \frac{a}{f_a'} \frac{e^2}{32\pi^2} F^{b,\mu\nu} \tilde{F}_{b,\mu\nu} = \frac{1}{4} g_{a\gamma\gamma}^0 a F^{b,\mu\nu} \tilde{F}_{b,\mu\nu}, \tag{2.24}$$

however the expression fo gluon and axion interaction is not change. Below QCD, scale, the quark condensate states form and break $SU(2)_L \times SU(2)_R$ symmetry

down to $SU(2)_D$. If we require that this breaking removes completely the axion-gluon coupling then the (2.15) must contain additional terms coming from the axial current of the u and d quarks. In particular

$$J^a_\mu = J^{PQ}_\mu - \frac{N}{1+z+w}(\bar{u}\gamma^\mu\gamma_5 u + z\bar{d}\gamma^\mu\gamma_5 d), \tag{2.25}$$

divergence of axion current is

$$\partial^\mu J^a_\mu = \frac{Ne^2}{16\pi^2}F^{b,\mu\nu}\tilde{F}_{b,\mu\nu}\Big[\frac{E}{N} - \frac{2}{3}\frac{4+z}{1+z}\Big] + ..., \tag{2.26}$$

where we can use (2.3) with $F^{\mu\nu,c}$ is electromagnetic field and we have anomalies of u, d, s current are

$$\begin{aligned}\partial_\mu(\bar{u}\gamma^\mu\gamma_5 u) &= Q_u^2 D(3)\frac{g^2}{8\pi^2}F^{b,\mu\nu}\tilde{F}_{b,\mu\nu} \\ &= \frac{4}{9}3\frac{g^2}{8\pi^2}F^{b,\mu\nu}\tilde{F}_{b,\mu\nu} \\ &= 2\frac{4}{3}\frac{g^2}{16\pi^2}F^{b,\mu\nu}\tilde{F}_{b,\mu\nu} \qquad (2.27)\\ \partial_\mu(\bar{d}\gamma^\mu\gamma_5 d) &= \frac{1}{9}3\frac{g^2}{8\pi^2}F^{b,\mu\nu}\tilde{F}_{b,\mu\nu} \\ &= 2\frac{1}{3}\frac{g^2}{16\pi^2}F^{b,\mu\nu}\tilde{F}_{b,\mu\nu} \qquad (2.28)\end{aligned}$$

We can get interaction lagrangian of axion and photon below QCD scale energy scale is

$$\begin{aligned}\mathcal{L} &= \Big[\frac{E}{N} - \frac{2}{3}\frac{4+z}{1+z}\Big]\frac{E}{N}\frac{a}{f'_a}\frac{e^2}{16\pi^2}F^{b,\mu\nu}\tilde{F}_{b,\mu\nu} \\ &= \frac{1}{2}g_{a\gamma\gamma}aF^{b,\mu\nu}\tilde{F}_{b,\mu\nu}, \end{aligned}\tag{2.29}$$

with coupling axion-photon is corrected

$$\begin{aligned}g_{a\gamma\gamma} &= \frac{\alpha}{2\pi f'_a}\Big[\frac{E}{N} - \frac{2}{3}\frac{4+z}{1+z}\Big], \qquad z = \frac{m_u}{m_d} \approx 0.586 \\ &= \frac{\alpha}{2\pi f'_a}\Big[\frac{E}{N} - 1.92\Big]. \end{aligned}\tag{2.30}$$

We see that he term 1.92 is model independent contribution and the term E/N is the model dependent contribution.

2.1.3 Axion- Fermion Couplings

At electroweak energy scale axion can interact with fermions as in Eq. (2.9). After the spontaneous symmetry $SU(2)_L \times U(1)_Y$ breaking, scalar complex field φ_n can also create Goldstone boson. Care must be taken to define the axion so that it does not mix with the Goldstone boson y that becomes the longitudinal Z^0. That Goldstone boson can be defined as

$$\begin{aligned}y &= f^{-1}\sum_n Y_n V_n \epsilon_n(x) \\ f^2 &= \sum_n Y_n^2 V_n^2, \end{aligned}\tag{2.31}$$

where the Y_n are the hypercharges of the φ_n. So now the axion must be shifted so that it doesnot mix with y, in particular

$$a' = a - (f_a f)^{-1}(\sum_n Z_n Y_n V_n^2)y. \tag{2.32}$$

Note that we can see n Goldstone boson as n basic vector and $\epsilon_n^2 = 1$, then

$$\begin{aligned} ay &= (f_a f)^{-1} \sum_n Z_n Y_n V_n^2 \\ y^2 &= f^{-2}(\sum_n Y_n V_n)^2 = 1 \\ a'y &= ay - (f_a f)^{-1} \sum_n Z_n Y_n V_n^2 y^2 \\ &= 0. \end{aligned} \tag{2.33}$$

We have shown that axion a' does not overlap with the y field. Substituting Eq. (2.15) in to Eq. (2.32) we obtain

$$\begin{aligned} a' &= f_a^{-1} \sum_n (Z_n - f^{-1} Y_n (\sum_m Z_m Y_m V_m^2)) V_n \epsilon_n \\ &= f_a^{-1} \sum_n Z'_n V_n \epsilon_n, \end{aligned} \tag{2.34}$$

where PQ charge of φ_n changed

$$Z'_n = Z_n - f^{-2} Y_n \sum_m Z_m Y_m V_m^2. \tag{2.35}$$

The change in PQ charge of φ leads a change in PQ charge (X_i) of fermion in order to preserve the properties of the divergence of the axion current.

Now, if fermion is electron has $Y_e = -1$ and we consider the second term in Eq. (2.9) (assume that $X'_{i,e} = X'_{j,e}$) we obtain

$$\begin{aligned} Z'_n = -2X'_{i,e} \Rightarrow X'_{i,e} &= -\frac{1}{2}(Z_n + f^{-2} \sum_m Z_m Y_m V_m^2) \\ &= -\frac{1}{2}(-2X_{i,e} + f^{-2} \sum_m Z_m Y_m V_m^2) \\ &= X_{i,e} - \frac{1}{2} \sum_m f^{-2} Z_m Y_m V_m^2 \end{aligned} \tag{2.36}$$

Using this procedure we can derive a new PQ charge for any charged lepton or quark.

We consider Eq. (2.19) in the case four component

$$J_\mu^{PQ} = f_a \partial_\mu a + \sum_i X'_i \bar{\psi}_i \gamma_\mu \gamma_5 \psi_i \tag{2.37}$$

$$\begin{aligned} \partial^\mu J_\mu^{PQ} &= f_a \partial^\mu \partial_\mu a + \sum_i X'_i \partial_\mu (\bar{\psi}_i \gamma_\mu \gamma_5 \psi_i) \\ &= f_a \partial^\mu \partial_\mu a + \sum_i 2X'_i m_i \bar{\psi}_i i\gamma_5 \psi_i + ..., \end{aligned} \tag{2.38}$$

Hence an effective Lagrangian for axions and fermion contains the interaction term

$$\mathcal{L}_{\text{axion-fermion}} = \frac{2m_i X_i'}{f_a} a\bar{\psi}_i i\gamma_5\psi_i, \tag{2.39}$$

from which we can define axion-fermion coupling

$$g_{a,f} = \frac{2m_f X_i}{f_a}, \qquad m_f \text{ is mass of fermion} \tag{2.40}$$

It should be noted that we still have anomalies term in Eq. (2.38). They gave rise to the axion-gluon and axion-photon interactions which we discussed.

In the KSVZ axion model, no ordinary quarks, leptons, or Higgs fields carry PQ charge, $X_i' = 0 \longrightarrow g_{a,f} = 0$ at tree level however they can be induced by radiation can exist Ref. [33]

In the DFSZ model $X_f' = \cos(\beta)/N_f$ where $\tan(\beta) = \frac{v_u}{v_d}$ (see Ref.) and N_f the number of families.

2.1.4 Axion-nucleon coupling

The interaction between the axion and the nucleon occurs only at low energies. The cause may be due to mixing with pion. From Eq. (2.25) we rewrite axion current after after the spontaneous symmetry $SU(2)_L \times U(1)_Y$ breaking

$$J_\mu^{a'} = J_\mu^{PQ'} - \frac{N}{1+z}(\bar{u}\gamma^\mu\gamma_5 u + z\bar{d}\gamma^\mu\gamma_5 d), \tag{2.41}$$

where we have

$$J_\mu^{PQ'} = f_a\partial_\mu a + X_u'\bar{u}\gamma_\mu\gamma_5 u + X_d'\bar{d}\gamma_\mu\gamma_5 d + ... \tag{2.42}$$

$$J_\mu^0 = \frac{1}{2}\bar{u}\gamma_\mu\gamma_5 u + \frac{1}{2}\bar{d}\gamma_\mu\gamma_5 d \tag{2.43}$$

$$J_\mu^3 = \frac{1}{2}\bar{u}\gamma_\mu\gamma_5 u - \frac{1}{2}\bar{d}\gamma_\mu\gamma_5 d, \tag{2.44}$$

Here we focus on only the u and d quark. Eq . (2.41) can be expressed in term of J_μ^0, J_μ^3 as

$$\begin{aligned} J_\mu^{a'} &= f_a\partial_\mu a' + X_u'(J_\mu^0 + J_\mu^3) + X_u'(J_\mu^0 - J_\mu^3) \\ &\quad - \frac{N}{1+z}(J_\mu^0 + J_\mu^3 + z(J_\mu^0 - J_\mu^3)) + ..., \\ &= (X_u' + X_d' - N)J_\mu^0 + (X_u' - X_d' - \frac{(1-z)N}{1+z})J_\mu^3 + ... \end{aligned} \tag{2.45}$$

At low energy u and d quark combine to create proton and neutron. J_μ^0,J_μ^3 can be understood as neutron current. The Goldberger-Treiman relation may be used to translate the coefficients of J_μ^0 and J_μ^3 into the couplings in an effective lagrangian.

$$\left\langle N(p1)\middle|J_\mu^0\middle|N(p2)\right\rangle = \bar{u}_N(p_1)\gamma_5 u_N(p_2)\tau^0(F_{A0})M_N \tag{2.46}$$

$$\left\langle N(p1)\middle|J_\mu^3\middle|N(p2)\right\rangle = \bar{u}_N(p_1)\gamma_5 u_N(p_2)\tau^3(F_{A3})M_N, \tag{2.47}$$

where $u_N(p_1), u_N(p_2)$ are understood as nucleon isospinors, τ^0, τ^3 are the Pauli isospin matrix, M_N is mass of nucleon. $F_{A3} = g_A$ is measured to be 1.27 and $F_{A0} = g_0^{ud} = 0.52$ see [20]. For axion current we have

$$\left\langle N(p1)\right|\frac{J_\mu^{a'}}{f_a}\left|N(p2)\right\rangle = \bar{u}_N(p_1)(g^0\tau^0 + g^3\tau^3)i\gamma_5 u_N(p_2), \tag{2.48}$$

where

$$g^0 = (X'_u + X'_d - N)M_N F_{A0} \tag{2.49}$$

$$g^3 = (X'_u - X'_d - \frac{1-z}{1+z}N)M_N F_{A3} \tag{2.50}$$

We define a doublet of pronton P and neutron N

$$\psi = \begin{pmatrix} P \\ N \end{pmatrix} \tag{2.51}$$

The effective Lagrangian is

$$\mathcal{L} = \bar{\psi}(g^0\tau^0 + g^3\tau^3)i\gamma_5\psi a, \tag{2.52}$$

and axion-proton coupling

$$C_{a,p} = g^0 + g^3, \tag{2.53}$$

axion-neutron coupling

$$C_{a,p} = g^0 - g^3. \tag{2.54}$$

2.2 SMASH model

In this section I will will discuss an example of high energy theory : Standard Model - Axion - Seesaw - Higgs portal inflation (SMASH) model first proposed in [14]. This model can solve five fundamental problems of particle physics and cosmology:

- the strong CP problem,
- the origin of neutrino masses and their flavour mixing,
- the nature of the inflaton,
- the generation of the matter-antimatter asymmetry in the Universe, and
- the identity of dark matter.

We will not going to discuss how this model can solve the all the problems, but we will just focus on the strong CP problem in this section. SMASH is extended from SM by adding:

- A new complex singlet σ in scalar sector
- Three SM-singlet neutrinos N_i with $i = 1, 2, 3$
- A new quark Q in the fundamental of $SU(3)_c$ ($\tilde{Q}$ in anti fundamental of $SU(3)_c$). It has hypercharge $-1/3$ ($1/3$ for $\tilde{Q}$) under $U(1)_Y$.

The most general Yukawa couplings invariant under $U(1)_{PQ}$ symmetry using the two-component Weyl spinor language

$$\begin{aligned}\mathcal{L} \supset\ & Y^u_{i,j} q_i \epsilon H u_i + Y^d_{,i,j} q_i H^\dagger d_j + G_{i,j} L_i H^\dagger N_j + F_{ij} L_i \epsilon H N_j \\ & + \frac{1}{2} Y_{ij} N_i \sigma N_j + y \tilde{Q} \sigma Q + y_{Q,di} Q \sigma d_i + h.c,\end{aligned} \tag{2.55}$$

where $u_i = u_R$, $d_i = d_R$ and

$$\epsilon = \begin{pmatrix} 0 & 1 \\ -1 & 0 \end{pmatrix}, \qquad L_i = \begin{pmatrix} \bar{\nu}_L & \bar{e}_L \end{pmatrix}, \qquad q_i = \begin{pmatrix} \bar{u}_L & \bar{d}_L \end{pmatrix}, \qquad H = \begin{pmatrix} \phi'(x) \\ \phi(x) \end{pmatrix} \tag{2.56}$$

and $Y^u_{ij}, Y^d_{ij}, Gij, F_{ij}, Y_{ij}, y$ and y_{Q,d_i} are YuKawa coupling. SMASH is built on a simpler axion model: KSVZ which only includes $y\tilde{Q}\sigma Q + h.c$ term. Thus, only $Q, \tilde{Q}$ and σ have PQ charge. However, in SMASH Q and σ are combined with d and N_i. This leads to our system have PQ charge

q	u	d	L	N	E	Q	$\tilde{Q}$	σ
1/2	-1/2	-1/2	1/2	-1/2	-1/2	-1/2	-1/2	1

Table 2.1: PQ charge assignment for fields in SMASH. The remaining fields do not carry PQ charge.

In Eq. (2.55) we have two scalar fields in our scalar potential of system. In general, the Higgs scalar Lagrangian is

$$L_H = (D_\mu H)^\dagger (D^\mu H) + (D_\mu \sigma)^\dagger (D^\mu \sigma) + V(H, \sigma) \tag{2.57}$$

with

$$\begin{aligned}V(H,\sigma) = & -\frac{1}{2}[m^2_{11}(H^\dagger H) + m^2_{22}(\sigma^\dagger \sigma)] \\ & + \frac{\lambda_1}{2}(H^\dagger H)^2 + \frac{\lambda_2}{2}(\sigma^\dagger \sigma)^2 \\ & + \frac{\lambda_3}{2}(H^\dagger H)(\sigma^\dagger \sigma),\end{aligned} \tag{2.58}$$

where $m^2_{11}, m^2_{22}, \lambda_1, \lambda_2$ and λ_3 are real parameters.

The conditions for extreme of the scalar potential

$$\begin{cases} \frac{\partial V(H,\sigma)}{\partial |H|} = -m^2_{11}|H| + 2\lambda_1 |H|^3 + \lambda_3 |H||\sigma|^2 = 0 \\ \frac{\partial V(H,\sigma)}{\partial |\sigma|} = -m^2_{22}|\sigma| + 2\lambda_2 |\sigma|^3 + \lambda_3 |H|^2 |\sigma| = 0 \end{cases}$$
$$\Rightarrow \begin{cases} 2\lambda_1 |H|^2 + \lambda_3 |\sigma|^2 = m^2_{11} \\ 2\lambda_2 |\sigma|^2 + \lambda_3 |H|^2 = m^2_{22} \end{cases} \tag{2.59}$$

At the minimum of the scalar potential, the scalar fields have vacuum expectation values

$$|H|^2 = \frac{v^2}{2}, \qquad |\sigma|^2 = \frac{v^2_\sigma}{2}, \tag{2.60}$$

Eq. (2.60) become

$$\begin{cases} 2\lambda_1 \frac{v^2}{2} + \lambda_3 \frac{v_\sigma^2}{2} = m_{11}^2 \\ 2\lambda_2 \frac{v_\sigma^2}{2} + \lambda_3 \frac{v^2}{2} = m_{22}^2 \end{cases} \tag{2.61}$$

If we set $\lambda_1 = 2\lambda_H, \lambda_2 = 2\lambda_\sigma$, $\lambda_3 = 4\lambda_{H\sigma}$, Eq. (2.58) gives us the same as results Ref. [8]

$$V(H,\sigma) = \lambda_H\Big(|H|^2 - \frac{v^2}{2}\Big)^2 + \lambda_\sigma\Big(|\sigma|^2 - \frac{v_\sigma^2}{2}\Big)^2 + 2\lambda_{H\sigma}\Big(|H|^2 - \frac{v^2}{2}\Big)\Big(|\sigma|^2 - \frac{v_\sigma^2}{2}\Big), \tag{2.62}$$

where, in SMASH $v = 246$GeV and v_σ corresponds to a much higher scale $v_\sigma \sim 10^{11}$ GeV. λ_σ is the quartic self-coupling of the new scalar. λ_H is the Higgs quartic coupling. In order to the potential is bounded from below one requires that $\lambda_H, \lambda_\sigma > 0$ and $\lambda_{H\sigma}^2 < \lambda_h \lambda_\sigma$. The scalar ρ can be defined as a fluctuation around the VEV v_σ :

$$\sigma = \frac{1}{\sqrt{2}}[v_\sigma + \rho(x)]e^{\frac{iA(x)}{v_\sigma}} \approx \frac{1}{\sqrt{2}}[v_\sigma + \rho(x) + iA(x)] \tag{2.63}$$

and Higg field

$$H = \begin{pmatrix} \phi' \\ \frac{1}{\sqrt{2}}[v + h(x) + iG(x)] \end{pmatrix}, \tag{2.64}$$

where $A(x), G(x)$ are Goldstone bosons and $\rho(x)$ and $h(x)$ are mass fields. We can obtain their mass matrix by combining Eqs. (2.64), (2.63) and (2.62)

$$\begin{aligned} V(H,\sigma) &\supset \lambda_H v^2 h^2(x) + \lambda_\sigma v_\sigma^2 \rho^2(x) + 2v_\sigma v \lambda_{H,\sigma} \rho(x) h(x) \\ &\subset \begin{pmatrix} \rho & h \end{pmatrix} \begin{pmatrix} \lambda_\sigma v_\sigma^2 & v_\sigma v \lambda_{H,\sigma} \\ v_\sigma v \lambda_{H,\sigma} & \lambda_H v^2 \end{pmatrix} \begin{pmatrix} \rho \\ h \end{pmatrix} \end{aligned} \tag{2.65}$$

Diagonalizable the above matrix we get the eigenvalue corresponding to ρ

$$\begin{aligned} K &= \frac{\lambda_\sigma v_\sigma^2 + \lambda_H v^2}{2} + \frac{1}{2}\sqrt{(\lambda_\sigma v_\sigma^2 + \lambda_H v^2)^2 - 4v^2 v_\sigma^2 (\lambda_H \lambda_\sigma - \lambda_{H\sigma}^2)} \\ &\approx \lambda_\sigma v_\sigma^2 + \mathcal{O}(\frac{v}{v_\sigma}), \end{aligned} \tag{2.66}$$

thus the mass of ρ is

$$m_\rho^2 = 2\lambda_\sigma v_\sigma^2 + \mathcal{O}(\frac{v}{v_\sigma}). \tag{2.67}$$

We can also easily obtain the mass of the new quark by substituting Eq. (2.63) into term $y\tilde{Q}\sigma Q$ we obtain

$$m_Q = \frac{y}{\sqrt{2}} v_\sigma + \mathcal{O}(\frac{v}{v_\sigma}), \tag{2.68}$$

and mass of Neutrino (by seesaw mechanism see [8])

$$M_{ij} = \frac{Y_{ij}}{\sqrt{2}} v_\sigma + \mathcal{O}(\frac{v}{v_\sigma}). \tag{2.69}$$

Because v_σ is so large and λ_σ, y and Y_{ij} are sizeable, all these masses will be large. We can integrate out these heavy particles at around the electroweak scale energy scale or below. Note that $A(x)$ is a Goldstone boson of scalar complex field which carries PQ charge. From Eq. (2.15) we can conclude that $A(x)$ is axion with axion decay constant $v_\sigma = f_A$. At energies Λ_{QCD}, but below electroweak symmetry breaking scale v, the low-energy effective Lagrangian of the field (see Eq. (2.64))

$$\mathcal{L} = \frac{A(x)}{f_a}\frac{g^2}{32\pi^2}G^{\alpha,\mu\nu}\tilde{G}_{\alpha\mu\nu} - \frac{1}{4}g^0_{a\gamma\gamma}A(x)F^{\alpha,\mu\nu}\tilde{F}_{\alpha\mu\nu} - \frac{1}{2}\partial_\mu A\partial^\mu A + \frac{1}{4}\frac{\partial_\mu A}{f_a}\bar{\nu}i\gamma^\mu\gamma^5\nu. \tag{2.70}$$

Where we can compute coupling of axion and photon by

$$\begin{aligned} N &= \sum_{j=1}^{n} X_j T(R) = -\frac{1}{2}\frac{1}{2} - \frac{1}{2}\frac{1}{2} = \frac{1}{2}, \\ E &= \sum_{j=1}^{n} X_j Q^2 D_f = -2\frac{1}{2}(\frac{1}{3})^2 3 = -\frac{1}{3}, \\ g^0_{a\gamma\gamma} &= \frac{\alpha}{2\pi f'_a}\frac{E}{N} = \frac{\alpha}{2\pi f'_a}\frac{2}{3}. \end{aligned} \tag{2.71}$$

Note that Eq. (2.71) we only the use PQ charge of new quark Q. Because just new quark interacts with axion via term $y\tilde{Q}\sigma Q$ and this quark can interact with itself to create photon. The final term of Lagrangian (2.70) is interaction of axion with neutrino. The reason for that is because axion can interact with N_i neutrino ($\frac{1}{2}Y_{ij}\sigma N_i N_j$), and this neutrino can product ν neutrino via higgs ($G_{i,j}L_i H^\dagger N_j$). This interaction is represented by a triangle-loop like axion with photon. Similarly we can also see that the SMASH axion has no tree-level interactions with SM quarks and charged leptons but loop level

At energies below Λ_{QCD}, free quarks do not exist due to confinement. Chiral theory give us a effective potential to create mass for axion. At this scale axion do not interact with gluon but mixing with π_0. This mixing can lead to an effective coupling of axion with nucleons

$$\mathcal{L} = V(a) - \frac{1}{4}g_{a\gamma\gamma}A(x)F^{\alpha,\mu\nu}\tilde{F}^{\sigma\rho}_{\alpha} - \frac{1}{2}\partial_\mu A\partial^\mu A + \frac{1}{4}\frac{\partial_\mu A}{f_a}\bar{\nu}i\gamma^\mu\gamma^5\nu + \frac{1}{2}\bar{\psi}_N\gamma^\mu\gamma_5\psi_N C_{AN}, \tag{2.72}$$

where $\psi_N = p, n$ and nucleon-axion coupling calculated by (2.53) and (2.54) ($z = 0.48$ and $X'_u = X'_d = 0$)

$$C_{Ap} = -0.47, \tag{2.73}$$

and

$$C_{An} = -0.037. \tag{2.74}$$

Axion-photon coupling is

$$g_{a\gamma\gamma} = \frac{\alpha}{2\pi f'_a}\Big[\frac{2}{3} - 1.92\Big]. \tag{2.75}$$

2.3 Astrophysical Axion Bounds

In experiment, the two important relevant couplings are the axion-photon and axion-electron couplings. They are considered as a free parameters independent of the axion models. The most stringent bounds on the interaction of the axion with have been obtained from astrophysical and cosmological data. The astrophysics provides a natural laboratory for the elementary particle physics. Especially for axions, the low energy environment available in stars are well suited for very sensitive tests.

The sun can be seen as an abundant source of axion production due to photon in the interior converting into axion via Primakoff process. From the standard solar model, the solar axion luminosity is (see Ref. [28])

$$L_{axion} = g_{10}^2 \times 1.85 \times 10^{-3} \times L_{\odot}, \tag{2.76}$$

where $L_{\odot} = 3.90 \times 10^{25} W$ is the solar luminosity and $g_{10} = g_{a\gamma\gamma}/(10^{-10} GeV^{-1})$. Because the sun is in the middle of burning hydrogen phase. The solar axion luminosity should not exceed its photon luminosity $L_{axion} < L_{\odot}$ and that constrains

$$g_{a\gamma\gamma} < 3 \times 10^{-9} GeV^{-1} \tag{2.77}$$

However, according to Ref. [28] if $g_{a\gamma\gamma} = 2 - 5 \times 10^{-6} GeV^{-1}$ the Sun could live only for 1000 years. That said, we need to introduce a stricter constraint. Helioseismology study of the structure and dynamics of the Sun through its oscillations and derive new limits (Ref. [28], [31])

$$g_{a\gamma\gamma} < 1 \times 10^{-9} GeV^{-1}. \tag{2.78}$$

More stringent constrains have been obtained by other experiments. For example, the measured neutrino fluxes (Ref. [28] [31]), provide more a conservative limit

$$g_{a\gamma\gamma} < 5 \times 10^{-10} GeV^{-1}, \tag{2.79}$$

corresponding to $L_{axion} < 0.04 L_{\odot}$. The CERN Axion Solar Telescope (CAST) experiment constrains light axion with (Ref.[39])

$$g_{a\gamma\gamma} < 1.16 \times 10^{-10} GeV^{-1} \qquad m_a = 0.02 eV. \tag{2.80}$$

Axion limit from Globular-Cluster Stars

Another restrictive limit $g_{a\gamma\gamma}$ is gave from globular-cluster stars, that is quite close to CAST constrains, but applies for higher masses. We can define a globular cluster to be a system of stars bound together by gravity. Those are formed at the same time and thus differ primarily in their mass. One can identify star state of evolution and estimate the accelerated consumption of helium due to axion production that is related with the axion coupling by use a color-magnitude diagram.

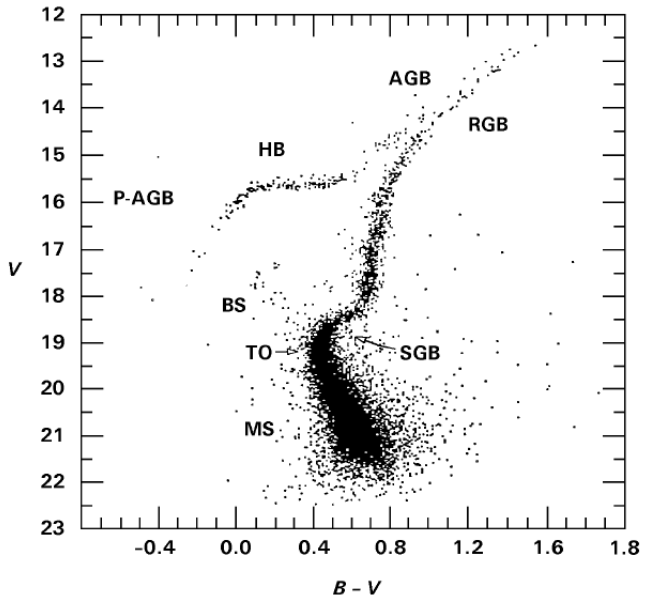

Figure 2.2: A globular cluster color-magnitude diagram which shows the different evolutionary stages of stars. The V-axis represents the brightness of the star. The horizontal axis is the difference of blueness B (blue meaning hot and lying to the left side) and brightness V is a measure of color. So this axis relates to the surface temperature of the star. The stages of evolution can be listed as follows, main sequence (MS): core hydrogen is burning, main-sequence turnoff (TO): central hydrogen is exhausted, red-giant branch (RGB): growing radius till helium ignites, and horizontal branch (HB) stars: helium burning in the core. Further regions such blue stragglers (BS), sub giant branch (SGB), asymptotic giant branch (AGB), post-asymptotic giant branch (P-AGB) are not needed in the present discussion. Taken from Ref.[36]

We consider stars on the horizontal branch which have reached helium burning. Some of the energy released from their cores is used for the production of axions through the Primakoff process. The energy loss rate of this process reduce the HB life time by a factor $8/(8+3g_{10}^2)$. And thus we can calculate HB life time by axion production. In addition, the HB lifetime can be measured by the ratio between the HB and RGB stars. From Ref. [28] a reasonable conservative bound for the coupling constant is

$$g_{a\gamma\gamma} < 10^{-10} GeV^{-1}. \tag{2.81}$$

White-dwarf cooling

When helium burning has ended, low-mass stars from HB move up to the red giant branch. They grow up to the asymptotic red giant branch (AGB). AGB stars, which have a degenerate carbon-oxygen core, are called white-dwarf. Their helium burning occurs in a shell. It leads to fast mass loss which creates a "planetary nebula". The planetary nebula surrounds a compact remnant and the core remains as a white dwarf. It has been found that the cooling of the white dwarf is due to the emission of neutrino and photon. The observed luminosity reveals that the cooling speed can constrain axion emission. The resulting limit on the axion-electron

coupling is (see Ref. [28])

$$g_{aee} < 1.3 \times 10^{-13} GeV^{-1}. \tag{2.82}$$

In addition to the condition given above, the axion searches from LUX suggest $g_{ae} < 3.5 \times 10^{-12} GeV^{-1}$ (Ref. [3]). The axion searches from PandaX suggest $g_{ae} < 4.35 \times 10^{-12} GeV^{-1}$ (Ref. [18]).

Chapter 3

The Direct Detection Proccesses of Axions and Axion-like Particles

3.1 Introduction

The QCD axion is a hypothetical particle as result of the Peicei-Quinn mechanism. Its mass and couplings with the SM fermions and bosons are related. The axion-like particle (ALP) is a generalization of the QCD axion. It can be associated with the breaking of a global U(1) symmetry (for example family, lepton number symmetry). Unlike the QCD axion, the mass and couplings can be treated independently. This property makes ALPs have much wider parameter space and generate rich phenomenology at low- and high-energy experiments and hence motivate the construction of thousand experiments in the past, present and future to search for them. In this chapter we use the word axion for both the QCD axion and the axion-like particles. This means that we treat its mass and couplings independently. Before mentioning about the processes which can be used to discover the axion we summarize here its general properties:

1) It is a pseudo scalar particle.

2) Its mass is very light. It is less than eV.

3) Its couplings to the SM particles arise from the dimentsion five operators and are suppressed by the energy scale that characterize of the breaking of the $U(1)$ global symmetry. The energy scale is assumed to be much larger than the electroweak symmetry breaking scale. The axion having this kind of couplings is also called the invisible axion.

There have been many experiments that make used of these properties to search for the axion. Most of experiments can be classified into three main categories which are based on the source of the axion productions. In the first case, the axion are produced in hot astrophysical plasma. These axions travel to the earth and scatter off targets, and cause nuclear and/or electron recoils which will be detected by detectors with high sensitivity. The second one is the accelerator-based experiments. The axions are produced accelerator-based facilities including beam-dump type and reactor experiments (DUNE, LDMX, T2K, ...) and collider experiments (LHC, ILC, CLIC just to name a few), therefore the environmental parameters associated with the production are more under control. The third case, axions are produced thermally in the early universe by processes involving quarks and gluons, hence axions would contribute to hot dark matter. In addition to these processes axions

can be produced by the vacuum re-alignment mechanism and constitute the cold dark matter. These axions can decay slowly into photons. As results the signature would be a quasi-monochromatic emission line from galaxies and galaxy clusters, that can be detected by telescopes. The frequency of that photons depends on the mass of axion and the galactic environment.

The three main search categories are all equivalently important, since they give complementary information. They can give also conflict results but that can be helpful to scrutinize the evidences for the existence of axions.

The objective of this chapter is the search for axions having astrophysical origin. The promising and closest source for this type of axons is our sun. However, the axions are produced in the Sun can be observed by XENON1T experiment with deposit energies in KeV range. As Ref.[29] mentioned we have two scattering cases that need attention. That is the electron recoil and the nuclear recoil. For low energy axions, they could scatter off atomic electrons rather than the nuclei. Since electrons are much lighter than nuclei. In this chapter, we will discuss the three electron recoil processes. They are known as three direct detection processes of axions. They are considered not only in the XENON1T experiment but also in a number of other axions search experiments . (shown in figure (3.1))

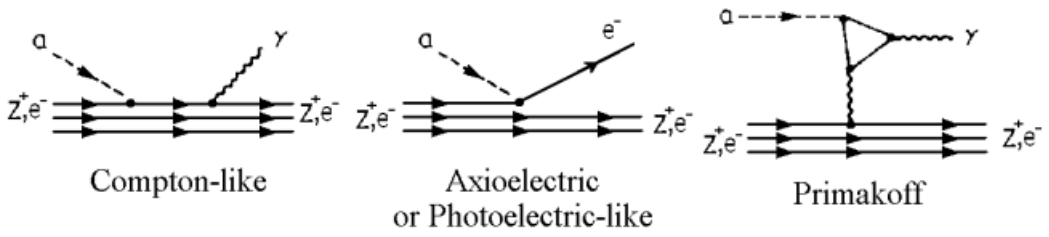

Figure 3.1: The direct detection processes of axion. From the right to the left: inverse Primakoff effect, ; "Axioelectric" or photoelectric effect; "Compton - like" effect, the figure is taken from Ref.[9]

In section (3.2), (3.3) and (3.4), I will present my detailed calculations of cross section these process and verify the results obtained by comparing with the existing results pretend in some papers. Next, to see more clearly the significance of these three processes in the search for dark matter, I will to briefly present the results obtained from the XENON1T experiment for axion in section (3.4).

3.2 The Inverse Primakoff Process

In 1983, Sikivie [32] proposed that invisible axions could be traced by several experiments, all based on the axion-photon conversion, i.e. the Primakoff effect. Figure (3.2) show this process. The sun can be seen as a huge source of reaction where photon interacts with the static Coulomb field (virtual photons) of atom to produce axions (this is Primakoff process, $\gamma + Ze \longrightarrow a + Ze$). This particle go to the Earth and scatters atom in the projection chamber to create photon that would

be detected by the detector. This process is called the inverse Primakoff,

$$a + Ze \longrightarrow \gamma + Ze'.$$

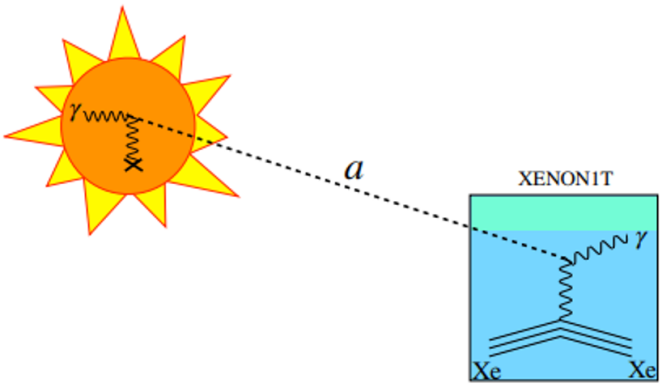

Figure 3.2: Primakoff and inverse Primakoff process. Extract from Ref.[19]

The Lagrangian describing the interaction process is given by

$$\mathcal{L}_{int} = \frac{1}{4} g_{a\gamma\gamma} \epsilon^{\mu\nu\sigma\rho} F_{\mu\nu} \tilde{F}^{\mu\nu} a + eA^{\eta} J_{\eta}, \tag{3.1}$$

The first term of Eq (3.1) describe the interaction of axions to photon via coupling $g_{a\gamma\gamma}$ and the other term is QED Lagrangian. In this case, J^{μ} is a conserved current of Ze atom. We do not know information about this current. The axion field a is a pseudo scalar field. We call p_1, p_3 are momentum of axion and photon. The momentum of the atom before and after the collision are p_2 and p_4. Before calculating S-matrix, we need to assume that the scattering is elastic in which the state of atom is unchanged during the scattering process.

The S-matrix

$$\langle p_3 p_4 | S | p_1 p_2 \rangle = \langle p_3 p_4 | T\Big(exp(-i \int \mathrm{d}^4 x L_{int}) \Big) | p_1 p_2 \rangle \,, \tag{3.2}$$

the expansion of exponential function is :

$$T\Big(exp(-i \int \mathrm{d}^4 x L_{int} \Big) = 1 - i \int \mathrm{d}^4 x L_{int} + \frac{(-i)^2}{2!} \int \mathrm{d}^4 x \int \mathrm{d}^4 y T\Big(L_{int}(x) L_{int}(y) \Big) + ..., \tag{3.3}$$

where $T\Big(L_{int}(x) L_{int}(y) \Big)$ is time-order as in Ref. [24]. Wick's theorem gives us the relationship between time-order T and normal order N (see Ref. [24])

$$T\Big(\int \mathrm{d}^4 x L_{int} \int \mathrm{d}^4 y L_{int} \Big) = N\Big(L_{int}(x) L_{int}(y) + \text{all possible contraction} \Big) \tag{3.4}$$

We can ignore factor 1 in Eqs. (3.3) since it represents the non-interactive system. The second term gives us zero contribution because the number of fields is

odd, hence they are not fully contracted. . Let, us substitute $\mathcal{L}_{int}$ as in Eqs. (3.1) and right hand of Eqs. (3.3) become :

$$T\Big(\frac{(-i)^2}{2!}\int \mathrm{d}^4x\frac{1}{8}g_{a\gamma\gamma}\epsilon^{\mu\nu\sigma\rho}F_{\mu\nu}F_{\sigma\rho}a\int \mathrm{d}^4yeA^\eta J_\eta + x\longleftrightarrow y\Big), \tag{3.5}$$

where the notation x $\leftrightarrow$ y means that the term is obtained by interchanging the role of x and y. This term is going to contribute the same as the first term. Therefore the factor $\frac{1}{2!}$ will be vanish. Note that $(\epsilon^{\mu\nu\sigma\rho}F_{\mu\nu}F_{\sigma\rho}a)^2$ and $(A^\eta J_\eta)^2$ have been ignored in Eq. (3.5) since they give zero contribution due to Wick's theorem. It leads to exchanging terms as in Eq. (3.5) which have the non-zero contribution. Next, we need to

$$\epsilon^{\mu\nu\sigma\rho}F_{\mu\nu}F_{\sigma\rho} = \epsilon^{\mu\nu\sigma\rho}(\partial_\mu A_\nu - \partial_\nu A_\mu)(\partial_\sigma A_\rho - \partial_\rho A_\sigma) = 4\epsilon^{\mu\nu\sigma\rho}\partial_\mu A_\nu \partial_\sigma A_\rho. \tag{3.6}$$

We use Eqs. (3.6), Eqs. (3.5) and substitute in Eqs. (3.2). The right hand of this equation is

$$\frac{1}{2}\langle p_3 p_4|T\Big((-i)^2\int \mathrm{d}^4x g_{a\gamma\gamma}\epsilon^{\mu\nu\sigma\rho}\partial_\mu A_\nu\partial_\sigma A_\rho a\int \mathrm{d}^4yeA^\eta J_\eta\Big)|p_1p_2\rangle\,. \tag{3.7}$$

This is the lowest order contribution, called the tree approximation. The higher order terms in the expansion in Eq. (3.3)) give quantum corrections and are not considered here. (see for the contribution are called quantum correction. Applying Wick's theorem at Eqs. (3.7), one obtains

$$2\frac{1}{2}eg_{a\gamma\gamma}(-i)^2\langle \overbrace{p_3, p_4|\int \mathrm{d}^4x\epsilon^{\mu\nu\sigma\rho}}\partial_\mu A_\nu \overbrace{\partial_\sigma A_\rho a\int \mathrm{d}^4yA^\eta J_\eta|p_1, p_2}\rangle. \tag{3.8}$$

The factor 2 results from the other possibility of the contraction which gives the same result. Using the following contractions (see Ref. [24])

$$\begin{aligned}
&\langle \overbrace{p,\sigma|A_\mu(x)}|0\rangle = \varepsilon^*_\mu(p,s)e^{ipx} \Rightarrow \langle \overbrace{p,\sigma|\partial_\nu A_\mu(x)}|0\rangle = \varepsilon^*_\mu(p,s)e^{ipx}(ip_\nu)\\
&\langle 0|\overbrace{a(x)|p,\sigma}\rangle = e^{-ipx},
\end{aligned} \tag{3.9}$$

where $\varepsilon_\mu(p,s)$ is the photon polarization vector and

$$\begin{aligned}
\overbrace{\partial_\sigma A_\rho(x)A_\eta}(y) &= \partial_\sigma A_\rho(x)A_\eta(y) - A_\eta(y)\partial_\sigma A_\rho(x)\\
&= \partial_\sigma(A_\rho(x)A_\eta(y) - A_\eta(y)A_\rho(x))\\
&= \partial_\sigma\Pi^F_{\rho\eta} \qquad (\ \Pi^F_{\rho\eta}\text{ is Feynman propagator of photon field }\ )\\
&= \partial_\sigma(\int\frac{d^4l}{(2\pi)^4}\frac{(-ig_{\rho\eta})}{l^2}e^{-i(x-y)l})\\
&= (-i)^2\int\frac{d^4l}{(2\pi)^4}\frac{g_{\rho\eta}}{l^2}e^{-i(x-y)l}l_\sigma.
\end{aligned} \tag{3.10}$$

We get the expression for S-matrix

$$\langle p_3 p_4|S|p_1 p_2\rangle = e g_{a\gamma\gamma}\epsilon^{\mu\nu\sigma\rho}\int\int\int d^4x d^4y \frac{d^4l}{(2\pi)^4}\frac{g_{\rho\eta}}{l^2}e^{-i(x-y)l}l_\sigma \times \varepsilon^*_\nu(p_3,s)e^{ip_3x}(ip_{3\mu})e^{-ip_1x}\langle p_4|J^\eta(y)|p_2\rangle \quad (3.11)$$

$$= e g_{a\gamma\gamma}\epsilon^{\mu\nu\sigma\rho}\int\int d^4y d^4l\delta^4(p_3-p_1-l)\frac{g_{\rho\eta}}{l^2}l_\sigma(ip_{3\mu})\varepsilon^*_\nu(p_3,s) \times \langle p_4|e^{iyl}J^\eta(y)|p_2\rangle$$

$$= ie g_{a\gamma\gamma}\epsilon^{\mu\nu\sigma\rho}l_\sigma p_{3\mu}\varepsilon^*_\nu(p_3,s)\frac{g_{\rho\eta}}{l^2}\langle p_4|\int d^4y e^{iyl}J^\eta(y)|p_2\rangle\Big|_{l=p_3-p_1}. \quad (3.12)$$

In the non-relativistic limit for the atomic state the current operator $\boldsymbol{J}(\vec{y})$ is vanish and hence, S-matrix become:

$$\langle p_3 p_4|S|p_1 p_2\rangle = ie g_{a\gamma\gamma}\epsilon^{\mu\nu\sigma 0}\frac{l_\sigma p_{3\mu}}{l^2}\varepsilon^*_\nu(p_3,s)\langle p_4|\int d^4y e^{iyl}J^0(\vec{y})|p_2\rangle\Big|_{l=p_3-p_1}. \quad (3.13)$$

It is easy to see that we can integrate the time dimension of Eq. (3.13)

$$\langle p_3 p_4|S|p_1 p_2\rangle = ie g_{a\gamma\gamma}\epsilon^{\mu\nu\sigma 0}\frac{l_\sigma p_{3\mu}}{(p_3-p_1)^2}\varepsilon^*_\nu(p_3,s)\langle p_4|\int d^3y e^{-i\vec{y}(\vec{p}_3-\vec{p}_1)}J^0(\vec{y})|p_2\rangle \times (2\pi)\delta(E_3-E_1). \quad (3.14)$$

The delta function of Eq. (3.14) tell us that the energy of atom is conserved during the scattering process and energy of axions completely convert to photon. However, momentum conservation is invisible. The reason for that we donot know explicit about the wavefunction of atom. Figure. (3.3) show Feynman diagram of this process corresponding to Eqs. (3.14)

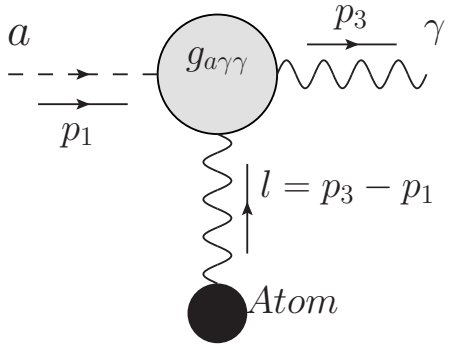

Figure 3.3: Feynman diagram for inverse Priamkoff process

$\mathcal{M}$-matrix

Now, we define $\mathcal{M}$-matrix as

$$\langle p_3 p_4|S|p_1 p_2\rangle = i(2\pi)\mathcal{M}\delta(E_3-E_1), \quad (3.15)$$

and

$$I(\vec{l}) = I(\vec{p_3}-\vec{p_1}) = \langle p_4|\int d^3y e^{-i\vec{y}(\vec{p}_3-\vec{p}_1)}J^0(\vec{y})|p_2\rangle. \quad (3.16)$$

Comparing to Eq. (3.14), we get

$$\begin{aligned}\mathcal{M} &= e g_{a\gamma\gamma}\epsilon^{\mu\nu\sigma 0}\frac{l_\sigma p_{3\mu}}{(p_3-p_1)^2}\varepsilon^*_\nu(p_3,s)I(\vec{l}) \\ &= e g_{a\gamma\gamma}\epsilon^{\mu\nu\sigma 0}\frac{(p_{3\sigma}-p_{1\sigma})p_{3\mu}}{(p_3-p_1)^2}\varepsilon^*_\nu(p_3,s)I(\vec{l}) \\ &= -e g_{a\gamma\gamma}\epsilon^{\mu\nu\sigma 0}\frac{p_{1\sigma}p_{3\mu}}{(p_3-p_1)^2}\varepsilon^*_\nu(p_3,s)I(\vec{l}). \end{aligned} \tag{3.17}$$

It is easy to get $\mathcal{M}$ squared

$$\begin{aligned}|\mathcal{M}|^2 &= \sum_{spin} e^2 g^2_{a\gamma\gamma}\epsilon^{\mu\nu\sigma 0}\epsilon^{\eta\kappa\gamma 0}\frac{(p_{1\sigma}p_{3\mu})(p_{1\gamma}p_{3\eta})}{(p_3-p_1)^4}\varepsilon^*_\nu(p_3,s)\varepsilon_\kappa(p_3,s)\Big|I(\vec{l})\Big|^2 \\ &= e^2 g^2_{a\gamma\gamma}\epsilon^{\mu\nu\sigma 0}\epsilon^{\eta\kappa\gamma 0}\frac{(p_{1\sigma}p_{3\mu})(p_{1\gamma}p_{3\eta})}{(p_3-p_1)^4}(-g_{\nu\kappa})\Big|I(\vec{l})\Big|^2, \end{aligned} \tag{3.18}$$

where we are used relation

$$\sum_{spin}\varepsilon^*_\nu(p_3,s)\varepsilon_\kappa(p_3,s) \longrightarrow -g_{\nu\kappa}. \tag{3.19}$$

Eq. (3.18) is not equal to zero when every index run from 1 to 3 and thus $g_{\nu\kappa} \to -\vec{e}_\nu\vec{e}_\kappa$ ($\vec{e}_{\nu=1,2,3} = \boldsymbol{i},\boldsymbol{j},\boldsymbol{k}$ in Cartesian coordinate system). Using $\vec{a}\times\vec{b} = \epsilon^{ijk}\vec{e}_i a_j b_k$, we can rewrite Eq. (3.18)

$$\begin{aligned}|\mathcal{M}|^2 &= e^2 g^2_{a\gamma\gamma}\epsilon^{\mu\nu\sigma 0}\epsilon^{\eta\kappa\gamma 0}\frac{(p_{1\sigma}p_{3\mu})(p_{1\gamma}p_{3\eta})}{(p_3-p_1)^4}(\vec{e}_\nu\vec{e}_\kappa)\Big|I(\vec{l})\Big|^2 \\ &= e^2 g^2_{a\gamma\gamma}\frac{|\vec{p}_1\times\vec{p}_3|^2}{(p_3-p_1)^4}\Big|I(\vec{l})\Big|^2. \end{aligned} \tag{3.20}$$

The differential cross section

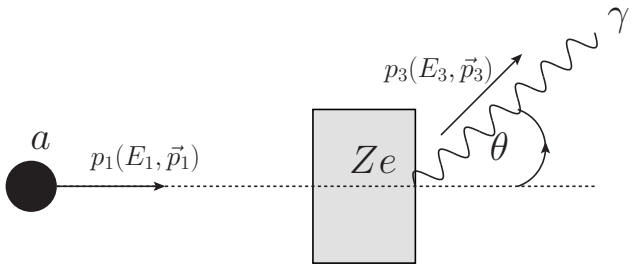

Figure 3.4: Priamkoff Scattering

In this case, because of the atom state and its energy is unchanged during the process the differential cross section can be calculate as

$$d\sigma = \frac{1}{2E_1|v_1|}\int\frac{d^3p_3}{(2\pi)^3}\frac{1}{2E_3}(2\pi)\delta(E_1-E_3)\Big|\mathcal{M}(p_1\to p_3)\Big|^2. \tag{3.21}$$

Note that, momentum conservation is forbidden in Eq. (3.21). As a result, E_1 and E_3 are two independent variables. In addition, because of photon mass equal

zero, we can change variable momentum to energy and take integral. Calling $d\Omega$ is solid angle in momentum space of photon, from Eq. (3.21) we get:

$$\begin{aligned} d\sigma &= \frac{1}{E_1 E_3 |v_1|} \int dp_3 \frac{p_3^2 d\Omega}{16\pi^2} \delta(E_1 - E_3) |\mathcal{M}|^2 \\ &= \frac{1}{E_1 E_3 |v_1|} \int dE_3 \frac{E_3^2 d\Omega}{16\pi^2} \delta(E_1 - E_3) |\mathcal{M}|^2 \\ \Rightarrow \frac{d\sigma}{d\Omega} &= \frac{1}{|v_1|} \frac{|\mathcal{M}|^2}{16\pi^2}. \end{aligned} \tag{3.22}$$

Assume that, atom is initially at rest ($v_2 = 0$). Let us substitute Eqs. (3.20) in Eqs. (3.22).

$$\begin{aligned} \frac{d\sigma}{d\Omega} &= \frac{1}{16\pi^2} \frac{1}{|v_1|} e^2 g_{a\gamma\gamma}^2 \frac{|\vec{p}_1 \times \vec{p}_3|^2}{(p_3 - p_1)^4} \left| I(\vec{l}) \right|^2 \\ &= \frac{e^2 g_{a\gamma\gamma}^2}{16\pi^2} \frac{1}{|v_1|} \frac{(|\vec{p}_1||\vec{p}_3| \sin\theta)^2}{(E_1^2 + |\vec{p}_1|^2 - 2|\vec{p}_1||\vec{p}_3| \cos\theta)^2} \left| I(\vec{l}) \right|^2 \\ &= \frac{e^2 g_{a\gamma\gamma}^2}{16\pi^2} \frac{E_1^3 |\vec{p}_1| \sin\theta^2}{(E_1^2 + |\vec{p}_1|^2 - 2E_1|\vec{p}_1| \cos\theta)^2} \left| I(\vec{l}) \right|^2. \end{aligned} \tag{3.23}$$

In the third line of Eq. (3.23), we have used $|\vec{p}_3| = E_3 = E_1$ and $E_1 = \frac{|\vec{p}_1|}{|\vec{v}_1|}$. θ is the angle formed by the two momentum vectors $\vec{p}_1$ and $\vec{p}_3$.

Eq. (3.23) is the same as the result quoted in Ref. [1]. The final step to acquire the complete result is to evaluate the $\left| I(\vec{l}) \right|^2$ term as defined in Eq. (3.16).

Atomic Form Factor

Now,choosing the origin at the nucleus of the atom, the charge density operator $J^0(\vec{y})$ of an atom of atomic number Z can be written as sum of the nucleus and electrons change density

$$J^0(\vec{y}) = Ze\delta^3(\vec{y}) - e \sum_i \delta^3(\vec{y} - \vec{y}_i), \tag{3.24}$$

where $e > 0$ and $\vec{y}_i$ is position of electrons.

According to Eqs. (3.24), Eqs. (3.16) will become

$$\begin{aligned} \left| I(\vec{l}) \right|^2 &= \left| \langle p_4 | \int d^3y e^{-i\vec{y}\vec{l}} (Ze\delta^3(\vec{y}) - e \sum_i \delta^3(\vec{y} - \vec{y}_i)) | p_2 \rangle \right|^2 \\ &= \left| Z - e \sum_i \langle A | e^{-i\vec{y}_i\vec{l}} | A \rangle \right|^2, \end{aligned} \tag{3.25}$$

where,the atom state is not change ,$|p_2\rangle = |p_4\rangle = |A\rangle$. $|A\rangle$ is consider as ground state of atom.

We will now define an important quantity called the atomic form factor

$$F(\vec{l}) = \sum_i \langle A | e^{-i\vec{y}_i\vec{l}} | A \rangle . \tag{3.26}$$

The atomic form factor is the Fourier transform of the electron density of an atom. It is also a measure of the scattering power of an individual atom. The exact analytic calculation of the atomic form factor for an arbitray value of momentum transverse is not possible since the exact distribution of the electron in atom is not well understood. However, this job will not be easy. First, we need calculate atom wave function at ground sate. This was done by Coulthard (1967). By utilizing the relativistic Hartree-Fock equation were derived by Swirles (1935) and by Grant (1961), he/she had evaluated numerically the relativistic Hartree-Fock (RHF) wave function of atom.Then compare the energy obtained from the calculation with the experiment to correct the (RHF) wave function as in Ref. [11]. The result of Xenon form factor can be found in Ref. [10] based on calculation in Ref. [17] which use relativistic Hartree-Fock (RHF) wave function in Ref. [11]. According to the Ref. [10] we can we can obtain an approximation for Eqs. (3.26)

$$F(\vec{l}) \simeq \sum_{i}^{4} a_i exp\Big(- \Big|\vec{l}\Big|^2 \frac{b_i}{16\pi^2}\Big) + c \tag{3.27}$$

where $c = 3.71180$ and the value of a_i and b_i are given by the table 3.1

a_1	a_2	a_3	a_4
20.2933	19.0298	8.97670	1.99000
b_1	b_2	b_3	b_4
3.92820	0.344000	26.4659	64.2658

Table 3.1: Table value of the parameters a_i and b_i

Figure (3.5) shows the matching of form factor computed by (RHF) and approximated by Eqs. (3.27).

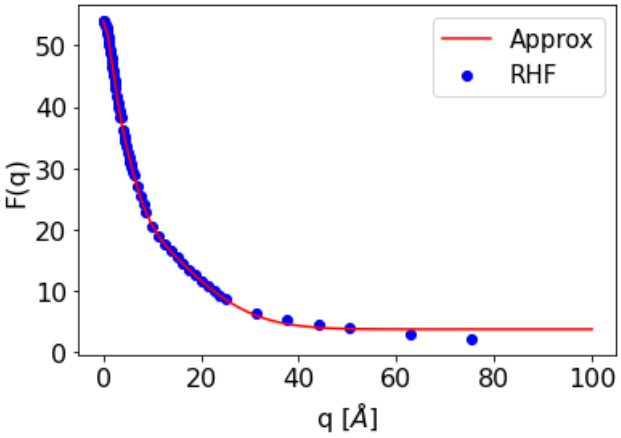

Figure 3.5: Form Factor

By using Eqs. (3.27) and (3.23), we can calculate cross section of Primakoff process.

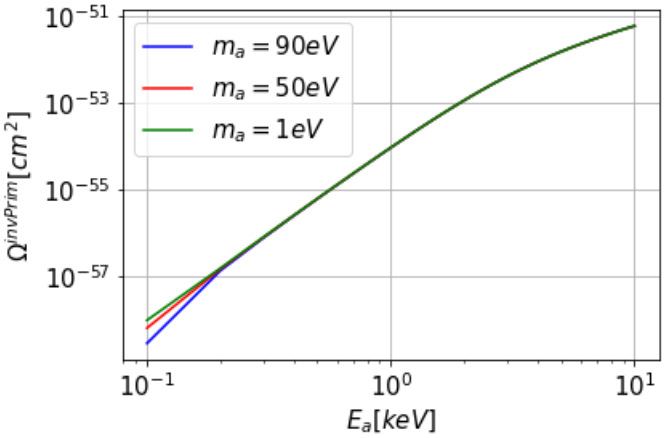

Figure 3.6: The total elastic scattering cross section of the inverse Primakoff process on Xe as a function of the axion energy E_a with $g_{a\gamma\gamma} = 10^{-10}\text{GeV}^{-1}$.

In figure (3.6), we can see that the value of the cross section increases when the energy of axion rises. Particularly, from 0.15 to 10 keV, at different masses, the cross sections are the same. On the other hand, from 0.1 to 0.15 keV, the cross sections are not equivalent for each values of masses.

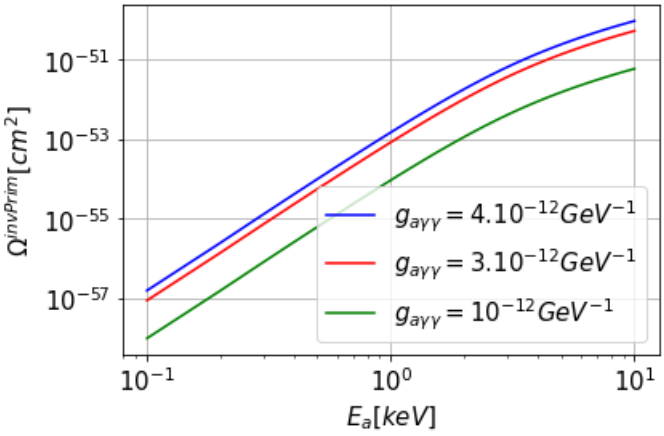

Figure 3.7: The total elastic scattering cross section of the inverse Primakoff process on Xe as a function of the axion energy E_a with axion mass $m_a = 1\text{eV}$.

Considering the cross section with respect to the axion energy at three different axion-photon couplings $g_{a\gamma\gamma}$, as shown in figure (3.7) , it is clear that the cross section strongly depends on the coupling.

3.3 Compton-like Cross section

A axion having a momentum k is absorbed by a charged free and point-like electron (momentum p) and a photon (momentum k) is emitted. The outgoing electron has momentum p'. In this case, the effective Lagrangian of interaction is:

$$\mathcal{L}_{int(2)} = e\bar{\psi}\gamma_\nu A^\nu \psi + \frac{\partial_\mu a}{f_a}\bar{\psi}\gamma^\mu\gamma^5\psi, \tag{3.28}$$

where, the second term describes the interaction between the axion (a) and the electron (ψ)

The S-matrix

$$\langle k'p'|S|kp\rangle = \langle k'p'|T\Big(exp(-i\int \mathrm{d}^4x L_{int(2)})\Big)|kp\rangle\,. \tag{3.29}$$

We now perform the perturbation expansion of T function in the way of Section. (3.1) and combine with similar arguments to obtain the formula Eqs. (3.7), we can write the function T in above equation to

$$T\Big(exp(-i\int \mathrm{d}^4x L_{int(2)})\Big) = T\Big((-i)^2\int \mathrm{d}^4x e\bar{\psi}\gamma_\nu A^\nu\psi\int \mathrm{d}^4y\frac{\partial_\mu a}{f_a}\bar{\psi}\gamma^\mu\gamma^5\psi\Big). \tag{3.30}$$

Applying Wick theorem give us two contribution corresponding to two Feynmann diagram. The first contribution is

$$\langle k'p'|S_1|kp\rangle = \langle \overbrace{k',p'|\int \mathrm{d}^4x e\bar{\psi}\gamma^\eta\psi A_\eta\int \mathrm{d}^4y\frac{1}{f_a}\partial_\mu a\bar{\psi}\gamma^\mu\gamma^5\psi|k,p}\rangle. \tag{3.31}$$

The contraction of electron fields operator with external states reads as (see Ref. [24])

$$\begin{aligned}
\langle 0|\overbrace{\psi(x)|\sigma,p}\rangle &= u(p,\sigma)e^{-ipx},\\
\langle \overbrace{p,\sigma|\bar{\psi}(x)}|0\rangle &= \bar{u}(p,\sigma)e^{ipx},\\
\overbrace{\psi(x)\bar{\psi}}(y) &= \int\frac{d^4l}{(2\pi)^4}\frac{i(\not{l}+m)}{l^2-m^2}e^{-il(x-y)},
\end{aligned} \tag{3.32}$$

where $u(p,s)$ is known as plane wave solution of Dirac equation with p being momentum and s spin of fermion. $\vec{l}$ and m momentum and mass of fermion in the internal line respectively. Using Eqs. (3.32) and (3.9), the expression (3.31) become:

$$\begin{aligned}
\langle k'p'|S_1|kp\rangle &= \int\int d^4xd^4y\bar{u}(p',s)\gamma^\eta\int\frac{d^4l}{(2\pi)^4}\frac{i(\not{l}+m)}{l^2-m^2}\gamma^\mu\gamma^5u(p,s)\varepsilon^*_\eta(k')(-ik_\mu)\\
&\qquad\times\frac{e}{f_a}e^{ip'x}e^{-i(x-y)l}e^{-ipy}e^{ik'x}e^{-iky}\\
&= \frac{e}{f_a}(2\pi)^4\delta^4(k+p-k'-p')\varepsilon^*_\eta(k')(-ik_\mu)\\
&\qquad\times\frac{\bar{u}(p',s)\gamma^\eta i(\not{l}+m)\gamma^\mu\gamma^5u(p,s)}{l^2-m^2}\Bigg|_{l=k+p}.
\end{aligned} \tag{3.33}$$

In the second line of Eq. (3.33), we have in turn integrated the variables d^4x, d^4l and d^4y. The conservation of momentum-energy of this process is satisfied by the delta function in Eq. (3.33). The Feynman diagram corresponds to the above expression in depicted in figure. (3.8)

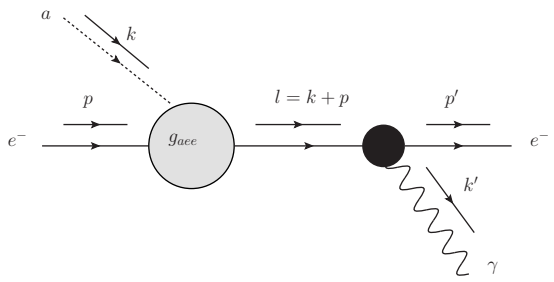

Figure 3.8: Feynman diagram for the first contribution

Next, the second contribution

$$\begin{aligned}
\langle k'p'|S_2|kp\rangle &= \langle k', p'| \int \mathrm{d}^4y \frac{1}{f_a} \partial_\mu a \bar{\psi}\gamma^\mu\gamma^5\psi \int \mathrm{d}^4x \bar{\psi}\gamma^\eta\psi A_\eta |k, p\rangle \\
&= \int\int d^4y d^4x \bar{u}(p', s)\gamma^\mu\gamma^5 \int \frac{d^4l}{(2\pi)^4} \frac{i(\not{l} + m)}{l^2 - m^2}\gamma^\eta u(p, s)\varepsilon^*_\eta(k')(-ik_\mu) \\
&\qquad \times \frac{e}{f_a} e^{ip'y} e^{-i(y-x)l} e^{ipx} e^{ik'x} e^{-iky} \\
&= \frac{e}{f_a}(2\pi)^4\delta^4(k + p - k' - p')\varepsilon^*_\eta(k')(-ik_\mu) \\
&\qquad \times \left. \frac{\bar{u}(p', s)\gamma^\mu\gamma^5 i(\not{l} + m)\gamma^\eta u(p, s)}{l^2 - m^2} \right|_{l=p-k'}, \quad (3.34)
\end{aligned}$$

corresponding to the Feynman diagram depicted in figure. (3.9)

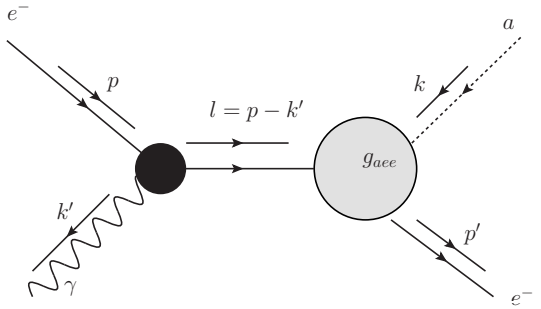

Figure 3.9: Feynman diagram for the second contribution

The two Feynman diagrams above describe the absorption of an axion by an electron through the s- and t-channels. The products obtained after scattering are a free photon and a free electron

Combining the two contributions in Eqs. (3.34) and (3.33), we get the S-matrix

element at tree-level

$$\begin{aligned}\langle k'p'|S|kp\rangle &= \langle k'p'|S_1|kp\rangle + \langle k'p'|S_2|kp\rangle \\ &= \frac{e}{f_a}(2\pi)^4\delta^4(k+p-k'-p')\varepsilon^*_\eta(k')(-ik_\mu)\bar{u}(p',s') \\ &\quad\times\left\{\frac{\gamma^\eta i(\not{k}+\not{p}+m)\gamma^\mu\gamma^5}{(k+p)^2-m^2}+\frac{\gamma^\mu\gamma^5 i(\not{p}-\not{k}'+m)\gamma^\eta}{(p-k')^2-m^2}\right\}u(p,s). \quad (3.35)\end{aligned}$$

The $\mathcal{M}$- amplitude

From Eqs. (3.35), we can define $\mathcal{M}_{cp}$-matrix for Compton-like process

$$\begin{aligned}\mathcal{M}_{cp} &= \frac{\langle k'p'|S|kp\rangle}{i(2\pi)^4\delta^4(k+p-k'-p')} \\ &= \frac{\langle k'p'|S_1|kp\rangle}{i(2\pi)^4\delta^4(k+p-k'-p')}+\frac{\langle k'p'|S_2|kp\rangle}{i(2\pi)^4\delta^4(k+p-k'-p')} \\ &= \mathcal{M}_1+\mathcal{M}_2, \quad (3.36)\end{aligned}$$

where

$$\begin{aligned}\mathcal{M}_1 &= \bar{u}(p',s')_\beta\left[\frac{\gamma^\eta i(\not{k}+\not{p}+m)\gamma^\mu\gamma^5}{(k+p)^2-m^2}\right]^\beta_\lambda u(p,s)^\lambda\varepsilon^*_\eta(k',\sigma)(-k_\mu) \\ \mathcal{M}_2 &= \bar{u}(p',s')_\beta\left[\frac{\gamma^\mu\gamma^5 i(\not{p}-\not{k}'+m)\gamma^\eta}{(p-k')^2-m^2}\right]^\beta_\lambda u(p,s)^\lambda\varepsilon^*_\eta(k',\sigma)(-k_\mu). \quad (3.37)\end{aligned}$$

The Dirac spinor indices ($\beta,\lambda=1,2,3,4$) are explicitly written included for the purpose of making the calculation more convenient.

The amplitude of this process is given by

$$\begin{aligned}|\bar{\mathcal{M}}_{cp}|^2 &= \frac{1}{2}\sum_{s,s',\sigma=1}^{2}\mathcal{M}^\dagger_{cp}\mathcal{M}_{cp} \\ &= \frac{1}{2}\sum_{s,s',\sigma=1}^{2}(\mathcal{M}_1+\mathcal{M}_2)^\dagger(\mathcal{M}_1+\mathcal{M}_2) \\ &= \frac{1}{2}\sum_{s,s',\sigma=1}^{2}(\mathcal{M}^\dagger_1\mathcal{M}_1+\mathcal{M}^\dagger_2\mathcal{M}_2+\mathcal{M}^\dagger_1\mathcal{M}_2+\mathcal{M}^\dagger_2\mathcal{M}_1). \quad (3.38)\end{aligned}$$

The factor $\frac{1}{2}$ appears in the Eq. (3.38) because we have averaged the initial electron spin. We have assumed that the incoming electron is unpolarized.

Using Eqs. (3.37) and (3.19), we can calculate each term in Eq. (3.38) that reads

$$\begin{aligned}\sum_{s,s',\sigma=1}^{2}\mathcal{M}^\dagger_1\mathcal{M}_1 = \frac{e^2}{f_a^2}Tr\Bigg[&(\not{p}+m)\frac{\gamma^{\mu'}\gamma^5(\not{k}+\not{p}+m)\gamma^{\eta'}}{(k+p)^2-m^2}(\not{p}'+m) \\ &\times\frac{\gamma^\eta(\not{k}+\not{p}+m)\gamma^\mu\gamma^5}{(k+p)^2-m^2}\Bigg]g_{\eta\eta'}k_\mu k_{\mu'}, \quad (3.39)\end{aligned}$$

$$\sum_{s,s',\sigma=1}^{2}\mathcal{M}_2^{\dagger}\mathcal{M}_2=\frac{e^2}{f_a^2}Tr\Bigg[(\not{p}+m)\frac{\gamma^{\eta}(\not{p}-\not{k}'+m)\gamma^{\mu}\gamma^5}{(p-k')^2-m^2}(\not{p}'+m)\times\frac{\gamma^{\mu'}\gamma^5(\not{p}-\not{k}'+m)\gamma^{\eta'}}{(p-k')^2-m^2}\Bigg]g_{\eta\eta'}k_{\mu}k_{\mu'},\tag{3.40}$$

$$\sum_{s,s',\sigma=1}^{2}\mathcal{M}_2^{\dagger}\mathcal{M}_1=\frac{e^2}{f_a^2}Tr\Bigg[(\not{p}+m)\frac{\gamma^{\eta}(\not{p}-\not{k}'+m)\gamma^{\mu}\gamma^5}{(p-k')^2-m^2}(\not{p}'+m)\times\frac{\gamma^{\eta}(\not{k}+\not{p}+m)\gamma^{\mu}\gamma^5}{(k+p)^2-m^2}\Bigg]g_{\eta\eta'}k_{\mu}k_{\mu'},\tag{3.41}$$

$$\sum_{s,s',\sigma=1}^{2}\mathcal{M}_1^{\dagger}\mathcal{M}_2=\frac{e^2}{f_a^2}Tr\Bigg[(\not{p}+m)\frac{\gamma^{\mu'}\gamma^5(\not{k}+\not{p}+m)\gamma^{\eta'}}{(k+p)^2-m^2}(\not{p}'+m)\times\frac{\gamma^{\mu'}\gamma^5(\not{p}-\not{k}'+m)\gamma^{\eta'}}{(p-k')^2-m^2}\Bigg]g_{\eta\eta'}k_{\mu}k_{\mu'}.\tag{3.42}$$

It is easy to see that because of $\mathcal{M}_1^{\dagger}\mathcal{M}_2$ must be real therefore $\mathcal{M}_1^{\dagger}\mathcal{M}_2=\mathcal{M}_2^{\dagger}\mathcal{M}_1$. Let us utilizes traces of products of γ-matrices and consequence of the law of conservation of momentum given in Appendix A for Eq. (3.39) to (3.42). After some algebraic manipulations, we obtain

$$\frac{f_a^2}{e^2}\sum_{s,s',\sigma=1}^{2}\mathcal{M}_1^{\dagger}\mathcal{M}_1=-4(2m^2+m_a^2)+8\Big(\frac{m^4m_a^2}{(p'.k')^2}+\frac{m^2m_a^2}{p'.k.}+p'.k'\Big)-8p.k',\tag{3.43}$$

$$\frac{f_a^2}{e^2}\sum_{s,s',\sigma=1}^{2}\mathcal{M}_2^{\dagger}\mathcal{M}_2=\frac{8m^4m_a^2}{(p.k')^2}-\frac{8m^2m_a^2}{p.k'}-8m^2-4m_a^2-8p.k'+8p'.k',\tag{3.44}$$

$$2\frac{f_a^2}{e^2}\sum_{s,s',\sigma=1}^{2}\mathcal{M}_1^{\dagger}\mathcal{M}_2=\frac{-16m^4m_a^2}{(p.k')(p'.k')}+\frac{8m^2m_a^4}{(p.k')(p'.k')}+\frac{8m^2m_a^2}{p'.k'}-\frac{8m^2m_a^2}{p.k'}+16m^2\Big(\frac{p'.k'}{p.k'}+\frac{p.k'}{p'.k'}\Big)-16m^2+8m_a^2+16p.k'-16p.k'.\tag{3.45}$$

The calculation of the scattering amplitude squared is presented in detain in Appendix A, here we quote only the final expression

$$\left|\bar{\mathcal{M}}_{cp}\right|^2=\frac{4m^2e^2}{f_a^2}\Big[B\left|\vec{k}\right|^2\sin^2\theta+2A\Big],\tag{3.46}$$

with

$$A=\frac{2(p.k)+m_a^2}{2(p.k')}+\frac{2(p.k')}{2(p.k)+m_a^2}-2$$
$$B=\frac{-4}{2(p.k)+m_a^2}+\frac{8(p.k)}{2(p.k)+m_a^2}.\tag{3.47}$$

Our result is equivalent to the one presented in Ref.[9]. We now proceed to compute the cross section and compare it with the cross section the Compton process. To make the comparison we assume that the energy of the incoming axion is equal to the energy of the incoming photon. The reason why we want to relate to two processes because they look rather similar. The free electron density in matter environment of the detector is not well define, one can then exploit the well-known data of the Compton process to evalutae the unknown cross section for the axion.

The Cross section

The cross section for $2 \to 2$ process reads

$$d\sigma = \frac{1}{2k_0 2p_0|v_1 - v_2|} \int \frac{d^3k'}{(2\pi)^3}\frac{1}{2k'_0} \int \frac{d^3p'}{(2\pi)^3}\frac{1}{2p'_0} \times (2\pi)^4\delta^4(k + p - p' - k')\left|\mathcal{M}_{cp}(k, p \to p', k')\right|^2. \tag{3.48}$$

If we consider the initial electron at rest ($|v_2| = 0$) and take integrate d^3p'

$$d\sigma = \frac{1}{2k_0 2p_0|v_1|} \int \frac{d^3k'}{16\pi^2}\frac{1}{k'_0 p'_0} \times \delta(k_0 + p_0 - p'_0 - k'_0)\left|\mathcal{M}_{cp}(k, p \to p', k')\right|^2. \tag{3.49}$$

We chose the laboratory frame of reference. To work on the two-body phase space, we can set $d^3k' = k'^2 dk' d\Omega_{k'} = \omega'^2 d\omega' d\Omega_{k'}$ with $\omega' = k'_0$, $\omega = k_0$ where k'_0 and k_0 are repsectively the energy of final photon and initial axion. We can rewrite Eq. (3.49) (see Appendix B)

$$d\sigma = \frac{1}{4\omega m|v_1|} \int \frac{d\cos\theta}{8\pi} \frac{\omega'}{(m + \omega - \left|\vec{k}\right|\cos\theta)}\left|\mathcal{M}_{cp}(k, p \to p', k')\right|^2 \tag{3.50}$$

where, θ is the angle between emitted photon and incoming axion we have a relation between ω and ω'

$$\omega' = \frac{m_a^2 + 2(p.k)}{2(\omega - \left|\vec{k}\right|\cos\theta + m)} \tag{3.51}$$

The above equation appear because of energy conversion (see Appdendix A). We will calculate Eqs. (3.50) in two cases

The case 1: $\beta = \frac{v_1}{c} \longrightarrow 0$

For $\omega \approx m_a \ll m$, we obtain

$$\omega' = \frac{m_a^2 + 2m\omega}{2(\omega - \left|\vec{k}\right|\cos\theta + m)} \Rightarrow \frac{\omega'}{\omega} = \frac{(\frac{m_a^2}{2m\omega} + 1)}{\frac{\omega - \left|\vec{k}\right|\cos\theta}{m} + 1}. \tag{3.52}$$

The speed of axion is very small compared to the speed of light, this means that we are working in the nonrelativistic limit. In fact, we can calculate exactly Eqs. (3.50) and then consider taking the limit $\beta \longrightarrow 0$. However, the calculation becomes more complicated if we do not bring the scattering amplitude (Eqs. (3.46)) to this limit .

We consider term A

$$\begin{aligned} A &= \frac{2m\omega + m_a^2}{2m\omega'} + \frac{2m\omega'}{2m\omega + m_a^2} - 2 \\ &= \frac{\omega}{\omega'}(1 + \frac{m_a^2}{2m\omega}) + \frac{\omega'}{\omega}\frac{1}{1 + \frac{m_a^2}{2m\omega}} - 2 \\ &= 1 + \frac{\omega - \left|\vec{k}\right|\cos\theta}{m} + \frac{1}{1 + \frac{\omega - \left|\vec{k}\right|\cos\theta}{m}} - 2. \end{aligned} \tag{3.53}$$

Because of the mass of the axion is much smaller than that of the electron ($m_a \ll m$). We can expand the Taylor series for the above expression at $\frac{m_a}{m} = 0$ in the nonrelativistic limit

$$\begin{aligned} \lim_{\beta \longrightarrow 0} A &= 1 + \frac{\omega}{m} + \frac{1}{1 + \frac{\omega}{m}} - 2 \\ &\approx 1 + \frac{\omega}{m} + (1 - \frac{\omega}{m} + \frac{\omega^2}{m^2} + \mathcal{O}(\frac{\omega^3}{m^3})) - 2 = \frac{\omega^2}{m^2} \approx \frac{m_a^2}{m^2}. \end{aligned} \tag{3.54}$$

We continue the term B (in Eq. (3.47)):

$$\begin{aligned} B &= \frac{-4}{m_a^2 + 2m\omega} + \frac{8m\omega}{(m_a^2 + 2m\omega)^2} \\ &= \frac{-2}{m\omega}\frac{1}{1 + \frac{m_a^2}{2m\omega}} + \frac{2}{m\omega}\frac{1}{(1 + \frac{m_a^2}{2m\omega})^2} \\ \Rightarrow \lim_{\beta \longrightarrow 0} B &\approx \frac{-2}{m\omega}\Big(1 - \frac{m_a^2}{2m\omega} + \mathcal{O}(\Big(\frac{m_a^2}{2m\omega}\Big)^2)\Big) + \frac{2}{m\omega}\Big(1 - 2\frac{m_a^2}{2m\omega} + \mathcal{O}(\Big(\frac{m_a^2}{2m\omega}\Big)^2)\Big) \\ &\approx -\frac{m_a^2}{m^2\omega^2} \approx -\frac{1}{m^2}, \end{aligned} \tag{3.55}$$

At the third line of Eq. (3.55), in the limit $\beta \longrightarrow 0$, $\omega \longrightarrow m_a$ and for $m_a \ll m$, we have used Taylor serious at $\frac{m_a^2}{2m\omega} = 0$. Finally we can derive the expression (from Eq. (3.46)) for the scattering amplitude in the nonrelativistic limit:

$$\begin{aligned} \lim_{\beta \longrightarrow 0} \left|\bar{\mathcal{M}}_{cp}\right|^2 &= \frac{4m^2e^2}{f_a^2}\Big[- \frac{1}{m^2}0\sin^2\theta + 2\frac{m_a^2}{m^2}] \\ &= \frac{8m^2e^2}{f_a^2}\frac{m_a^2}{m^2}. \end{aligned} \tag{3.56}$$

Eq. (3.56) tell us that, the scattering amplitude of Compton-like process is independent of the angle θ of the emitted photon in this limit.

According to Eq. (3.52), and Eq. (3.50), cross section of this process is :

$$\begin{aligned}
\lim_{\beta\longrightarrow 0} d\sigma_{cp} &= \frac{1}{4m\beta}\int \frac{d\cos\theta}{8\pi}\lim_{\beta\longrightarrow 0}\Big(\frac{\omega'}{\omega(m+\omega+\left|\vec{k}\right|\cos\theta)}\left|\mathcal{M}_{cp}(k,p\to p',k')\right|^2\Big)\\
&= \frac{1}{4m\beta}\int \frac{d\cos\theta}{8\pi}\frac{\frac{m_a}{2m}+1}{\frac{m_a}{m}+1}\frac{1}{(m+m_a)}\frac{8m^2e^2}{f_a^2}\frac{m_a^2}{m^2}\\
&= \frac{1}{4m\beta}\int \frac{d\cos\theta}{8\pi}\frac{\frac{m_a}{2m}+1}{m(\frac{m_a}{m}+1)^2}\frac{8m^2e^2}{f_a^2}\frac{m_a^2}{m^2}\\
&\approx \frac{1}{4m^2\beta}\int \frac{d\cos\theta}{8\pi}(\frac{m_a}{2m}+1)(1-2\frac{m_a}{m}+\mathcal{O}(\frac{m_a^2}{m^2}))\frac{8m^2e^2}{f_a^2}\frac{m_a^2}{m^2}\\
&\approx \frac{\alpha}{f_a^2\beta}\frac{m_a^2}{m^2}\int_{-1}^{1} d\cos\theta\\
\Rightarrow \sigma_{cp} &\approx \frac{2\alpha}{\beta f_a^2}\frac{m_a^2}{m^2}.
\end{aligned} \tag{3.57}$$

We need the Compton cross section to compare with the Compton process. According to the Ref. [24], the formula for calculating the scattering cross-section of the Compton process is known as Klei-Nishina formula, first derived in 1928 (Ref. ([22])):

$$\frac{d\sigma_{\gamma\to\gamma}}{d\cos\theta} = \frac{\pi\alpha^2}{m^2}\frac{\omega'_\gamma}{\omega_\gamma}\Big[\frac{\omega'_\gamma}{\omega_\gamma}+\frac{\omega_\gamma}{\omega'_\gamma}-\sin^2\theta\Big], \tag{3.58}$$

where ω_γ and ω'_γ are energy of initial and final photon respectively.

From Eq. (3.52) in the nonrelativistic limit ,we have the following approximation

$$\begin{aligned}
\lim_{\beta\to 0}\frac{\omega}{\omega'} = \Big(\frac{m_a}{2m}+1\Big)\Big(\frac{m_a}{m}+1\Big)^{-1} &\approx \Big(\frac{m_a}{2m}+1\Big)\Big(1-\frac{m_a}{m}+\mathcal{O}(\frac{m_a^2}{m^2})\Big)\\
&\approx 1-\frac{m_a}{2m}.
\end{aligned} \tag{3.59}$$

From the Eq. (3.59), we can see that the energy ratio between the input (axion) and output (photon) particles is almost equal (because $m_a \ll m$). Therefore, Eq. (3.58) also needs to return to the limit $\frac{\omega_\gamma}{\omega'_\gamma}\to 1$. Using this limit and performing integration over θ, this leads to Thomson cross section formula:

$$\sigma_{\gamma\to\gamma} = \frac{8}{3}\frac{\alpha^2\pi}{m^2}. \tag{3.60}$$

According to Eqs. (3.60) and (3.57), we get

$$\frac{\lim_{\beta\to 0}\sigma_{cp}}{\sigma_{\gamma\to\gamma}} = \frac{3}{4}\frac{m_a^2}{\pi\beta\alpha f_a^2} = g_{ae}^2\frac{3}{16}\frac{m_a^2}{\pi\beta\alpha m^2}, \tag{3.61}$$

where the coupling of axion with electron given by $g_{ae}=\frac{2m}{f_a}$ and $\alpha=\frac{e^2}{4\pi}$

The case 2: $\beta\longrightarrow 1$

This limit is equivalent to $m_a\longrightarrow 0$ and $\left|\vec{k}\right| = \omega\beta\longrightarrow\omega$.

At the first line of Eq. (3.55), it is easy to see that term $B \longrightarrow 0$ in this limit. From Eqs. (3.46) and (3.50) the differential cross section in the case 2 is:

$$\lim_{m_a\to 0} d\sigma = \frac{1}{4m\beta}\int \frac{d\cos\theta}{8\pi}\lim_{m_a\to 0}\Big(\frac{\omega'}{\omega(m+\omega-\left|\vec{k}\right|\cos\theta)}\frac{8m^2e^2}{f_a^2}A\Big) \tag{3.62}$$

In the limit $m_a \longrightarrow 0$ term A (Eq. (3.53)) become :

$$\lim_{m_a\to 0} A = 1 + x + \frac{1}{1+x} - 2, \tag{3.63}$$

where, we defined

$$x = \frac{\omega(1-\cos\theta)}{m} \tag{3.64}$$

Note that, the energy of axion is much less than electrons mass ($\omega \ll m$), so $x \ll 1$.

Next, substitute A as in Eq. (3.63) into Eq. (3.62):

$$\lim_{m_a\to 0} d\sigma = \frac{1}{4m^2\beta}\int \frac{d\cos\theta}{8\pi}\frac{8m^2e^2}{f_a^2}(\frac{1}{1+x} - \frac{2}{(1+x^2)} + \frac{1}{(1+x)^3}), \tag{3.65}$$

Taylor approximation for the Eq. (3.65) at $x = 0$, we obtain:

$$\begin{aligned}\lim_{m_a\to 0} d\sigma &\approx \frac{1}{4m^2\beta}\int \frac{d\cos\theta}{8\pi}\frac{8m^2e^2}{f_a^2}(x^2+\mathcal{O}(x^3))\\ &\approx \frac{1}{4m^2\beta}\int_{-1}^{1} \frac{d\cos\theta}{8\pi}\frac{8m^2e^2}{f_a^2}\frac{\omega^2}{m^2}(1-\cos\theta)^2\\ \Rightarrow \lim_{m_a\longrightarrow 0}\sigma_{cp} &\approx \frac{\alpha}{f_a^2\beta}\frac{8}{3}\frac{\omega^2}{m^2}.\end{aligned} \tag{3.66}$$

We need to check the ratio between the energy axion and photon. From Eq. (3.52), we get:

$$\lim_{m_a\to 0}\frac{\omega}{\omega'} = 1 + \frac{\omega(1-\cos\theta)}{m} = 1 + x \tag{3.67}$$

Because of $x \ll 1$, the energy of axion and photon are almost equal. This is similar to the case one

According to Eqs. (3.66) and Eqs. (3.60), we acquire:

$$\frac{\lim_{\beta\longrightarrow 1}\sigma_{cp}}{\sigma_{\gamma\longrightarrow\gamma}} = \frac{\omega^2}{f_a^2\beta\alpha\pi} = g_{ae}^2\frac{\omega^2}{4\beta\alpha\pi m^2}. \tag{3.68}$$

In general, we can compute Compton-like cross section through Compton cross section by the expression

$$\sigma_{cp} = \sigma_{\gamma\longrightarrow\gamma}\frac{3g_{ae}^2\omega^2}{16\beta\pi\alpha m^2}(1+\frac{\beta}{3}). \tag{3.69}$$

If we take the limit Eqs. (3.69) with $\beta \longrightarrow 0$ and $\beta \longrightarrow 1$, we will get back Eqs. (3.61) and (3.69). The data for Compton cross section was obtain from [35]

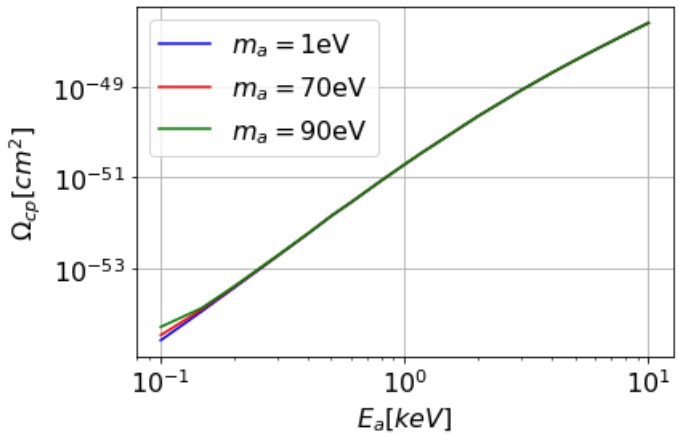

Figure 3.10: The total cross section of the Compton-like process on Xe as a function of the axion energy E_a with $g_{ae} = 10^{-12}$.

In figure (3.10), the value of the cross section dramatically increases when the energy of axion rises. Moreover, there is a possibility that the mass of axion slightly affects to the Compton-like cross section.

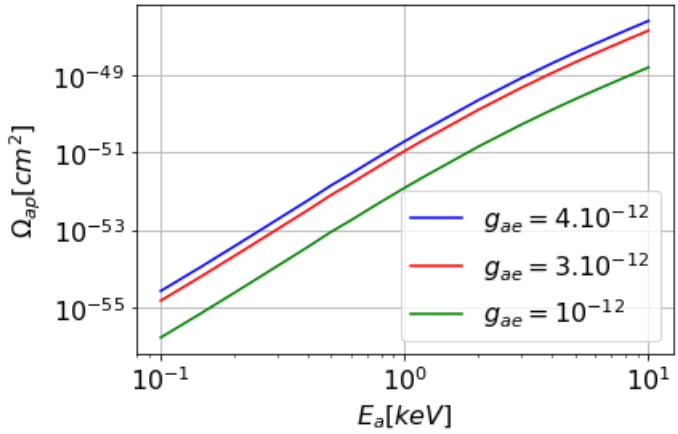

Figure 3.11: The total cross section of the Compton-like process on Xe as a function of the axion energy E_a with axion mass $m = 1$eV .

Figure (3.11) illustrates that the cross section significantly depends on axion-electron coupling.

3.4 Axioelectric process

Axion is absorbed by a bound electron of the atom and the excited electron to fly out of the atom. Note that this process does not produce photons like Compton scattering. A discussion and calculation about axioelectric process was performed in Ref.[16] and corrected by Ref.[26]. In this section, we will calculate in detail cross section of axioelectric process in nonrelativistic limit as in Ref.[26], because energy of axion is so small. Like the two previous processes, the cross section of this one will be calculated through the well-known photoelectric process. Unlike the two processes we can use the quantum field theory to compute the cross section, in this

process we will make use of the quantum mechanics. In this language, one have to write down the interaction Hamiltonian operator which has dimension of energy. The transformation from interaction Lagrangian in QFT to Hamiltonian operator in QM is not straight forward. The easiest way for us is to accept the form of the non relativistic Hamiltonian for the electromagnetic interaction which is well known in literature. We however want to derive it directly from the relativistic Lagrangian using several tricks. This method will then be applied to derive the non-relativistic Hamiltonian for the interaction of axion with electrons.

3.4.1 Photoelectric process

The photoelectric effect is a direct example for the energy quantization of light. Electrons were observed to be ejected from metals when irradiated with light, which was discovered by Hertz (1887). The basic process can be considered as photon is absorbed a bound electron $|i\rangle$ of the atom and transfer it to free electron $|f\rangle$. The Quantum field theory give us interaction Lagrangian of electron and photon:

$$\mathcal{L}_{int(3)} = eA^{\mu}\bar{\psi}\gamma_{\mu}\psi, \tag{3.70}$$

where ψ is electron field. Our aim is to bring the Eq. (3.70) to nonrelativistic limit, which mean that, we consider physical system in quantum mechanism. Because Lagragian of above equation is independent of the first derivative of field. So interaction Hamiltonian is

$$\mathcal{H}_{int(3)} = -\mathcal{L}_{int(3)} = -eA^{\mu}\bar{\psi}\gamma_{\mu}\psi. \tag{3.71}$$

Here we have to clarify several notations before going further. The electron field ψ in QFT has mass dimension of 3/2 and is expressed as $\psi = (\psi_L, \psi_R)$ in Weys representation. However the electron is moving slowly in the electromagnetic potential A^{μ}, we donot treat ψ as a field operator anymore, but a Dirac spinor normalized in such a way that it is dimensionless. In particular we use the plane wave solution of the Dirac equation and define plane wave solution of Dirac equation of electron:

$$\psi = \begin{bmatrix} \sqrt{p.\sigma}\chi \\ \sqrt{p.\bar{\sigma}}\chi \end{bmatrix} \qquad \bar{\psi} = \begin{bmatrix} \chi^{\dagger}\sqrt{p.\bar{\sigma}} & \chi^{\dagger}\sqrt{p.\sigma} \end{bmatrix}, \tag{3.72}$$

where p is 4-momentum of electron, σ is Pauli matrix and χ is two component spinor state normalized as $\chi^{\dagger}\chi = 1/\sqrt{2m}$ of electrons.

Using Eq. (3.72) and γ-matrix in the chiral representation given in Ref. [24] substitute into Eq. (3.71), giving:

$$\mathcal{H}_{int(3)} = -eA_{\mu}\Big(\chi^{\dagger}\sqrt{p.\bar{\sigma}}(\sigma^{\mu})\sqrt{p.\bar{\sigma}}\chi + \chi^{\dagger}\sqrt{p.\sigma}(\bar{\sigma}^{\mu})\sqrt{p.\sigma}\chi\Big), \tag{3.73}$$

In the case $\mu = 0$

$$\begin{aligned} \mathcal{H}_{int(3)}\Big|_{\mu=0} &= -eA_{\mu}\Big(\chi^{\dagger}(p.\bar{\sigma})\chi + \chi^{\dagger}(p.\sigma)\chi\Big) \\ &= -2ep_0A_0\chi^{\dagger}\chi, \end{aligned} \tag{3.74}$$

In the second line of Eq. (3.74), we defined

$$\begin{aligned} p\sigma &= p_0\sigma^0 - \vec{p}.\vec{\sigma} = p_0 - \vec{p}.\vec{\sigma} \\ p\bar{\sigma} &= p_0\sigma^0 - \vec{p}.(-\vec{\sigma}) = p_0 + \vec{p}.\vec{\sigma}. \end{aligned} \tag{3.75}$$

Now, we can transform Eq. (3.74) into the operator Hamiltonian. Considering normalization condition of spin state:

$$2m\chi^\dagger\chi = 1 \tag{3.76}$$

Here, we can define eigenvectors for spin state of electron:

$$|\chi\rangle = \sqrt{2m}\chi, \tag{3.77}$$

With this definition, Eq. (3.74) is understood as expected value of Hamiltonian.

In the nonrelativistic limit Eq. (3.74) become:

$$\begin{aligned} \mathcal{H}_{int(3)}\Big|_{\mu=0} = -e\,\langle\chi|\frac{p_0A_0}{m}|\chi\rangle &= -e\,\langle\chi|\frac{\sqrt{\vec{p}^2+m^2}}{m}A_0|\chi\rangle \\ &\approx -e\,\langle\chi|\Big(1+\frac{1}{2}\frac{\vec{p}^2}{m^2}+\mathcal{O}(\frac{\vec{p}^4}{m^4})\Big)A_0|\chi\rangle \\ &\approx -e\,\langle\chi|A_0|\chi\rangle\,. \end{aligned} \tag{3.78}$$

In this limit, we leave out the term proportional to the square of velocity at Eq. (3.78). Finally, Hamiltionian operator is:

$$\hat{\mathcal{H}}_{int(3)}\Big|_{\mu=0} = -eA_0. \tag{3.79}$$

Next, we continue with the case $\mu = 1, 2, 3$ in which Eq. (3.73) become :

$$\mathcal{H}_{int(3)}\Big|_{\mu=1,2,3} = -e\chi^\dagger\Big(\sqrt{p.\bar{\sigma}}(-\vec{A}.\vec{\sigma})\sqrt{p.\bar{\sigma}} + \sqrt{p.\sigma}(\vec{A}.\vec{\sigma})\sqrt{p.\sigma}\Big)\chi, \tag{3.80}$$

The product of p and σ into square root make the calculation very difficult. To resolve the issue, we can use an interesting computational technique that is square root of a 2×2- matrix

$$\begin{aligned} \sqrt{p.\sigma} &= \frac{1}{\sqrt{2p_0+2m}}(p.\sigma + mI) \\ \sqrt{p.\bar{\sigma}} &= \frac{1}{\sqrt{2p_0+2m}}(p.\bar{\sigma} + mI). \end{aligned} \tag{3.81}$$

According to Eqs. (3.81) and (3.75),

$$\begin{aligned} \mathcal{H}_{int(3)}\Big|_{\mu=1,2,3} = \frac{e}{2p_0+2m}\chi^\dagger\Big(&2p_0[(\vec{A}.\vec{\sigma})(\vec{p}.\vec{\sigma}) + (\vec{p}\vec{\sigma})(\vec{A}.\vec{\sigma})] \\ &+ 2m[(\vec{A}.\vec{\sigma})(\vec{p}.\vec{\sigma}) + (\vec{p}\vec{\sigma})(\vec{A}.\vec{\sigma})]\Big)\chi. \end{aligned} \tag{3.82}$$

Using the relation between dot and cross products of Pauli matrix:

$$(\vec{A}.\vec{\sigma})(\vec{p}.\vec{\sigma}) = \vec{A}.\vec{p} + i(\vec{A}\times\vec{p}).\sigma, \tag{3.83}$$

Eq. (3.82) becomes

$$\mathcal{H}_{int(3)}\Big|_{\mu=1,2,3} = \frac{e}{2p_0+2m}\chi^\dagger\Big(4p_0(\vec{A}.\vec{p}) + 4m(\vec{A}.\vec{p})\Big)\chi$$
$$= e2m\chi^\dagger\frac{\vec{A}.\vec{p}}{m}\chi = e\,\langle\chi|\frac{\vec{A}.\vec{p}}{m}|\chi\rangle\,. \tag{3.84}$$

From Eqs. (3.79) and (3.84), we acquire Hamiltonian operator for electron move in with electromagnetic field in quantum mechanics

$$\hat{\mathcal{H}}_{int(3)} = -eA_0 + e\frac{\boldsymbol{A}.\boldsymbol{p}}{m}, \tag{3.85}$$

where potential and momentum vector become potential and momentum operator. This expression is well-known in any quantum mechanics book. The first term in Eq. (3.85) is considered as electric potential. It is usually placed in electron Hamiltonian $\boldsymbol{\mathcal{H}}_e = \frac{\boldsymbol{p}^2}{2m} + V(r)(= -eA_0)$ which act on eigenstates $|i\rangle$ of electron produces eigensvalue.

$$\boldsymbol{\mathcal{H}}_e\,|i\rangle = E_i\,|i\rangle\,. \tag{3.86}$$

The rest can be seen as perturbation and it is the main contribution to the scattering amplitude. Now, we can calculate cross section of photoelectric process.

Cross section

We consider physical situation of a photon absorbed by on an atom in a volume of detector material. We assume that, $\boldsymbol{A}$ is a monochromatic field of the plane wave

$$\boldsymbol{A} = \hat{\boldsymbol{\varepsilon}}(e^{i\omega\boldsymbol{r}.\hat{\boldsymbol{n}}-i\omega t} + e^{-i\omega\boldsymbol{r}.\hat{\boldsymbol{n}}+i\omega t}), \tag{3.87}$$

where $\hat{\boldsymbol{\varepsilon}}$ is polarization vector and $\hat{\boldsymbol{n}}$ is propagation direction. The energy of this field is ω. $\boldsymbol{r}$ is position vector of electron move in electromagnetic and $\boldsymbol{r}^2 = |r|^2$ (with r is algebraic value of $\boldsymbol{r}$). The term $e^{-i\omega\boldsymbol{r}.\hat{\boldsymbol{n}}+i\omega t}$ is is responsible for stimulated emission of photon, and $e^{i\omega\boldsymbol{r}.\hat{\boldsymbol{n}}-i\omega t}$ is responsible for photons are absorbed.

In the absorption case, matrix element given by:

$$\mathcal{M} = e\,\langle f|e^{i\omega\hat{\boldsymbol{n}}.\boldsymbol{r}-i\omega t}\frac{\hat{\boldsymbol{\varepsilon}}.\boldsymbol{p}}{m}|i\rangle\,, \tag{3.88}$$

We have (see Ref. [30])

$$im[\boldsymbol{\mathcal{H}}_{\boldsymbol{e}}, \boldsymbol{r}] = \boldsymbol{p}, \tag{3.89}$$

Eqs. (3.88) become

$$\mathcal{M} = e\,\langle f|e^{i\omega\hat{\boldsymbol{n}}.\boldsymbol{r}-i\omega t}\boldsymbol{\varepsilon}[\boldsymbol{\mathcal{H}}_{\boldsymbol{e}}, \boldsymbol{r}]|i\rangle$$
$$= e\boldsymbol{\varepsilon}\,\langle f|(E_f - E_i)\boldsymbol{r}e^{i\omega\hat{\boldsymbol{n}}.\boldsymbol{r}-i\omega t}|i\rangle$$
$$= e\omega\,\langle f|\boldsymbol{\varepsilon}\boldsymbol{r}e^{i\omega\hat{\boldsymbol{n}}.\boldsymbol{r}-i\omega t}|i\rangle\,, \tag{3.90}$$

At the third line of Eqs. (3.90), we need to note that, the energy required for the electron to transform from i-level to f-level is exactly the same as the absorbed photon energy.

Because of the wavelength of the photon field, in fact, is far longer than the atomic dimension. The electric dipole approximation is useful

$$e^{i\omega\hat{\boldsymbol{n}}.\boldsymbol{r}} = 1 + i\omega\boldsymbol{n}.\boldsymbol{r} + ..., \tag{3.91}$$

We work with its leading term, 1 (see chapter 5 in [30]). The matrix element can be written as

$$\mathcal{M} = e\omega \langle f|\hat{\boldsymbol{\varepsilon}}\boldsymbol{r}|i\rangle \, e^{-i\omega t}. \tag{3.92}$$

Now we need a very important assumption to get the desired result that the wave function is spherically symmetric. This means that the wave function of electrons depends only on the variable r (not $\boldsymbol{r}$). We can write bound state $|i\rangle$ and free state $|f\rangle$ of electron as $\psi_b(r)$ and $\psi_f(r)$. The amplitude of scattering is:

$$\begin{aligned}\left|\bar{\mathcal{M}}\right|^2 = \sum_{spin} \frac{|\mathcal{M}|^2}{4} &= \frac{\omega^2 e^2}{4} \langle f|\hat{\boldsymbol{\varepsilon}}\boldsymbol{r})|i\rangle \, (\, \langle f|\hat{\boldsymbol{\varepsilon}}\boldsymbol{r'})|i\rangle)^\dagger \\ &= \frac{\omega^2 e^2}{4} \int dr \psi_f^*(r)(\hat{\boldsymbol{\varepsilon}}\boldsymbol{r})\psi_b(r) \int dr' \psi_b^*(r')(\hat{\boldsymbol{\varepsilon}}\boldsymbol{r'})\psi_f(r')\end{aligned} \tag{3.93}$$

Where, as explained in section (3.2) the factor $\frac{1}{4}$ by the probabilistic contribution of electrons $(\frac{1}{2})$ and photons $(\frac{1}{2})$. Mathematically, we need to write $\boldsymbol{r'}$ and $\boldsymbol{r}$ to represent two independent integrals. However, physically we only have one initial state and one final state so $\boldsymbol{r} = \boldsymbol{r'}$.

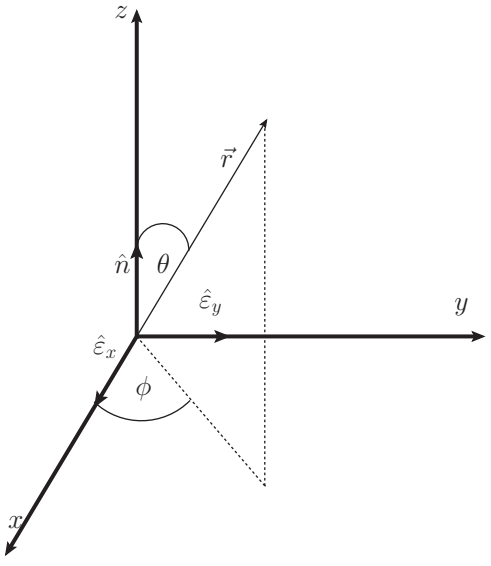

Figure 3.12: Polar coordinate system

From figure. (3.12) we can choose xOy is polarization plane with two polarization vectors being the two basis vectors :

$$\begin{aligned}\hat{\boldsymbol{\varepsilon}}_x &= \hat{\boldsymbol{x}} = (1, 0, 0), \\ \hat{\boldsymbol{\varepsilon}}_y &= \hat{\boldsymbol{y}} = (0, 1, 0).\end{aligned} \tag{3.94}$$

We also have

$$(\boldsymbol{\varepsilon r})^2 = (\boldsymbol{\varepsilon}_x \boldsymbol{r} + \boldsymbol{\varepsilon}_x \boldsymbol{r})^2 = |r|^2(\sin\theta\cos\phi + \sin\theta\sin\phi)^2$$
$$= |r|^2(\sin^2\theta + \sin^2\theta\sin 2\phi). \tag{3.95}$$

Substituting Eqs. (3.95) into Eqs. (3.93), giving:

$$\left|\bar{\mathcal{M}}\right|^2 = \frac{\omega^2 e^2}{4} S^2(\sin^2\theta + \sin^2\theta\sin 2\phi), \tag{3.96}$$

where we defined the functional S^2

$$S^2 = \int dr\psi_f^*(r)|r|\psi_b(r) \int dr\psi_b^*(r)|r|\psi_f(r). \tag{3.97}$$

Now, let's go back to the cross section calculation. In quantum mechanics, an absorption cross section given by: (see Ref. [30])

$$d\sigma = (2\pi)\frac{\left|\bar{\mathcal{M}}\right|^2}{J} d\rho, \tag{3.98}$$

where J is the incident flux (in this case is photon flux)

$$J = 2 \times \text{Energy of Incident particle} \times \left|v_{\text{incident particale}} - v_{\text{bound electron}}\right|, \tag{3.99}$$

and the density of states for the outgoing electron is:

$$d\rho = \frac{V}{(2\pi)^3} p_e^2 dp_e d\Omega \delta(E_p - E_{nl} - E_e)$$
$$= dP d\phi \sin\theta d\theta, \tag{3.100}$$

We have three things to note in the Eqs. (3.100). Firstly, the delta function tells us that the energy of the system is conservative. E_p and E_e are energy of photon and the escaping electron. (-E_{nl}) is the binding energy of the atomic electron in the nl shell. Secondly, $d\Omega$ is solid angle of free electron in momentum space. We can choose origin at atom and assume that immediately after the scattering, electron is not affected by the external force. When the vector momentum has the same direction as the vector position. Finally, the term $dP = \frac{V}{(2\pi)^3} p_e^2 dp_e \delta(E_p - E_{nl} - E_e)$ is depends only on the electron's momentum so we can integrate out the delta function the momentum without affecting other integration variables :

$$d\rho = P d\phi \sin\theta d\theta. \tag{3.101}$$

According to Eqs. (3.101), (3.99), (3.98) and (3.96), the cross section for photo-electric is :

$$d\sigma_{ph} = \frac{2\pi}{2\omega}\frac{\omega^2 e^2}{4} S^2(\sin^2\theta + \sin^2\theta\sin 2\phi) P d\phi \sin\theta d\theta$$
$$\Rightarrow \sigma_{ph} = \frac{\pi}{4}\omega e^2 2\pi \frac{4}{3} S^2 P$$
$$= 2\pi^2 \omega\alpha \frac{4\pi}{3} S^2 P. \tag{3.102}$$

Now, the remaining problem that we need to solve is cross section of axioelectric process.

3.4.2 Axioelectric cross section

The process is typically similar to the photoelectric process. However, the axion is an incident particle instead of a photon with the same energy. We need to first introduce the Hamiltonian operator for the system in the nonrelativistic limit. We follow the same method applied for the electromagnetic interaction.

Hamiltonian operator in quantum mechanic

In quantum field theory, interaction lagrangian for axion and electron given by (see section. (3.3.1))

$$\mathcal{L}_{int(4)} = -\frac{\partial_\mu a}{f_a}\bar{\psi}\gamma^\mu\gamma 5\psi = -\mathcal{H}_{int(4)}. \tag{3.103}$$

Using Eq. (3.72) we get

$$\begin{aligned}\mathcal{H}_{int(4)} &= \frac{\partial_\mu a}{f_a}\bar{\psi}\gamma^\mu\gamma 5\psi \\ &= \frac{\partial_\mu a}{f_a}\Big(\chi^\dagger\sqrt{p.\bar{\sigma}}(\sigma^\mu)\sqrt{p.\bar{\sigma}}\chi + \chi^\dagger\sqrt{p.\sigma}(-\bar{\sigma}^\mu)\sqrt{p.\sigma}\chi\Big).\end{aligned} \tag{3.104}$$

In the case $\mu = 0$

$$\begin{aligned}\mathcal{H}_a &= \frac{\partial_t a}{f_a}\Big(\chi^\dagger(p.\bar{\sigma})\chi - \chi^\dagger(p.\sigma)\chi\Big) \\ &= 2\frac{\partial_t a}{f_a}\chi^\dagger(\vec{p}.\vec{\sigma})\chi = 2m\frac{\partial_t a}{f_a}\chi^\dagger\frac{\vec{p}.\vec{\sigma}}{m}\chi = \frac{\partial_t a}{f_a}\left\langle\chi\right|\frac{\vec{p}.\vec{\sigma}}{m}\left|\chi\right\rangle.\end{aligned} \tag{3.105}$$

In the case $\mu = 1, 2, 3$

$$\begin{aligned}\mathcal{H}_b &= -\frac{1}{f_a}\Big(\chi^\dagger\sqrt{p.\bar{\sigma}}(\boldsymbol{\nabla}(a).\vec{\sigma})\sqrt{p.\bar{\sigma}}\chi + \chi^\dagger\sqrt{p.\sigma}(\boldsymbol{\nabla}(a)\vec{\sigma})\sqrt{p.\sigma}\chi\Big) \\ &= -\frac{1}{f_a}\frac{1}{2p_0+2m}\chi^\dagger\Big[(p.\sigma)(\boldsymbol{\nabla}a.\vec{\sigma})(p.\sigma) + (p.\bar{\sigma})(\boldsymbol{\nabla}a.\vec{\sigma})(p.\bar{\sigma}) \\ &\quad + 2m^2(\boldsymbol{\nabla}a.\vec{\sigma}) + m(p.\sigma + p.\bar{\sigma})(\boldsymbol{\nabla}a.\vec{\sigma}) + m(\boldsymbol{\nabla}a.\vec{\sigma})(p.\sigma + p.\bar{\sigma})\Big]\chi.\end{aligned} \tag{3.106}$$

Substituting Eq. (3.75) in Eq. (3.106) and using

$$\begin{aligned}(\vec{p}.\vec{\sigma})(\boldsymbol{\nabla}a.\vec{\sigma})(\vec{p}.\vec{\sigma}) &= (p_i\sigma^i\partial_j a\sigma^j)(\vec{p}.\vec{\sigma}) \\ &= p_i\partial_j a(2\delta^{ij} - \sigma^j\sigma^i)(\vec{p}.\vec{\sigma}) \\ &= 2(\vec{p}.\boldsymbol{\nabla}a)(\vec{p}.\vec{\sigma}) - (\boldsymbol{\nabla}a.\vec{\sigma})(\vec{p}.\vec{\sigma})(\vec{p}.\vec{\sigma}) \\ &= 2(\vec{p}.\boldsymbol{\nabla}a)(\vec{p}.\vec{\sigma}) - (\boldsymbol{\nabla}a.\vec{\sigma})\vec{p}^2,\end{aligned} \tag{3.107}$$

we obtains,

$$\begin{aligned}\mathcal{H}_b = -\frac{1}{f_a}\frac{1}{2p_0+2m}\chi^\dagger\Big[&2(\boldsymbol{\nabla}a.\vec{\sigma})(p_0^2 - \vec{p}^2) + 2m^2(\boldsymbol{\nabla}a.\vec{\sigma}) \\ &+ 4(\vec{p}.\boldsymbol{\nabla}a)(\vec{p}.\vec{\sigma}) + 4mp_0(\boldsymbol{\nabla}a.\vec{\sigma})\Big]\chi.\end{aligned} \tag{3.108}$$

In the nonrelativistic limit, we ignore the term related to the square of velocity $4(\vec{p}.\boldsymbol{\nabla}a)(\vec{p}.\vec{\sigma})$ then

$$\begin{aligned}\mathcal{H}_b &= -\frac{1}{f_a}\frac{1}{2p_0+2m}\chi^\dagger\Big[4(\boldsymbol{\nabla}a.\vec{\sigma})m^2+4mp_0(\boldsymbol{\nabla}a.\vec{\sigma})\Big]\chi \\ &= -\frac{2m}{f_a}\chi^\dagger(\boldsymbol{\nabla}a.\vec{\sigma})\chi = -\frac{1}{f_a}\langle\chi|\boldsymbol{\nabla}a.\vec{\sigma}|\chi\rangle\,. \end{aligned} \tag{3.109}$$

From Eqs. (3.109) and (3.105) we acquire Hamiltonian operator for axioelectric interaction

$$\begin{aligned}\hat{\mathcal{H}}_{(4)} &= \hat{\mathcal{H}}_a+\hat{\mathcal{H}}_b \\ &= \frac{\partial_t a}{f_a}\frac{\boldsymbol{p}.\boldsymbol{\sigma}}{m}-\frac{1}{f_a}\boldsymbol{\nabla}a.\boldsymbol{\sigma}. \end{aligned} \tag{3.110}$$

Cross section

Axion is a scalar field. In the simplest case it can be written as $a=e^{-ikr}$ with k,r is momentum and position vector in 4-dimension space.Now. we will it to calculate cross section in two different situations like section. (3.2).

The case 1: $\beta=\frac{v_1}{c}\longrightarrow 0$

In this case, the energy of axion $k_0=\omega=m_a$ and $\vec{k}\longrightarrow 0$. The field of axion can be considered as $a=e^{-im_at}e^{i\vec{k}\vec{r}}$. In addition $\boldsymbol{\nabla}a\longrightarrow 0$ so only $-\frac{\partial_t a}{f_a}\bar{\psi}\gamma^0\gamma 5\psi$ term corresponding $\hat{\mathcal{H}}_a$ contributes to this process. The matrix element

$$\begin{aligned}\mathcal{M}_a = \langle f|\frac{\partial_t a}{f_a}\frac{\boldsymbol{p}.\boldsymbol{\sigma}}{m}|i\rangle &= \frac{m_a e^{-im_at}}{f_a}\langle f|e^{i\boldsymbol{kr}}\frac{\boldsymbol{p}.\boldsymbol{\sigma}}{m}|i\rangle \\ &= \frac{m_a e^{-im_at}}{f_a}\langle f|[\boldsymbol{\mathcal{H}_e},\boldsymbol{r}].\boldsymbol{\sigma}|i\rangle \\ &= \frac{m_a^2 e^{-im_at}}{f_a}\langle f|\boldsymbol{r}.\boldsymbol{\sigma}|i\rangle\,. \end{aligned} \tag{3.111}$$

At the first line of Eqs. (3.111), we made approximation dipole $e^{i\boldsymbol{kr}}=1+i\boldsymbol{kr}+...$ and ignored term proportional to the square of the velocity.

The amplitude of scattering

$$\begin{aligned}\left|\bar{\mathcal{M}}\right|_a^2 &= \sum_{spin}\frac{1}{2}\frac{m_a^4}{f_a^2}\langle f|\boldsymbol{r}.\boldsymbol{\sigma}|i\rangle\left(\langle f|\boldsymbol{r'}.\boldsymbol{\sigma}|i\rangle\right)^\dagger \\ &= \frac{1}{2}\frac{m_a^4}{f_a^2}S^2, \end{aligned} \tag{3.112}$$

where, we have argued like Eq. (3.93) and used Eqs.(3.83) and (3.97) to derive (3.112). According to Eqs. (3.98), (3.99) and (3.101), the cross section in this case is

$$\begin{aligned} d\sigma_{a,e} &= (2\pi)\frac{\left|\bar{\mathcal{M}}\right|_a^2}{2m_a\beta}Pd\phi\sin\theta d\theta \\ \Rightarrow\sigma_a &= \frac{\pi}{m_a\beta}\int_0^{2\pi}d\phi\int_0^{\pi}\sin\theta d\theta\frac{1}{2}\frac{m_a^4}{f_a^2}S^2P \\ &= \frac{(2\pi^2)}{\beta}\frac{m_a^3}{f_a^2}PS^2. \end{aligned} \tag{3.113}$$

Now, we can make a ratio between cross section of axioelectric and photoelectric process (note that energy of axion and electron are equal and $g_{a,e} = 2m/f_a$)

$$\left.\frac{\sigma_{a,e}}{\sigma_{ph}}\right|_{\beta\longrightarrow 0} = \frac{3}{4\pi\alpha}\frac{1}{\beta}\frac{m_a^2}{f_a^2} = g_{ae}^2\frac{3}{16\pi\alpha}\frac{1}{\beta}\frac{m_a^2}{m^2}. \tag{3.114}$$

This result is interesting. It turns out that in the $\beta \longrightarrow 0$ limit the ratio of Compton-like to Compton process is the same ratio of axioelectric to photoelectric (Eqs. (3.61) and (3.114)). Although the energy scale takes place the two processes occur at different energy scales.

The case 2 $\beta = \frac{v_1}{c} \longrightarrow 1$:

$$\begin{aligned}\mathcal{M}_{(4)} =& \langle f|\frac{\partial_t a}{f_a}\frac{\boldsymbol{p}.\boldsymbol{\sigma}}{m} - \frac{1}{f_a}\boldsymbol{\nabla}a.\boldsymbol{\sigma}|i\rangle \\ =& \frac{\omega}{f_a}e^{-i\omega t}\langle f|e^{i\boldsymbol{k}\boldsymbol{r}}\boldsymbol{p}.\boldsymbol{\sigma}|i\rangle - \frac{1}{f_a}e^{-i\omega t}\langle f|e^{i\boldsymbol{k}\boldsymbol{r}}\boldsymbol{k}.\boldsymbol{\sigma}|i\rangle .\end{aligned} \tag{3.115}$$

If we make the dipole approximation $e^{i\boldsymbol{k}\boldsymbol{r}} = 1 + i\boldsymbol{k}\boldsymbol{r} + ...$ for Eqs. (3.115). The first term is treated the same way as case $\beta \longrightarrow 0$. The second term became $-\frac{1}{f_a}e^{-i\omega t}\langle f|(i\boldsymbol{k}\boldsymbol{r})\boldsymbol{k}.\boldsymbol{\sigma}|i\rangle$, because $\langle f|\boldsymbol{k}.\boldsymbol{\sigma}|i\rangle = \langle f|1|i\rangle\,\boldsymbol{k}.\boldsymbol{\sigma} = 0$. We can write $\boldsymbol{k} = \omega\hat{\boldsymbol{n}}$ with $|\hat{\boldsymbol{n}}| = 1$ is magnitude of direction vector of axion momentum, Eqs. (3.115) is approximated

$$\mathcal{M}_{(4)} \approx \frac{\omega^2}{f_a}e^{-i\omega t}\langle f|\boldsymbol{r}.\boldsymbol{\sigma}|i\rangle - \frac{\omega^2}{f_a}e^{-i\omega t}\langle f|(\hat{\boldsymbol{n}}.\boldsymbol{r})(\hat{\boldsymbol{n}}.\boldsymbol{\sigma})|i\rangle . \tag{3.116}$$

The scattering amplitude squared reads

$$\begin{aligned}\left|\bar{\mathcal{M}}_{(4)}\right|^2 =& \sum_{spin}\frac{1}{2}\mathcal{M}_{(4)}^{\dagger}\mathcal{M}_{(4)} \\ =& \frac{\omega^4}{f_a^2}\frac{1}{2}\left|\langle f|\boldsymbol{r}.\boldsymbol{\sigma} - (\hat{\boldsymbol{n}}.\boldsymbol{r})(\hat{\boldsymbol{n}}.\boldsymbol{\sigma})|i\rangle\right|^2. \\ =& \left|\bar{\mathcal{M}}_a\right|^2 + \left|\bar{\mathcal{M}}_b\right|^2 - \left|\bar{\mathcal{M}}_{ab}\right|^2 - \left|\bar{\mathcal{M}}_{ba}\right|^2\end{aligned} \tag{3.117}$$

We will deal with each term in the Eqs. (3.117). By replacing ω (energy of axion) with m_a in Eqs. (3.112), we get the first term $\left|\bar{\mathcal{M}}_a\right|^2$ in the Eqs. (3.117). The remaining three terms indicate the difference between the calculation of the case $\beta \longrightarrow 0$ and $\beta \longrightarrow 1$. The second term is

$$\begin{aligned}\left|\bar{\mathcal{M}}_b\right|^2 =& \frac{\omega^4}{f_a^2}\frac{1}{2}\left|\langle f|(\hat{\boldsymbol{n}}.\boldsymbol{r})(\hat{\boldsymbol{n}}.\boldsymbol{\sigma})|i\rangle\right|^2 \\ =& \frac{\omega^4}{f_a^2}\frac{1}{2}\int dr\psi_f^*(r)\psi_b(r)\int dr'\psi_b^*(r)\psi_f(r)(\hat{\boldsymbol{n}}.\boldsymbol{r})(\hat{\boldsymbol{n}}.\boldsymbol{r}) \\ =& \frac{\omega^4}{f_a^2}\frac{1}{2}\cos\theta^2 S^2,\end{aligned} \tag{3.118}$$

where the $\hat{\boldsymbol{r}}$ makes an angle θ with $\hat{\boldsymbol{n}}$ as shown in figure (3.12), the third and fourth

are the interference terms and read

$$\begin{aligned}\left|\bar{\mathcal{M}}_{ab}\right|^2 &= \frac{\omega^4}{f_a^2}\frac{1}{2}\langle f|\boldsymbol{r}.\boldsymbol{\sigma}|i\rangle\,(\,\langle f|(\hat{\boldsymbol{n}}.\boldsymbol{r'})(\hat{\boldsymbol{n}}.\boldsymbol{\sigma})|i\rangle)^\dagger \\ &= \frac{\omega^4}{f_a^2}\frac{1}{2}\int dr\psi_f^*(r)\psi_b(r)\int dr'\psi_b^*(r')\psi_f(r')(\boldsymbol{r}.\boldsymbol{\sigma})(\hat{\boldsymbol{n}}.\boldsymbol{\sigma})(\hat{\boldsymbol{n}}.\boldsymbol{r'}) \qquad (3.119)\\ \left|\bar{\mathcal{M}}_{ba}\right|^2 &= \frac{\omega^4}{f_a^2}\frac{1}{2}\langle f|(\hat{\boldsymbol{n}}.\boldsymbol{r})(\hat{\boldsymbol{n}}.\boldsymbol{\sigma})|i\rangle\,(\,\langle f|\boldsymbol{r'}.\boldsymbol{\sigma}|i\rangle)^\dagger \\ &= \frac{\omega^4}{f_a^2}\frac{1}{2}\int dr\psi_f^*(r)\psi_b(r)\int dr'\psi_b^*(r')\psi_f(r')(\hat{\boldsymbol{n}}.\boldsymbol{r})(\hat{\boldsymbol{n}}.\boldsymbol{\sigma})(\boldsymbol{r'}.\boldsymbol{\sigma}) \qquad (3.120)\end{aligned}$$

if we use the condition $\boldsymbol{r} = \boldsymbol{r'}$. Then, we add both of the above equations and utilize Eqs. (3.83)

$$\begin{aligned}\left|\bar{\mathcal{M}}_{ab}\right|^2 + \left|\bar{\mathcal{M}}_{ba}\right|^2 &= 2\frac{\omega^4}{f_a^2}\frac{1}{2}\int dr\psi_f^*(r)\psi_b(r)\int dr'\psi_b^*(r)\psi_f(r)(\hat{\boldsymbol{n}}.\boldsymbol{r})(\hat{\boldsymbol{n}}.\boldsymbol{r}) \\ &= 2\left|\bar{\mathcal{M}}_b\right|^2. \qquad (3.121)\end{aligned}$$

According to Eqs. (3.98),(3.99), (3.101),(3.118),(3.121) and (3.117). The cross section is

$$\begin{aligned}d\sigma_{a,e} &= \frac{2\pi}{2\omega\beta}(\left|\bar{\mathcal{M}}_a\right|^2 - \left|\bar{\mathcal{M}}_b\right|^2)Pd\phi\sin\theta d\theta \\ \Rightarrow \sigma_{a,e} &= \frac{\pi}{\omega\beta}\int_0^{2\pi}d\phi\int_0^{\pi}\sin\theta d\theta(\frac{1}{2}\frac{\omega^4}{f_a^2}S^2 - \frac{\omega^4}{f_a^2}\frac{1}{2}\cos\theta^2 S^2)P \\ &= \frac{2\pi^2}{\beta}\frac{1}{2}\frac{\omega^3}{f_a^2}\frac{4}{3}S^2P, \qquad (3.122)\end{aligned}$$

we obtain

$$\frac{\lim_{\beta\longrightarrow 1}\sigma_{a,e}}{\sigma_{ph}} = \frac{\omega^2}{2\pi\alpha f_a^2} = g_{a,e}\frac{\omega^2}{8\pi\alpha m^2}. \qquad (3.123)$$

A convenient general formula which reduces to the asymptotic expressions of axioelectric cross section (From Eqs. (3.123) and (3.114)) is

$$\sigma_{a,c} = \sigma_{ph}\frac{3g_{ae}^2\omega^2}{16\beta\pi\alpha m^2}(1-\frac{\beta}{3}), \qquad (3.124)$$

which has been showed by Derbin et al. [12]. This result is twice as large as the formula of Ref [15]. The source of the discrepancy with previous calculation is omission of the first term in Eq. (3.116). However, Ref. [4] modified Eq. (3.124)to describes the cross section with a better accuracy over the full β range.

$$\sigma_{a,c} = \sigma_{ph}\frac{3g_{ae}^2\omega^2}{16\beta\pi\alpha m^2}(1-\frac{\beta^{2/3}}{3}), \qquad (3.125)$$

where the cross section for the photoelectric effect $\sigma_{ph}(\omega)$ for various energies of photon can be obtained from Ref. [35].

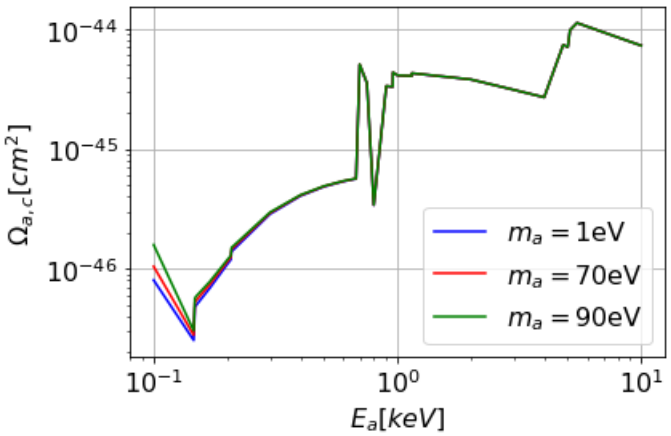

Figure 3.13: The total cross section of the axioelectric process on Xe as a function of the axion energy E_a with $g_{ae} = 10^{-12}$.

In general, the value of axioelectric cross section increases when the energy of axion rise (as shown figure (3.13)). However, we still see some peaks. The reason comes from experimental data of photoelectric cross section. Theoretically, we can explain that the energy difference of the electrons on the atomic shells is responsible for the peaks in the figure. Particularly, from 0.30 to 10 keV, at different masses, the cross sections are the same. From 0.1 to 0.15 keV, the larger the mass of the axion, the smaller its velocity. According to (3.125), the value of the axioelectric cross section will be proportional to the mass of the axion.

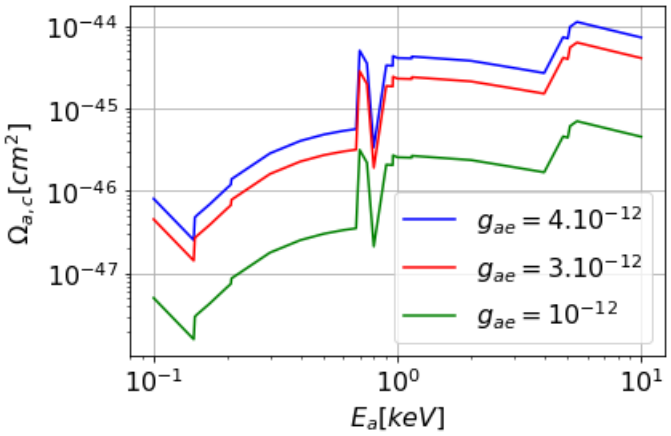

Figure 3.14: The total cross section of the axioelectric process on Xe as a function of the axion energy E_a with $m_a = 1\text{eV}$.

In figure (3.14), we see that the axion-electron coupling directly affects the axioelectric cross section. It is likely that the bigger axion-electron coupling, the greater the cross section.

We see that in the three cases: inverse Primakoff process, Comptom-like process and axioelectric effect with the same coupling value, axioelectric effect the largest contribution.

Now, we will learn how to use the calculation in the section (3.1),(3.2) and (3.3) to detect dark matter.

3.5 The Evidence of Axion

One of evidences for the of existence of axions is the anormaly observed recently by the XENONT experiment. To verify the existence of this theoretical particle, one constructs a quantity that can be calculated by theory and measured by experiment. Its name is the differential event rate. This quantity includes the axion detection processes that we described in the previous sections and the total solar axion flux.

The Sun can produce a an axion flux through the following three mechanisms. Atomic recombination and deexcitation, Bremsstrahlung, and Compton scattering that is known as the "ABC process" ($\Phi_a^{ABC} \propto g_{ae}^2$) given by [29]. Another important mechanism also contributes to total solar axion flux is Primakoff conversion of photons to axions in the Sun. The Primakoff flux is given by Ref. [28]

$$\frac{d\Phi_a^{Prim}}{dE_a} = 6 \times 10^{10} cm^{-2} s^{-1} keV^{-1} \times \Big(\frac{g_{a\gamma\gamma}}{10^{-10} GeV}\Big)^2 \Big(\frac{E_a}{keV}\Big)^{2.481} e^{-E_a/(1.205keV)}, \tag{3.126}$$

where E_a is energy of axion . In general, we have a third mechanism, a monoenergetic 14.4 keV M1 nuclear transition of Fe^{57} (see Ref. [4]) , that contributes to the total solar axion flux. However, we will focus on the range energy of axion < 5keV. This mechanism can be neglected.

The different event rate after including inverse Primakoff, Compton-like particle and axoelectric process in the detection is given by:

$$\frac{dR}{dE_r} = \frac{N_A}{A}\Big(\frac{d\Phi_a^{ABC}}{dE}(E_r) + \frac{d\Phi_a^{Prim}}{dE}(E_r)\Big) \times (\sigma^{Prim}(E_r) + \sigma_{cp}(E_r) + \sigma_{a,c}(E_r)), \tag{3.127}$$

where, N_A is Avogadro constant, $A = 131$ is the atomic weight of xenon, E_r is electronic recoil energy. The term $\frac{d\Phi_a^{ABC}}{dE}$ is not written explicitly like Ref. (3.126) since it is calculated numerically by some computational codes, for instance, Los Alamos opacities (LEDCOP) [23] (see Ref. ([29])). From Eq. (3.69), we see that cross section of Compton-like particle depended on the Compton cross section. The energy scale for the Compton process to occur is at $MeV - GeV$ (Ref. [5]). It is much larger than the energy scale we focus on. Therefore, we can ignore Compton-like particle process. Now, the different event rate is become

$$\frac{dR}{dE_r} = \frac{N_A}{A}\Big(\frac{d\Phi_a^{ABC}}{dE}(E_r) + \frac{d\Phi_a^{Prim}}{dE}(E_r)\Big) \times (\sigma^{Prim}(E_r) + \sigma_{a,c}(E_r)), \tag{3.128}$$

with cross section of Primakoff and axioelectric as in Eqs. (3.23) and (3.125). We note that we have assumed that at the keV energy range, the XENON1T detector can hardly distinguish the detector response of photons and that of electronic recoils.

On searches for electronic recoil (ER) signal with data acquired from February 2017 to February 2018 (a time period known as Science Run 1 (SR1)) [6] and using background model given by [7], they obtained an excess at low energies, that is displayed in figure. (3.15)

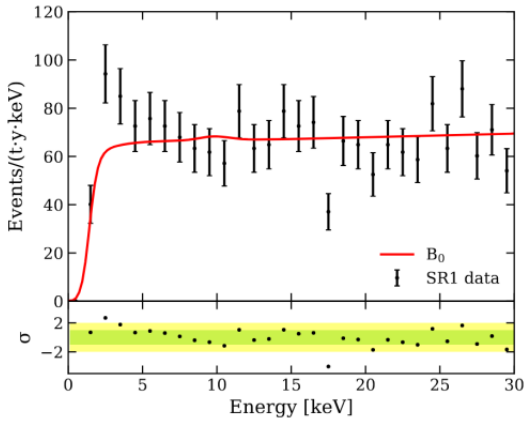

Figure 3.15: The Xenon1T experiment result. The red line represents the background. The lower plot shows the centre of experiment data deviated from the 1 sigma (green) and 2 sigma (yellow) significance bands. Extract from [7]

In the figure (3.15), at 6 keV, the data begins to deviate upward from the background. As the energy decreases, the deviation increases with a peak near 2-3 keV. However the deviation decreases to 1 sigma near 1-2 keV. The excess indicates that there may be new mechanism that is not accounted for in the background. It is most likely the new mechanism caused by a particle outside the standard model.

The excess of XENON1T can be well explained by solar axion, whose energy spectrum is quite coincident with the excess. The authors of Ref.[19] used Eq. (3.125) and then smeared the differential even rate with a Gaussian function and applied the detector efficiency. Two examples of the differential event rate of the electronic recoils are given in figure. (3.16) to illustrate the axion's interpretation of the excess .

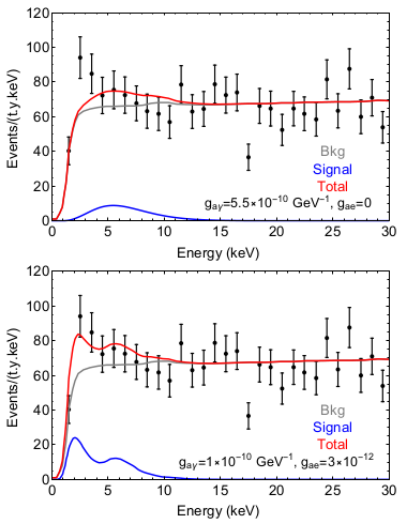

Figure 3.16: The differential event rate of the electronic recoils. Extract from [7]

Figure 3.16 shows that by choosing different $(g_{a\gamma}, g_{a,e})$-value pair we can get results that match the experimental data as closely as possible. It is also possible to vary both $g_{a\gamma}$ and g_{ae} simutaniously to find the best fit region, which is shown in figure (3.17).

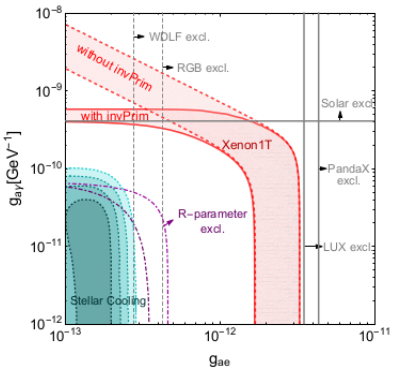

Figure 3.17: The 2D fit for axion coupling parameters. The best fit (90% confident level) to the XENON1T excess is shown in the red shaded region with the solid boundary. The gray lines represent the constraints from astrophysics which we mentioned in section. (2.3). Extract from Ref.[19]

If we ignore the inverse Primakoff process ($\sigma^{Prim}(E_r) = 0$) we will get the region (without invPrim) of value $(g_{a\gamma}, g_{a,e})$ highlighted in red as shown in figure. (3.17). In this region, the value of $g_{a\gamma}$ can be larger than $10^{-9}GeV^{-1}$. That is in higher tension with the astrophysical constraints (see Eq. (2.78)). Therefore, considering the inverse Primakoff process reduces tension with constraints from astrophysics. The value best fit of electron-axion coupling automatically satisfies some astrophysic constraints beautifully. However the best fit region of the XENON1T anomaly is in great tension with the region favoured by the stellar cooling anomaly, shown in shaded green region in figure (3.17). The solar axion gives a good explanation of the XENON1T excess as we have seen. However more data and better understanding of the background are needed to see if this anomaly persist.

Summary

In general, my thesis can be divided into two main parts: the theory of axion and the detection of axion.

In chapter 1, the U(1) problem led to an extra term $\mathcal{L}_\theta$ for QCD Lagrangian. The term $\mathcal{L}_\theta$ is CP violation and gives rise to the Strong CP problem. By the PQ mechanism, the CP violation term is vanished and generated a new term that preserves CP. This new term contains the axion field. To generate mass for the axion, we have to consider the system at low energies and the Chiral theory. Consequently, the mass of the axion is calculated through the mass of light quarks and pion decay constants.

In chapter 2, we have derived the formula for calculating the anomalies of an axial current. Then, we considered anomalies of divergence of PQ current and acquired interaction Lagrangian of axion with gluon and photon. After breaking the symmetry at the electroweak energy level, we introduced a correction for the PQ charge of the fermions thereby leading to the effective interaction Lagrangian for the axion-fermion interaction and its couplings. At below Λ_{QCD} scale, to create the mass of axion, we take the interaction term with the gluon out of the Lagrangian, this leads to the correction of the interaction coupling of the axion and the photon, and at this energy level, there is the interaction of the axion with the nucleon. Next, we introduced a specific axion model SMASH and applied the coupling formulas to this model.

In chapter 3, we considered three direct detection processes of axion: Primakoff, Compton-like scattering, and axioeletric effect. For the axioeletric effect, we are already familiar with the transition from the Lagrangian in QFT theory to the Hamiltonian operator in quantum mechanics. We have shown how the above processes play an essential role in the detection of axion.

Appendix A

The Amplitude scattering of Compton-like process

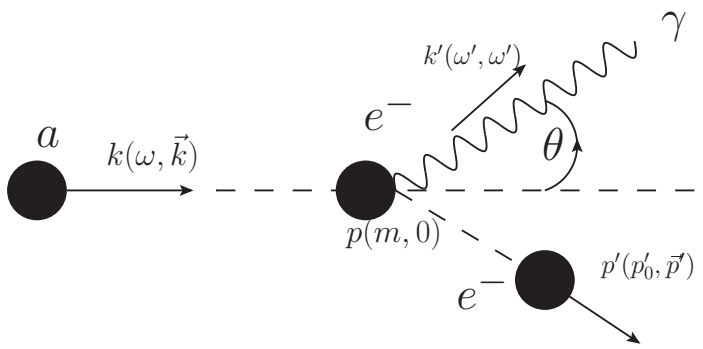

Figure A.1: Compton-like Scattering

According to Eqs. (3.38), (3.43)-(3.45), we obtain

$$|\bar{\mathcal{M}}_{cp}|^2 = 4m_a^2 m^2 \frac{e^2}{f_a^2}\Bigg[m^2\Big(\frac{1}{p'.k'} - \frac{1}{p.k'}\Big)^2 + 2\Big(\frac{1}{p'.k'} - \frac{1}{p.k'}\Big) + \frac{m_a^2}{(p'.k')(p.k')} + \frac{2}{m_a^2}\Big(\frac{p'.k'}{p.k'} + \frac{p.k'}{p'.k'}\Big) - \frac{4}{m_a^2}\Bigg] \tag{A.1}$$

and a number of equations obtained by the assumption in section. (3.2)

$$k.k = m_a^2 \tag{A.2}$$
$$k'k' = 0 \tag{A.3}$$
$$p.k' = m\omega' \tag{A.4}$$
$$p.k = m\omega \tag{A.5}$$
$$2p'k' = 2pk + m_a^2 \tag{A.6}$$
$$2kk' = m_a^2 - 2m^2 + 2pp' \tag{A.7}$$
$$2pp' = 2m^2 - m_a^2 + 2p'k' - 2pk' \tag{A.8}$$

The energy of system is conservation

$$\omega + m = \omega' + p'_0 \tag{A.9}$$

$$\Leftrightarrow \omega + m - \omega' = \sqrt{m^2 + (\vec{k} - \vec{k'})^2}$$

$$\Leftrightarrow (\omega + m - \omega')^2 = m^2 + \left|\vec{k}\right|^2 + \omega'^2 \Leftrightarrow -2\left|\vec{k}\right|\omega' \cos\theta$$

$$\Leftrightarrow \omega^2 + 2m\omega - 2m\omega' - 2\omega\omega' = \left|\vec{k}\right|^2 - 2\left|\vec{k}\right|\omega' \cos\theta$$

$$\Leftrightarrow m_a^2 + 2m\omega = 2\omega'(m + \omega - \left|\vec{k}\right| \cos\theta)$$

$$\Leftrightarrow \frac{m_a^2 + 2m\omega}{2(m + \omega - \left|\vec{k}\right| \cos\theta)} = \omega' \tag{A.10}$$

From Eq. (A.1), we define A term

$$A = \Big(\frac{p'.k'}{p.k'} + \frac{p.k'}{p'.k'}\Big) - 2 \tag{A.11}$$

$$= \frac{2m\omega + m_a^2}{2m\omega'} + \frac{2m\omega'}{2m\omega + m_a^2} - 2 \tag{A.12}$$

and C term is

$$C = m^2\Big(\frac{1}{p'.k'} - \frac{1}{p.k'}\Big)^2 + 2\Big(\frac{1}{p'.k'} - \frac{1}{p.k'}\Big) + \frac{m_a^2}{(p'.k')(p.k')} \tag{A.13}$$

$$= 4m^2\Big(\frac{1}{2p.k + m_a^2} - \frac{1}{2p.k'}\Big)^2 + 4\Big(\frac{1}{2p.k + m_a^2} - \frac{1}{2p.k'}\Big) + \frac{4m_a^2}{(2p.k + m_a^2)(2p.k')}$$

$$= 4m^2\Big(\frac{1}{2p.k + m_a^2} - \frac{1}{2p.k'}\Big)^2 + 4\frac{2p.k' - 2p.k}{(2p.k + m_a^2)(2p.k')}$$

$$= 4m^2\Big(\frac{1}{2p.k + m_a^2} - \frac{1}{2p.k'}\Big)^2 + \frac{4}{2p.k + m_a^2}(1 - \frac{2p.k}{2p.k'})$$

$$= C_1 + C_2, \tag{A.14}$$

where

$$C_1 = 4m^2\Big(\frac{1}{2p.k + m_a^2} - \frac{1}{2p.k'}\Big)^2 = 4m^2\Big(\frac{1}{2m\omega + m_a^2} - \frac{1}{2m\omega'}\Big)^2$$

$$= \frac{1}{\omega'^2}\frac{(2m\omega' - 2m\omega - m_a^2)^2}{(2m\omega + m_a^2)^2}$$

$$= 4\frac{(\omega - \left|\vec{k}\right| \cos\theta)^2}{(2m\omega + m_a^2)^2} \tag{A.15}$$

$$C_2 = \frac{4}{2p.k + m_a^2}(1 - \frac{2p.k}{2p.k'})$$

$$= \frac{4}{2m\omega + m_a^2}(1 - \frac{\omega}{\omega'})$$

$$= \frac{4}{2m\omega + m_a^2}(1 - \frac{2\omega(m + \omega - \left|\vec{k}\right| \cos\theta)}{2m\omega + m_a^2})$$

$$= \frac{4}{(2m\omega + m_a^2)^2}(m_a^2 - 2\omega^2 + 2\omega\left|\vec{k}\right| \cos\theta) \tag{A.16}$$

According to Eqs. (A.15), (A.16) and (A.14), we obtain

$$\begin{aligned} C &= \frac{4}{(2m\omega + m_a^2)^2}(m_a^2 - \omega^2 + \left|\vec{k}\right|^2 \cos\theta^2) \\ &= \frac{4}{(2m\omega + m_a^2)^2}(-\left|\vec{k}\right|^2 + \left|\vec{k}\right|^2 \cos\theta^2) \\ &= \frac{4}{(2m\omega + m_a^2)^2}(-\left|\vec{k}\right|^2 \sin\theta^2) \end{aligned} \tag{A.17}$$

Finally, we have the amplitude of Compton-like scattering is

$$\begin{aligned} \left|\bar{\mathcal{M}}_{cp}\right|^2 &= 4m_a^2 m^2 \frac{e^2}{f_a^2}(C + \frac{2A}{m_a^2}) \\ &= 4m^2 \frac{e^2}{f_a^2}\Big(\frac{4m_a^2}{(2m\omega + m_a^2)^2}(-\left|\vec{k}\right|^2 \sin\theta^2) + 2A\Big) \\ &= 4m^2 \frac{e^2}{f_a^2}\Big(\frac{4(2m\omega + m_a^2 - 2m\omega)}{(2m\omega + m_a^2)^2}(-\left|\vec{k}\right|^2 \sin\theta^2) + 2A\Big) \\ &= 4m^2 \frac{e^2}{f_a^2}\Big(\Big[\frac{-4}{2m\omega + m_a^2} + \frac{8m\omega}{(2m\omega + m_a^2)^2}\Big]\left|\vec{k}\right|^2 \sin\theta^2 + 2A\Big) \\ &= 4m^2 \frac{e^2}{f_a^2}(B\left|\vec{k}\right|^2 \sin\theta^2 + 2A), \end{aligned} \tag{A.18}$$

where

$$B = \frac{-4}{2m\omega + m_a^2} + \frac{8m\omega}{(2m\omega + m_a^2)^2} \tag{A.19}$$

Appendix B

Differential Cross Section of Compton-like Scattering

From section. (3.2) we have

$$d\sigma = \frac{1}{2k_0 2p_0|v_1|}\int \frac{d^3k'}{16\pi^2}\frac{1}{k'_0 p'_0} \times \delta(k_0 + p_0 - p'_0 - k'_0)\left|\mathcal{M}_{cp}(k, p \to p', k')\right|^2. \tag{B.1}$$

combining to figure. (A.4) we have

$$d\sigma = \frac{1}{4m\omega|v_1|}\int \frac{d\cos(\theta)}{8\pi^2}\frac{d\omega'\omega'}{p'_0} \times \delta(\omega + m - \omega' - p'_0)\left|\mathcal{M}_{cp}(k, p \to p', k')\right|^2, \tag{B.2}$$

note that in the delta function p'_0 is a function of ω'. In order to take integrate by ω', we need to calculate

$$f(\omega') = \omega + m - \omega' - p'_0 = 0, \tag{B.3}$$

with

$$p'_0 = \sqrt{m^2 + (\vec{k} - \vec{k'})^2}. \tag{B.4}$$

The solution of Eq. (B.3) is is exactly equal to Eq. (A.10), when

$$d\sigma = \frac{1}{4m\omega|v_1|}\int \frac{d\cos(\theta)}{8\pi^2}\frac{\omega'}{p'_0\left|f'(\omega')\right|} \times \delta(\omega + m - \omega' - p'_0)\left|\mathcal{M}_{cp}(k, p \to p', k')\right|^2, \tag{B.5}$$

where

$$\left|f'(\omega')\right| = \left|\frac{df(\omega')}{d\omega'}\right| = \left|-1 - \frac{d}{d\omega'}\sqrt{m^2 + \left|\vec{k}\right| + \left|\vec{k'}\right| - 2\left|\vec{k}\right|\left|\vec{k'}\right|\cos(\theta)}\right| = \left|\frac{p'_0 + \omega' - \left|\vec{k}\right|\cos(\theta)}{p'_0}\right|. \tag{B.6}$$

Finally, we get

$$d\sigma = \frac{1}{4\omega m|v_1|}\int \frac{d\cos\theta}{8\pi}\frac{\omega'}{(m+\omega-\left|\vec{k}\right|\cos\theta)}\left|\mathcal{M}_{cp}(k,p\to p',k')\right|^2 \qquad \textbf{Q.E.D} \tag{B.7}$$

Bibliography

[1] Tomohiro Abe, Koichi Hamaguchi, and Natsumi Nagata. Atomic Form Factors and Inverse Primakoff Scattering of Axion. *Phys. Lett. B*, 815:136174, 2021.

[2] Stephen L. Adler and William A. Bardeen. Absence of higher-order corrections in the anomalous axial-vector divergence equation. *Phys. Rev.*, 182:1517–1536, Jun 1969.

[3] D. S. Akerib et al. First Searches for Axions and Axionlike Particles with the LUX Experiment. *Phys. Rev. Lett.*, 118(26):261301, 2017.

[4] F. Alessandria et al. Search for 14.4 keV solar axions from M1 transition of Fe-57 with CUORE crystals. *JCAP*, 05:007, 2013.

[5] P. Ambrozewicz et al. High Precision Measurement of Compton Scattering in the 5 GeV region. *Phys. Lett. B*, 797:134884, 2019.

[6] E. Aprile et al. Dark matter search results from a one ton-year exposure of xenon1t. *Phys. Rev. Lett.*, 121:111302, Sep 2018.

[7] E. Aprile et al. Excess electronic recoil events in XENON1T. *Phys. Rev. D*, 102(7):072004, 2020.

[8] Guillermo Ballesteros, Javier Redondo, Andreas Ringwald, and Carlos Tamarit. Standard Model—axion—seesaw—Higgs portal inflation. Five problems of particle physics and cosmology solved in one stroke. *JCAP*, 08:001, 2017.

[9] R. Bernabei et al. Investigating pseudoscalar and scalar dark matter. *Int. J. Mod. Phys. A*, 21:1445–1470, 2006.

[10] P. J. Brown, A. G. Fox, E. N. Maslen, M. A. O'Keefe, and B. T. M. Willis. *Intensity of diffracted intensities*, pages 554–595. Springer Netherlands, Dordrecht, 2004.

[11] M A Coulthard. A relativistic hartree-fock atomic field calculation. *Proceedings of the Physical Society*, 91(1):44–49, may 1967.

[12] A. V. Derbin, I. S. Dratchnev, A. S. Kayunov, V. N. Muratova, D. A. Semenov, and E. V. Unzhakov. Search for solar axions produced by Compton process and bremsstrahlung using the resonant absorption and axioelectric effect. In *9th Patras Workshop on Axions, WIMPs and WISPs*, 12 2013.

[13] P. Di Vecchia and G. Veneziano. Chiral Dynamics in the Large n Limit. *Nucl. Phys. B*, 171:253–272, 1980.

[14] A. G. Dias, A. C. B. Machado, C. C. Nishi, A. Ringwald, and P. Vaudrevange. The Quest for an Intermediate-Scale Accidental Axion and Further ALPs. *JHEP*, 06:037, 2014.

[15] S. Dimopoulos, G. D. Starkman, and B. W. Lynn. Atomic Enhancements in the Detection of Axions. *Mod. Phys. Lett. A*, 1:491–500, 1986.

[16] Savas Dimopoulos, Joshua Frieman, Bryan W. Lynn, and Glenn D. Starkman. Axiorecombination: A new mechanism for stellar axion production. *Physics Letters B*, 179(3):223–227, 1986.

[17] P. A. Doyle and P. S. Turner. Relativistic Hartree–Fock X-ray and electron scattering factors. *Acta Crystallographica Section A*, 24(3):390–397, May 1968.

[18] Changbo Fu et al. Limits on Axion Couplings from the First 80 Days of Data of the PandaX-II Experiment. *Phys. Rev. Lett.*, 119(18):181806, 2017.

[19] Christina Gao, Jia Liu, Lian-Tao Wang, Xiao-Ping Wang, Wei Xue, and Yi-Ming Zhong. Reexamining the Solar Axion Explanation for the XENON1T Excess. *Phys. Rev. Lett.*, 125(13):131806, 2020.

[20] Giovanni Grilli di Cortona, Edward Hardy, Javier Pardo Vega, and Giovanni Villadoro. The QCD axion, precisely. *JHEP*, 01:034, 2016.

[21] B. L. Ioffe. Condensates in quantum chromodynamics. *Phys. Atom. Nucl.*, 66:30–43, 2003.

[22] O. Klein and Y. Nishina. The scattering of light by free electrons according to dirac's new relativistic dynamics. 1928.

[23] N. H. Magee, J. Abdallah, J. Colgan, P. Hakel, D. Kilcrease, S. Mazevet, M. Sherrill, C. Fontes, and H. L. Zhang. Los alamos opacities: Transition from ledcop to atomic. 2004.

[24] Michael E. Peskin and Daniel V. Schroeder. *An Introduction to quantum field theory*. Addison-Wesley, Reading, USA, 1995.

[25] Maxim Pospelov and Adam Ritz. Electric dipole moments as probes of new physics. *Annals Phys.*, 318:119–169, 2005.

[26] Maxim Pospelov, Adam Ritz, and Mikhail B. Voloshin. Bosonic super-WIMPs as keV-scale dark matter. *Phys. Rev. D*, 78:115012, 2008.

[27] Jérémie Quevillon and Christopher Smith. Axions are blind to anomalies. *Eur. Phys. J. C*, 79(10):822, 2019.

[28] Georg G. Raffelt. Astrophysical axion bounds. *Lect. Notes Phys.*, 741:51–71, 2008.

[29] Javier Redondo. Solar axion flux from the axion-electron coupling. *Journal of Cosmology and Astroparticle Physics*, 2013(12):008–008, dec 2013.

[30] Jun John Sakurai and Jim Napolitano. *Modern quantum mechanics; 2nd ed.* Addison-Wesley, San Francisco, CA, 2011.

[31] H. Schlattl, A. Weiss, and G. Raffelt. Helioseismological constraint on solar axion emission. *Astroparticle Physics*, 10(4):353–359, 1999.

[32] P. Sikivie. Experimental tests of the "invisible" axion. *Phys. Rev. Lett.*, 51:1415–1417, Oct 1983.

[33] Mark Srednicki. Axion Couplings to Matter. 1. CP Conserving Parts. *Nucl. Phys. B*, 260:689–700, 1985.

[34] Gerard 't Hooft. Symmetry Breaking Through Bell-Jackiw Anomalies. *Phys. Rev. Lett.*, 37:8–11, 1976.

[35] Wm. J. Veigele. Photon cross sections from 0.1 keV to 1 MeV for elements Z = 1 to Z = 94. *Atom. Data Nucl. Data Tabl.*, 5:51–111, 1973.

[36] Julia Vogel. Searching for solar axions in the ev-massregion with the ccd detector at cast. 01 2009.

[37] Steven Weinberg. The U(1) Problem. *Phys. Rev. D*, 11:3583–3593, 1975.

[38] Steven Weinberg. A New Light Boson? *Phys. Rev. Lett.*, 40:223–226, 1978.

[39] K. Zioutas et al. First results from the CERN Axion Solar Telescope (CAST). *Phys. Rev. Lett.*, 94:121301, 2005.